NOVEL TRENDS IN ANALYTICAL SCIENCES: CAPILLARY ELECTROPHORESIS AND MICROCHIP CAPILLARY ELECTROPHORESIS

NANTANA NUCHTAVORN

**A THESIS SUBMITTED IN PARTIAL FULFILLMENT
OF THE REQUIREMENTS FOR
THE DEGREE OF DOCTOR OF PHILOSOPHY
(PHARMACEUTICAL CHEMISTRY AND PHYTOCHEMISTRY)
FACULTY OF GRADUATE STUDIES
MAHIDOL UNIVERSITY
2011**

COPYRIGHT OF MAHIDOL UNIVERSITY

Thesis
entitled

NOVEL TRENDS IN ANALYTICAL SCIENCES: CAPILLARY ELECTROPHORESIS AND MICROCHIP CAPILLARY ELECTROPHORESIS

……
Miss Nantana Nuchtavorn
Candidate

……
Prof. Leena Suntornsuk,
Ph.D. (Pharmaceutical Chemistry)
Major advisor

……
Lect. Nimit Chomnawang,
Ph.D. (Electrical Engineering)
Co-advisor

……
Prof. Mirek Macka
Ph.D. (Chemistry)
Co-adivisor

……
Prof. Banchong Mahaisavariya,
M.D., Dip Thai Board of Orthopedics
Dean
Faculty of Graduate Studies
Mahidol University

……
Assoc. Prof. Opa Vajragupta
Ph.D. (Medicinal Chemistry)
Program Director
Doctor of Philosophy Program in
Pharmaceutical Chemistry and
Phytochemistry
Faculty of Pharmacy, Mahidol University

Thesis
entitled

NOVEL TRENDS IN ANALYTICAL SCIENCES: CAPILLARY ELECTROPHORESIS AND MICROCHIP CAPILLARY ELECTROPHORESIS

was submitted to the Faculty of Graduate Studies, Mahidol University
for the degree of Doctor of Philosophy
(Pharmaceutical Chemistry and Phytochemistry)
on
June 13, 2011

……
Miss Nantana Nuchtavorn
Candidate

……	……
Prof. Leena Suntornsuk, Ph.D. (Pharmaceutical Chemistry) Member	Lect. Walapa Thathong Ph.D. (Pharmaceutical Chemistry) Chair
……	……
Lect. Nimit Chomnawang, Ph.D. (Electrical Engineering) Member	Prof. Mirek Macka Ph.D. (Chemistry) Member
……	……
Prof. Banchong Mahaisavariya, M.D., Dip Thai Board of Orthopedics Dean Faculty of Graduate Studies Mahidol University	Assoc. Prof. Chuthamanee Suthisisang Ph.D. (Pharmacology) Dean Faculty of Pharmacy Mahidol University

ACKNOWLEDGEMENTS

First, I wish to extend my gratitude and great appreciation to my advisor, Professor Leena Suntornsuk, for her dedication to suggest, assist and give me a great deal of encouragement throughout my study. Secondly, I would like to thank Professor Mirek Macka, School of chemistry, Univeristy of Tasmania, Australia, my co-advisor, for providing knowledge, kindness, and useful advice during my work in School of Chemical Sciences, Dublin City University, Republic of Ireland. Next, I would like to thank Dr. Nimit Chomnawang, School of Electrical Engineering, Institute of Engineering, Suranaree University of Technology, my co-advisor, for his knowledge, helpful, and suggestions for this work.

I would like to thank Dr. Walapa Tatong for being a committee in my thesis examination and also give me valuable comments and suggestions. As well, I would like to thank Assistant Professor Nongluck Ruangwises for her kindness and assistance for being my proposal examination committee.

I would like to thank all of the staffs, friends and colleagues at the Department of Pharmaceutical Chemistry and the Central Laboratory, Faculty of Pharmacy, Mahidol University, for their kindness and help. Next, I would like to thank all of the staffs, friends and colleagues in Microfluidic analysis" (μ-FAn) research group, School of Chemical Sciences, Dublin City University, Republic of Ireland, the Microelectromechanical Systems Laboratory, School of Electrical Engineering, Institute of Engineering Suranaree University of Technology and other persons who have not been mentioned here for their help, friendship and encouragement.

I would like to thank the Royal Golden Jubilee Ph. D. program, Thailand Research fund for the financial support, which enables me to study my Ph.D. and to do this research work.

Finally, I wish to express my sincere gratitude and especially thanks to my family for their concern and support me to gain invaluable experience throughout my life.

Nantana Nuchtavorn

NOVEL TRENDS IN ANALYTICAL SCIENCES: CAPILLARY ELECTROPHORESIS AND MICROCHIP CAPILLARY ELECTROPHORESIS

NANTANA NUCHTAVORN 4937086 PYPP/ D

Ph.D. (PHARMACEUTICAL CHEMISTRY AND PHYTOCHEMISTRY)

THESIS ADVISORY COMMITTEE: LEENA SUNTORNSUK, Ph.D., MIREK MACKA, Ph.D., NIMIT CHOMNAWANG, Ph.D.

ABSTRACT

Recently, a demand for rapid, cost-effective, and environmentally friendly analytical methods has increased. These approaches can be achieved with electrically driven separation methods known as “capillary electrophoresis (CE)” due to short analysis time, low solvent and sample consumption, and high separation efficiency. Additionally, the miniaturization system, “microchip CE”, enables promise for higher sample throughput, lower solvent and sample consumption, and consideration as a portable instrument.

This work purposed to evaluate the merits of these techniques in chemical and biological fields towards green analytical chemistry. The CE method for the simultaneous analysis of nicotine, cotinine, nicotinamide, and nicotinic acid was established using triprolidine as an internal standard. The optimized condition was achieved in 25 mM sodium dihydrogen phosphate (pH 2.1) using a capillary with a L_{total} of 64.5 cm, 50 μm i.d. (extended path length), injection at 50 mbar for 10 s, and the applied voltage of 30 kV, and a baseline separation at 10 min. The validated method was applied for the determination of nicotine, cotinine (in a stress test of nicotine gum), nicotinamide, and nicotinic acid in pharmaceutical formulations with the results found within USP limit.

Furthermore, the performance of commercial microchip CE with a red laser induced fluorescence detection and its chips were evaluated. Simple and rapid chip-based non-aqueous CE separation of several structurally related basic dyes (*e.g.* methylene blue, toluidine blue, nile blue, and brilliant cresyl blue) was achieved in ~ 40 s in 80 mM NH_4OAc, 870 mM acetic acid in DMSO with a separation length of 14 mm and injection/separation voltages of 1,400/1,500 V. Then, single cell analysis of nile blue stained *E. coli*, *B. subtilis*, *M. luteus*, *S. aureus*, *C. albicans*, and *L. fungicola* was achieved in ~ 20 s in 1 mg/mL CTAB in 1 mM Tris/0.33 mM citric acid, pH 7.0, using 5 mg/mL SB3-10 as a blocking agent and injection/separation voltages of -1,000/-1,000 V providing S/N of 26.2 – 34.0 with % RSD within 2.45%. Separations of the bacteria and fungus mixture containing *E. coli*, *S. aureus* and *C. albicans* were re-optimized and achieved in 3.94 mM Tris, 0.56 mM boric acid and 0.013 mM Na_2EDTA pH 10.5, containing 0.025% PEO with injection/separation voltages of 1,000/1,000 V. Addtionally, the optimal condition was successfully applied for the separation of Gram positive bacteria (*i.e. B. subtilis*, *M. luteus*, and *S. aureus*).

KEY WORDS: CAPILLARY ELECTROPHORESIS/ PYRIDINE/ MICROCHIP CAPILLARY ELECTROPHORESIS/ FLUORESCENT DYE/ MICROORGANISM

178 pages

แนวโน้มใหม่ของศาสตร์ด้านการวิเคราะห์: แคปิลลารีอิเล็กโทรโฟรีซีสและไมโครชิพแคปิลลารีอิเล็กโทรโฟรีซีส
NOVEL TRENDS IN ANALYTICAL SCIENCES: CAPILLARY ELECTROPHORESIS AND MICROCHIP CAPILLARY ELECTROPHORESIS

นันทนา นุชถาวร 4937086 PYPP/ D

ปร.ด. (เภสัชเคมีและพฤกษเคมี)

คณะกรรมการที่ปรึกษาวิทยานิพนธ์ : ลีณา สุนทรสุข, Ph.D., Mirek Macka, Ph.D., นิมิต ชมนาวัง, Ph.D.

บทคัดย่อ

ปัจจุบันเทคนิคการวิเคราะห์ที่รวดเร็ว ราคาถูก และเป็นมิตรกับสิ่งแวดล้อมเป็นที่ต้องการมากขึ้น แนวทางที่สอดคล้องกับวัตถุประสงค์นี้ คือ การใช้เทคนิคแคปิลลารีอิเล็กโทรโฟรีซีสซึ่งเป็นการแยกสารภายใต้สนามไฟฟ้าได้อย่างรวดเร็ว ใช้สารตัวอย่างและตัวทำละลายน้อย และให้ประสิทธภาพในการแยกสูง นอกจากนี้ไมโครชิพแคปิลลารีอิเล็กโทรโฟรีซีสยังสามารถวิเคราะห์ได้รวดเร็วยิ่งขึ้น ใช้สารตัวอย่างและตัวทำละลายน้อยกว่า และสามารถพัฒนาเป็นเครื่องมือพกพาได้

ในการศึกษานี้มีวัตถุประสงค์ที่จะประเมินศักยภาพของเทคนิคแคปิลลารีและไมโครชิพแคปิลลารีอิเล็กโทรโฟรีซีสเพื่อการวิเคราะห์ทางเคมีและชีววิทยา ซึ่งได้พัฒนาเทคนิคแคปิลลารีอิเล็กโทรโฟรีซีสสำหรับการแยกนิโคติน โคตินิน นิโคตินาไมด์ และนิโคตินิก แอซิดในคราวเดียวกัน ในโดยใช้ไตรโพรลิดีนเป็นสารมาตรฐานภายใน สภาวะที่เหมาะสม ได้แก่ โซเดียมไดไฮโดรเจนฟอสเฟต 25 มิลลิโมลาร์ที่พีเอช 2.1 แคปิลลารียาว 64.5 เซนติเมตร, เส้นผ่าศูนย์กลางภายใน 50 ไมโครเมตร (ขยายส่วนที่แสงผ่าน), ฉีดสารด้วยแรงดัน 50 มิลลิบาร์ 10 วินาที และ ความต่างศักย์ไฟฟ้า 30 กิโลโวลต์ สภาวะดังกล่าวสามารถแยกสารได้อย่างสมบูรณ์ภายใน 10 นาที วิธีวิเคราะห์ที่ผ่านการประเมินได้ถูกนำไปประยุกต์ใช้ในการหาปริมาณของนิโคติน โคตินิน (ในสภาวะเร่งของหมากฝรั่งนิโคติน) นิโคตินาไมด์ และนิโคตินิก แอซิด ในเภสัชภัณฑ์ พบว่าปริมาณอยู่ในช่วงที่ตำรายากำหนดไว้

นอกจากนี้ได้ประเมินศักยภาพของไมโครชิพแคปิลลารีอิเล็กโทรโฟรีซีสที่ตรวจวัดด้วยฟลูออเรสเซนซ์ โดยใช้หลักการแยกสารแบบไม่ใช้น้ำอย่างง่ายและรวดเร็วในการวิเคราะห์เมทิลลีนบลู โทลูอิดีนบลู ไนล์บลู และบริลลิแอนท์เครซิลบลู ซึ่งวิเคราะห์ได้ภายใน 40 วินาที สภาวะที่เหมาะสม ได้แก่ แอมโมเนียมอะซิเตท 80 มิลลิโมลาร์ อะซิติก แอซิด 870 มิลลิโมลาร์ ในไดเมทิลซัลฟอกไซด์ จากนั้นเซลล์เดี่ยวของ *E. coli, B. subtilis, M. luteus, S. aureus, C. albicans* and *L. fungicola* ที่ย้อมด้วยไนล์บลู ถูกตรวจวัดได้ภายใน 20 วินาที ในเซทิลไตรเมทิลแอมโมเนียมโบรไมด์ 1 มิลลิกรัมต่อมิลลิลิตร ทริส/ซิตริก แอซิด 1/0.33 มิลลิโมลาร์ ที่พีเอช 7.0 เอสบี 3-10 5 มิลลิกรัมต่อมิลลิลิตร และพบว่าให้อัตราส่วนของสัญญาณต่อสัญญาณรบกวนในช่วง 26.2 – 34.0 สำหรับสภาวะที่เหมาะสมในการแยก *E. coli*, *S. aureus* and *C. albicans* ได้แก่ ทริส /บอริก แอซิด /ไดโซเดียมอีดีทีเอ 3.94/0.56/0.013 มิลลิโมลาร์ ที่พีเอช 10.5 และโพลีเอทิลลีนออกไซด์ 0.025 เปอร์เซนต์ และยังสามารถนำไปแยกแบคทีเรียแกรมบวก (*B. subtilis M. luteus* และ *S. aureus*)ได้

178 หน้า

CONTENTS

CONTENTS (cont.)

CONTENTS (cont.)

CONTENTS (cont.)

LIST OF TABLES

LIST OF TABLES (cont.)

LIST OF FIGURES

LIST OF FIGURES (cont.)

LIST OF FIGURES (cont.)

LIST OF FIGURES (cont.)

LIST OF ABBREVIATIONS

ACN	acetonitrile
AR	analytical grade
AVG	average
APCI	atmospheric pressure chemical ionization
BC	brilliant cresyl blue
BGE	background electrolyte
BP	British Pharmacopoeia
CE	capillary electrophoresis
CZE	capillary zone electrophoresis
CEC	capillary electrochromatography
CGE	capillary gel electrophoresis
CIEF	capillary electrophoretic focusing
CITP	isotechophoretic
cm	centimeter
COT	cotinine
DAD	photodiode array detector
EOF	electroosmotic flow
ESI	electrospray ionization
FIA	flow injection analysis
g	gram
GC	gas chromatography
h	hour
HPLC	high performance liquid chromatography
i.d.	inner diameter
I.S.	internal standard
kV	kilovoltage

LIST OF ABBREVIATIONS (cont.)

l	effective length of capillary
L	total length of capillary
LC	liquid chromatography
LED	Light emitting diode
LIF	Laser induced fluorescence
LOD	limit of detection
LOQ	limit of quantitation
M	molarity
MB	methylene blue
MEKC	micellar electrokinetic chromatography
MeOH	methanol
mg	milligram
min	minute
mL	millimeter
mm	millimeter
mM	milimolar
MS	mass spectrometry
N	number of theoretical plates
NA	nicotinic acid
NACE	non aqueous capillary electrophoresis
NaOH	sodium hydroxide
NIC	nicotine
nm	nanometer
nM	nanomolar
NM	nicotinamide
o.d.	external diameter
PDMS	poly(dimethylsiloxane)

LIST OF ABBREVIATIONS (cont.)

PETG	polyethylenephthalate
PI	polyimide
pH	negative logarithm of hydrogen ion concentration
pL	picoliter
PMMA	polymethyl methacrylate
ppm	part per million
psi	pound per square inch
q	charge of the molecule
r	ion radius
r^2	coefficient of determination
R_s	resolution
RSD	relative standard deviation
s	second
SD	standard deviation
SDS	sodium dodecyl sulfate
SP	system peak
TB	toluidine blue
TF	tailing factor
TLC	thin layer chromatography
$t_{I.S.}$	Migration time of internal standard
t_m	migration time
t_r	relative migration time
USP	United State Pharmacopeia
UV	ultraviolet
V	volt
ν_{ep}	velocity of anlayte
v/v	volume by volume

LIST OF ABBREVIATIONS (cont.)

W/m·K	watts per meter kelvin
°C	degree celcius
μ_a	apparent mobility of the analyte
μ_e	electrophoretic mobility
µg	microgram
µm	micrometer
µM	micromolar
η	viscosity of BGE
ξ	zeta potential

PART I: CAPILLARY ELECTROPHORESIS OF BIOLOGICALLY ACTIVE PYRIDINES

CHAPTER I
INTRODUCTION

Pyridine is a heterocyclic aromatic organic compound which presents in many biologically active substances including nicotine (NIC), cotinine (COT), nicotinic acid (NA) and nicotinamide (NM). NIC is a major alkaloid present in tobacco, which accounts for 98% of the total alkaloids (1-2) and is the main known addictive component of tobacco smoke (3-6). It is also the most frequently determined compound as a biomarker of tobacco exposure in both smokers and non-smokers exposed to environmental tobacco smoke (ETS). The relatively short plasma half-life of nicotine (t½ ~ 2.3 h) (7) and large inter-individual differences in the extent of nicotine metabolism precludes its uses as a single accurate marker of nicotine uptake from cigarette smoke. NIC is metabolized to more than 20 different derivatives, among them, COT is a primary metabolite (70-80%) with similar structure to NIC (2). COT has a longer plasma half-life of about 17 h and it has been assumed to be a better biochemical measurement of nicotine uptake in smokers and non-smokers. NIC and COT are frequently used as biomarkers of tobacco exposure, which appear in different human biological fluids and matrices. Additionally, NIC has been added to pharmaceutical formulations including chewing gums, spray, inhaler and beverages as smoke cessation products. Moreover, nicotine in chewing gum can lead to cotinine and further myosmine by the thermal and oxidative degradation (8). Therefore, detection of tobacco alkaloids especially for nicotine content and its oxidized compound (COT) content is obvious interest for both pharmaceutical and food industries in order to regulate commercially by nicotine-related products. The United States Pharmacopeia (USP) and British Pharmacopoeia (BP) recommend non-aqueous titration for the assay of NIC in raw material (9-10), whereas high performance liquid chromatography (HPLC) is for assay of NIC in gum (9). Additionally, analyses of NIC and COT in different matrices by several methods have been described in literatures, such as HPLC (11-18), gas chromatography (GC) (19-26) and capillary electrophoresis (CE) (1, 27-33). Most of these works focused on the analyses of NIC, its related alkaloids

and metabolites in biological samples (e.g. urine, plasma, saliva, brain tissue, human milk, hair, vegetables and food products), tobacco or cigarette smoke (4-5, 11-31). Thus, sample pre-treatment (e.g. liquid-liquid extraction, solid phase extraction (SPE), solid phase microextraction (SPME), microdialysis or cloud point extraction) and sensitive detectors such as mass spectrometer (MS), tandem MS and light emitted diode induced fluorescence are required to enable the detection of NIC and its derivatives in trace amounts. A few papers described the analysis of NIC in bulk material, extended and immediate release dosage forms (6) and the analysis of five NIC related alkaloids in chewing gums, beverage and tobacco (1).

Nicotinic acid (niacin, NA) and nicotinamide (niacinamide, NM) belong to vitamin B group, which are water-soluble vitamins (34-35). NA and NM are structurally related with a carboxylic or a carboxamide functional group respectively bounded on a pyridine ring (35). They are well–known precursors in the synthesis of the several co-enzymes, which involve in cell metabolism such as nicotinamide adenine dinucleotide (NAD) and nicotinamide adenine dinucleotide phosphate (NADP). Deficiency of these vitamins causes inflammation of mucus membranes and illness known as pellagra (36). In addition, NA is clinically used for treatment of dyslipidemia, which favorably affects all of the lipoprotein risk factors in atherosclerotic diseases (37-40). Therefore, determination of NA and NM in supplements, nutraceuticals and pharmaceuticals becomes necessary from pharmacological and pharmaceutical aspects. The USP suggests spectrophotometry for assay of NA in raw material and injection and HPLC for assay of NA in tablets, NM in raw material, injection and tablets (9). BP recommends aqueous titration for assay of NA in raw material and tablets and non-aqueous titration for assay of NM in raw material (10). Previous works on analyses of NA and NM by several analytical methods have been reported including spectrophotometry (41), voltammetry (42), HPLC (35, 38, 43-46) and CE (34, 47-49). HPLC with UV and diode array detectors (DAD) were mainly used for determination of NA and NM in multivitamin preparations, whereas SPE coupled with MS was employed for detection of both pyridines in industrial effluent (35) and in plasma (38, 43, 45-46).

Because of the related structures of NIC, COT, NA and NM, it is very interesting to establish a fast, simple and cost effective method for the analysis of

these compounds. Among several methods, CE has a high potential due to its advantages in terms of applicability for a wide range of compounds, high separation efficiency, simplicity, low solvent consumption and short analysis time. Therefore, this work aimed to develop a common capillary zone electrophoresis (CZE) method for the separation of NIC, COT, NA and NM and to apply the method for the analysis of these analytes in pharmaceutical formulations.

Optimization was performed by varying types of background electrolytes (BGEs), pH of BGEs, BGE concentration, applied voltage and injection time. The influence of BGE types (i.e. citric acid and sodium dihydrogen phosphate) was evaluated and sodium dihydrogen phosphate was chosen for further optimization on pH of 1.9-3.5 and concentration of 15-30 mM. The applied voltage was varied from 20 to 30 kV and the injection volume was optimized by varying the injection time from 5 to 20 s at 50 mbar. Resolution, percent relative standard deviation (RSD) of migration time, tailing factor and number of theoretical plate were used to determine the optimum condition. The analysis of biologically active pyridine was performed on the optimum condition of 25 mM sodium dihydrogenphosphate pH 2.1, the separation voltage at +30 kV, temperature 25°C in a fused silica capillary with a total length (L_{total}) of 64.5 cm, an effective length (L_{eff}) of 56 cm and an inner diameter of 50 μm i.d. (extended pathlength). Method validation was evaluated in term of linearity, recoveries, inter-day, intra-day and injection precision, limit of detection and limit of quantitation. Finally, this developed method was applied for the determination of NIC, COT, NA and NM in pharmaceutical formulations and COT in stability studies of NIC gum.

CHAPTER II
LITERATURE REVIEW

1. Biologically active pyridines

Pyridines are heterocyclic aromatic organic compounds, which present in many biologically active substances including nicotine (NIC), cotinine (COT), nicotinic acid (NA) and nicotinamide (NM) (Figure 2.1). NIC is the major alkaloid present in tobacco, which accounts for 98% of the total alkaloids (2) and the main known addictive component of tobacco smoke (2, 5-6). NIC is metabolized to more than 20 different derivatives, among them, COT is a primary metabolite (70-80%) with similar structure to NIC (2, 7) (Figure 2.2). NIC and COT are frequently used as biomarkers of tobacco exposure in both smokers and non-smokers exposed to environmental tobacco smoke (ETS), which are important in evaluating the risk of cancer (50-51). Additionally, NIC has been added to pharmaceutical formulations including chewing gums, spray, inhaler and beverages as smoke cessation products.

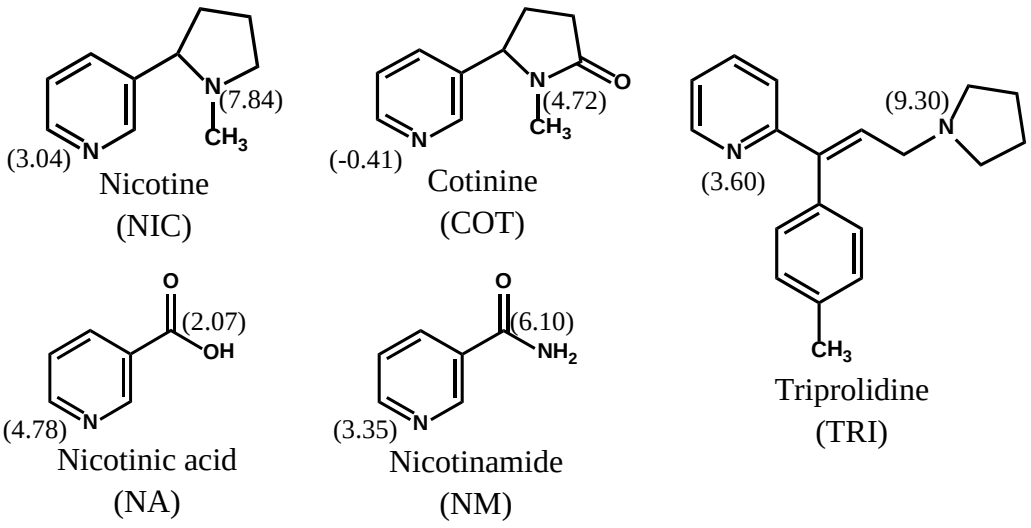

Figure 2.1 Structures of nicotine, cotinine, nicotinic acid, nicotinamide and triprolidine (as internal standard). Number in parentheses indicate pK_a of the compounds (32, 51-54).

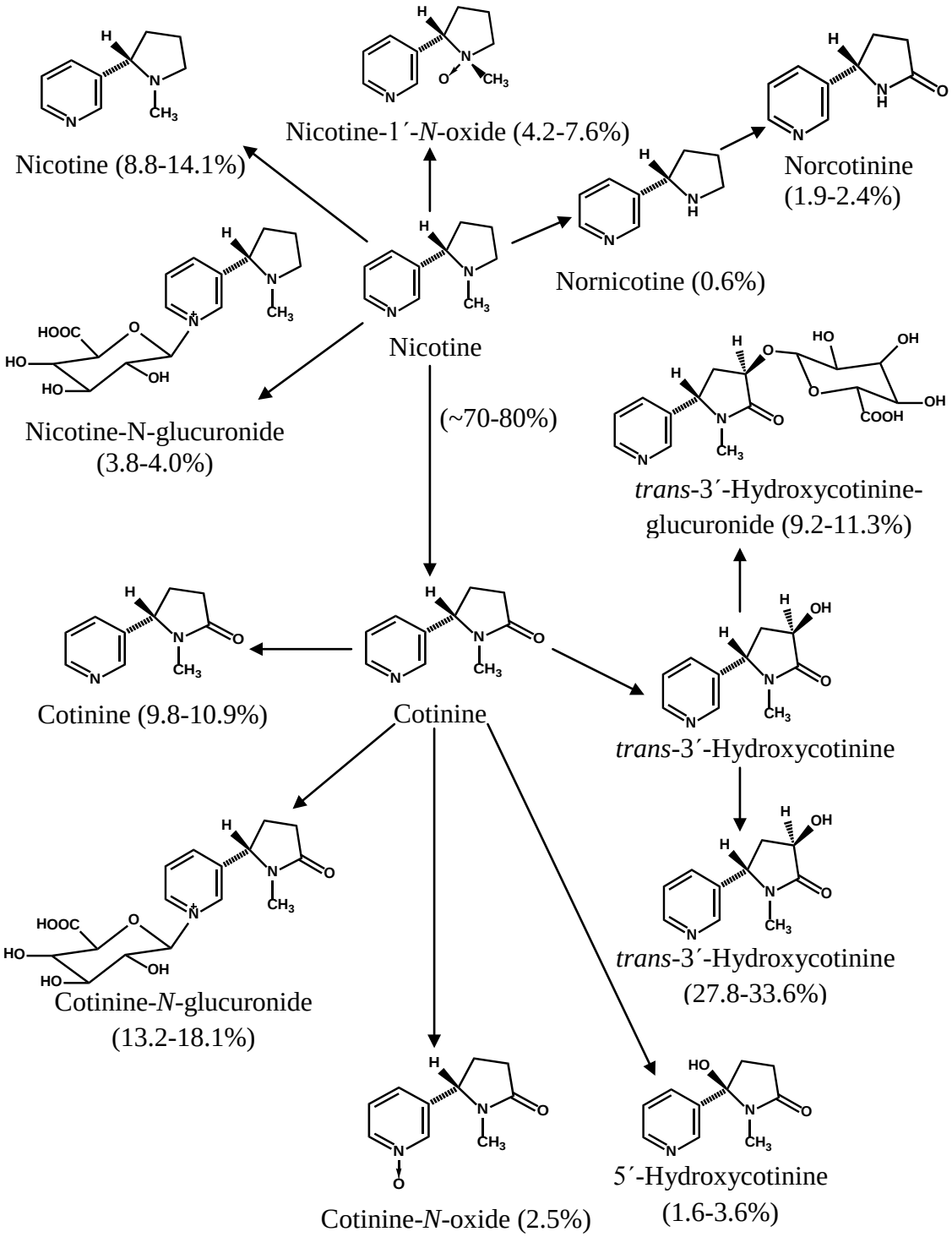

Figure 2.2 Quantitative scheme of nicotine metabolism, based on average excretion of metabolites as percentages of total urinary nicotine which present in parentheses. Nicotine, cotinine and trans-3′-hydroxycotinine detected in blood and other compounds indicate major metabolites excreted in urine (7, 55-57).

Nicotinic acid (niacin, NA) and nicotinamide (niacinamide, NM), are structurally related with a carboxylic or a carboxamide functional group respectively bounded on a pyridine ring (Figure 2.1). NA and NM belong to vitamin B group, which are water-soluble vitamins (35, 46). They are well–known precursors in the synthesis of the several co-enzymes, which involve in cell metabolism such as nicotinamide adenine dinucleotide (NAD) and nicotinamide adenine dinucleotide phosphate (NADP) involved in cell metabolism. Deficiency of these vitamins causes inflammation of mucus membranes and illness known as pellagra (38). In addition, NA is clinically used for treatment of dyslipidemia, which favorably affects all of the lipoprotein risk factors in atherosclerotic diseases (37).

2. Determination of biologically active pyridines

The detection of NIC content is important for both pharmaceutical and food industries in order to regulate commercial nicotine-related products. The United States Pharmacopeia (USP) and British Pharmacopoeia (BP) recommend non-aqueous titration for the assay of NIC in raw material (9-10), whereas high-performance liquid chromatography (HPLC) is for assay of NIC in gum (9). Additionally, analyses of NIC and COT in different matrices by several methods have been described in literatures, such as gas chromatography (GC) (19-20, 22-26, 58-64), HPLC (2, 11-18, 35, 38, 43, 65-83) and capillary electrophoresis (CE) (1, 27-32, 84-85). Most of these works focused on the analyses of NIC, its related alkaloids and metabolites in biological samples (e.g. urine, plasma, saliva, brain tissue, human milk and hair), vegetables, food products, tobacco or cigarette smoke (2, 5, 11-20, 22-24, 26-31, 58-59). Thus, sample pre-treatment (e.g. liquid-liquid extraction, liquid phase microextraction (LPME), solid phase extraction (SPE), solid phase microextraction (SPME), single-drop microextraction (SDME), microdialysis or cloud point extraction (CPE)) and sensitive detectors such as mass spectrometer (MS), tandem MS and light emitted diode induced fluorescence are required to enable the detection of NIC and its derivatives in trace amounts. A few literatures described the analysis of NIC in bulk material, extended and immediate release dosage forms (6) and the analysis of NIC and its related alkaloids in chewing gums, beverage and tobacco (1, 8).

Determination of NA and NM in supplements, nutraceuticals and pharmaceuticals becomes necessary from pharmacological and pharmaceutical aspects. The USP suggests spectrophotometry for assay of NA in raw material and injection and HPLC for assay of NA in tablets, NM in raw material, injection and tablets (9). BP recommends aqueous titration for assay of NA in raw material and tablets and non-aqueous titration for assay of NM in raw material (10). Previous works on analyses of NA and NM by HPLC have been reported (35, 38, 43-46). UV and diode array detectors (DAD) were mainly used for determination of NA and NM in multivitamin preparations, whereas SPE coupled with MS was employed for detection of both pyridines in industrial effluent (35) and in plasma (38, 43, 45-46).

Table 2.1 - 2.4 show the analytical methods that have been reported for the determination of the investigated pyridines.

Table 2.1 GC methods for the determination of the investigated pyridines

Method	Analyte	Sample	Significant finding	Reference
GC - nitrogen detection	• COT	• Saliva	• Linearity range 3.8 - 1,200 ng/mL • LOD 0.9 ng/mL • LOQ 3.8 ng/mL	(60)
GC - flame - ionization detection (FID)	• NA • NM	• β-picoline oxidation reaction	• Linearity range 0.15 – 6.22 µg/mL • LOD 0.15 - 0.37 µg/mL • RSDs = 0.6 -20 %	(61)
SDME - GC - FID	• NIC • COT • Anabasine	• Urine • Saliva	• Linearity range - NIC 0.5 - 25 mg/L - COT 0.5 - 45 mg/L - Anabasine 0.5 - 65 mg/L • LOD 0.33 - 0.45 mg/L • RSDs = 1.3 - 9.2 % • Recoveries = 71.2 - 111.0%	(59)

Table 2.1 (continued) GC methods for the determination of the investigated pyridines

Method	Analyte	Sample	Significant finding	Reference
GC-MS	• NIC	• Hair	• Linearity range 0.04 - 200 ng/mg, $r^2 > 0.9950$ • LOQ 0.04 ng/mg • RSDs = 0.7 - 11.3% • Recoveries = 92.6%	(23)
GC-MS	• COT	• Urine	• Linearity range 5 - 5,000 ng/mL, $r^2 = 0.9954$ • LOD 0.8 ng/mL	(62)
GC-MS	• NIC • Nornicotine • Myosmine • Anabasine • Nicotyrine • Anatabine	• Tobacco	• LOD 7.1 µg/g • RSDs = 2.77 - 9.97 % • Recoveries = 80.4 %	(26)

Table 2.1 (continued) GC methods for the determination of the investigated pyridines

Method	Analyte	Sample	Significant finding	Reference
GC-MS	• NIC • COT	• Hair	• LOD - NIC 0.04 ng/mg - COT 0.033 ng/mg	(63)
SPME-GC-MS	• NIC • COT	• Urine	• Linearity range 1 -500 µg/L, r^2 > 0.9998 • LOD 0.9 - 1.1 µg/L • RSDs < 9.0 % • Recoveries = 90.0 – 99.0 %	(58)
SMPE-GC-MS	• NIC • Benzene • Toluene • o, m, p-Xylene • Pyridine • Limonene • Naphthalene	• Mainstream and sidestream smoke	• Linearity range 4.17–133.40 µg/mL, r^2 = 0.9910	(64)

Table 2.1 (continued) GC methods for the determination of the investigated pyridines

Method	Analyte	Sample	Significant finding	Reference
LPME-GC-MS	• NIC	• Vegetables • Food products	• Linearity range 2.0 – 100.0 ng/g, r^2 > 0.9980 • LOD 0.2 - 0.5 ng/g • RSDs = 2.3 - 4.5 %	(19)
CPE-GC-MS	• NIC • Other six minor alkaloids	• Tobacco	• LOD = 7.1 µg/g • RSDs = 2.77 - 9.97 % • Recoveries = 80.4 %	(26)

Table 2.2 HPLC methods for the determination of the investigated pyridines

Method	Analyte	Sample	Significant finding	Reference
HPLC - UV	• NIC	• Saliva	• Linearity range 0.1 - 50 mg/L, r^2 = 0.9996 • LOD 0.05 mg/L • Recoveries 96.3 - 102.2% • RSDs < 5%	(17)
SPE - HPLC -UV	• COT	• Urine	• Linearity range 10 - 500 ng/mL, r^2 = 0.9980 • Recoveries 75.0 – 91.0 % • RSDs < 10.5 %	(65)
SPE - HPLC -DAD	• NIC • COT • Other eleven plant alkaloids	• Serum • Urine	• Linearity range 0.5-1,000 ng/mL, r^2 = 0.9992-0.9999 • Recoveries = 19.7- 91.7 % • LOQ 0.30 - 94 ng/mL	(66)
SPE - HPLC - DAD	• COT	• Urine	• Recoveries ≥ 80.0 % • Linearity range 0.05 - 5 µg/mL • RSDs ≤ 10.0 %	(18)

Table 2.2 (continued) HPLC methods for the determination of the investigated pyridines

Method	Analyte	Sample	Significant finding	Reference
LC - electrochemical detection	• NIC	• Chewing gum • Dermal patches • Tobacco • Serum	• Analysis time < 8 min • LOD 0.17 ng/mL • LOQ 0.4 ng/mL • Recoveries = 91.0 -109.0 % • RSDs < 1.8 %	(67)
LC - MS	• NIC • COT	• Cerebrospinal fluid	• Linearity range 1–500 ng/mL, r^2 > 0.9900 • LOD 1 ng/mL • LOQ 3 - 5 ng/mL • RSDs < 12.0 %	(68)
LC - MS	• NIC • COT	• Serum	• Linearity range 2 - 500 ng/mL, r^2 > 0.9900 • LOQ 2 - 5 ng/mL • Recoveries = 93.8 - 106.3 % • RSDs < 16.5 %	(69)

Table 2.2 (continued) HPLC methods for the determination of the investigated pyridines

Method	Analyte	Sample	Significant finding	Reference
SPE - LC - MS	• NIC • COT • *trans*-3′-Hydroxycotinine Norcotinine	• Plasma	• Linearity range 2.5 - 500 ng/mL, r^2 > 0.9980 • LOD 1.0 ng/mL • LOQ 2.5 ng/mL • Recoveries = 90.5 -109.5 % • RSDs < 15.0 %	(70)
SPME - LC - MS	• NIC • COT • Nornicotine • Anabasine • Anatabine	• Urine • Saliva	• Linearity range 0.5 – 20 ng/mL, r^2 = 0.9969 - 0.9994 • LOD 15- 40 pg/mL • RSDs < 11.3 % • Recoveries = 83.2 – 98.2 %	(2)
LC – MS - MS	• NIC • COT • Other eight metabolites	• Urine	• Linearity range 1 - 8,000 ng/mL, r^2 > 0.9980 • Recoveries = 78.4 - 115.6% • RSDs = 2.1 - 17.0%	(71)

Table 2.2 (continued) HPLC methods for the determination of the investigated pyridines

Method	Analyte	Sample	Significant finding	Reference
LC - MS - MS	• NIC • COT • *trans*-3-Hydroxycotinine • Opiates • Benzoylegonine	• Human fetal postmortem brain	• Linearity range 5 - 5,000 pg/mg, r^2 = 0.9979 - 0.9996 • Recoveries ≥ 92% • RSDs ≤ 14% • Extraction efficiencies ≥ 67.2%	(16)
LC - MS -MS	• NIC • COT • *trans*-3-Hydroxycotinine • NIC - *N′*-oxide • COT- *N′*- oxide	• Urine	• Linearity range 10 – 10,000 ng/mL, r^2 > 0.9500 • LOQ 10 ng/mL • Extraction efficiencies = 70.4 - 100.4 % • Recoveries = 89.6 – 109.1 % • RSDs < 10.0 %	(72)
LC - MS -MS	• COT • *trans* - 3′ - Hydroxycotinine	• Plasma • Urine • Saliva	• LOQ 0.02 - 0.1 ng/mL • Recoveries = 96.3 - 106 % • RSDs = 0.79 - 22 %	(73)

Table 2.2 (continued) HPLC methods for the determination of the investigated pyridines

Method	Analyte	Sample	Significant finding	Reference
LC - MS - MS	• NIC • COT • *trans* - 3′ - Hydroxycotinine • Buprenorphine • Methadone • Cocaine • Opiates	• Oral fluid	• Linearity range 1 - 500 µg/L, r^2 > 0.9940 • LOD 0.2 -0.8 µg/L • LOQ 0.5 - 1 µg/L • RSDs < 13% • Recoveries = 92.0 – 114.0 % • Extraction efficiencies > 77%	(74)
LC - MS - MS	• NIC • COT • *trans* - 3′ - Hydroxycotinine • Norcotinine	• Plasma	• Linearity range 1 - 500 ng/mL, $r^2 \geq 0.9983$ • Recoveries = 101.9 - 116.8% • RSDs < 11.0 % • Extraction efficiencies ≥ 70 %	(14)

Table 2.2 (continued) HPLC methods for the determination of the investigated pyridines

Method	Analyte	Sample	Significant finding	Reference
SPE - LC - MS - MS	• NIC • COT • Other seven metabolites • Two minor tobacco alkaloids	• Plasma • Urine	• LOQ 1.0 -2.5 ng/mL • Recoveries = 51.0 – 118.0 % • RSDs ≤17%	(12)
HPLC - DAD	• Vitamin B_1, B_2, B_5, B_6, B_9 and C • NA • Biotin	• Urine	• r^2 = 0.9270 - 0.9650	(75)
HPLC - DAD	• Vitamin B1, B2, B5, B6 and C • NM • Methyl paraben • Sodium benzoate	• Multivitamin syrup	• Linearity range 6 - 3,004 µg/mL, r^2 > 0.9950 • Recoveries = 97.5 - 100.6 % • LOD 0.1 - 0.7 µg/mL • LOQ 0.3 - 2.3 µg/mL	(76)

Table 2.2 (continued) HPLC methods for the determination of the investigated pyridines

Method	Analyte	Sample	Significant finding	Reference
HPLC - DAD	• NA • NM • 3-Cyanopyridine	• Industrial effluent	• LOD 0.70 - 1.18 mg/L • Recoveries = 87.0 – 102.0 % • Precision (RSDs) - Intra-day = 0.9-3.9 % - Inter-day = 1.2-5.6 %	(35)
HPLC - DAD	• Nicorandril • NA • Nitrate nicorandil • De-nitrated nicorandil	• Raw material • Tablets	• Linearity range 0.02 – 21.76 mg/L, r^2 = 0.9984 – 0.9998 • LOD 0.01 – 0.03 mg/L	(77)
HPLC - DAD and fluorescence detection	• Vitamin B_1, B_2, B_5, B_9, B_{12} and C • NA	• Milk products	• Linearity range 0.01 - 150 mg/kg, $r^2 \geq$ 0.9984 • LOQ 0.01 - 2.49 mg/kg • Recoveries = 90.0 - 100.0 % • RSDs = 0.5 - 3.7%	(78)

Table 2.2 (continued) HPLC methods for the determination of the investigated pyridines

Method	Analyte	Sample	Significant finding	Reference
Hydrophilic interaction liquid - chromatography (HILIC) - DAD	• Vitamin B_1, B_2 B_6, B_9, B_{12} and C • NA • NM	• Pharmaceutical formulation • Energy drink	• Linearity range 0.025 – 10 µg/mL, r^2 = 0.9933 - 0.9999 • LOD 0.005 - 0.3 µg/mL • RSDs = 0.38 - 2.9 %	(79)
HPLC - DAD -MS	• NA • NM • 6 - Hydroxynicotinic acid • 2 - Hydroxynicotinic acid	• Pear and apple blossoms	• LOD 4.0 - 14.8 µg/L • LOQ 13.2 - 49.4 µg/L • Recoveries = 50.7 - 94.1 %	(80)
LC - MS - MS	• NA • NM • Trigonelline • Pyridine derivatives	• Plasma • Urine • Coffee brew	• Linearity range 10 - 1,000 nM, $r^2 \geq$ 0.9950 • Recoveries = 92.4 - 113.0 % • RSDs = 4.9 - 11.9 %	(43)

Table 2.2 (continued) HPLC methods for the determination of the investigated pyridines

Method	Analyte	Sample	Significant finding	Reference
LC - MS - MS	• Vitamin B_1, B_2 B_6, B_8, B_9, B_{12} and C • NA • NM	• Multivitamin tablets	• Linearity range 0.01 - 50 mg/L, r^2 = 0.9963 -0.9999 • LOD 1 - 10 µg/L • LOQ 5 - 20 µg/L • Recoveries = 98.3 – 101.5 % • RSDs = 0.3 - 3.4 %	(81)
LC – MS - MS	• NA	• Plasma	• Linearity range 0.05 - 20 µg/mL, r^2 > 0.9900 • RSDs < 18%	(82)
LC - MS - MS	• NA • NM • Trigonelline	• Foods • Urine • Plasma	• Recoveries = 98.5 – 104.5 % • RSDs = 1.1 - 3.1 %	(83)
LC - MS - MS	• NA • NM • Other three NA metabolites	• Rat plasma	• Linearity range 10 - 2,000 ng/mL • Recoveries = 94.4 - 110.9 % • RSDs = 1.3 - 13.3 %	(38)

Table 2.3 CE methods for the determination of the investigated pyridines

Method	Analyte	Sample	Significant finding	Reference
CE-DAD	• Vitamin B_1, B_2, B_6, B_9, B_{12}, C • NA • NM • Calcium pantothenate • Biotin	• Corns	• Linearity range 1 - 40 µg/mL, r^2 = 0.9928 - 0.9999 • Recoveries = 90.0-96.0%, RSDs < 5.2%	(84)
CE-DAD	• NM • NA • Isonicotinic acid • Vitamin B_6	• Standard compounds	• α -Cyclodextrin and 2-hydroxypropyl- α -cyclodextrin form weak 1:1 complexes with NA and isonicotinic acids in aqueous media at 298.15 K, while β -cyclodextrin and its derivative did not form complexes.	(32)
CE-UV	• NA • Isonicotinic acid • Picolinic acid	• Standard compounds	• RSDs = 0.32 - 2.60%	(85)

Table 2.4 Miscellaneous methods for the determination of the investigated pyridines

Method	Analyte	Sample	Significant finding	Reference
SPE-spectrophotometry	• NIC • COT • Anabasine • Norcotinine • Caffeine	• Urine	• Linearity range 1.1 - 60 µM, r^2 > 0.9980 • LOQ 1.1 µM • Precision (RSDs) - Intra-day = 4-10% - Inter-day = 5-13%	(86)
Spectrofluorometry	• NIC	• Cigarettes	• Linearity range 0.2 - 8.0 µg/mL, r^2 = 0.9957 • LOD 0.05 µg/mL	(87)
Flow injection analysis-electroluminescence	• NIC	• Cigarettes	• Linearity range 2 - 100 µM, r^2= 0.9972 • LOD 1.2 nM • Recoveries = 94.0% • RSDs = 1.4%	(88)
Voltammetry	• NIC	• Tobacco samples	• LOD 0.2 µM • Linearity range 0.4 - 33.0 µM • Recoveries = 99.0 - 102.0 %	(89)

Table 2.4 (continued) Miscellaneous methods for the determination of the investigated pyridines

Method	Analyte	Sample	Significant finding	Reference
Voltammetry	• NIC	• Cigarettes	• Linearity range 7.6 - 107.5 µM, r^2= 0.9994 • LOD 2.0 µM • Recoveries = 96.1- 98.7%	(90)
ELISA	• COT	• Urine • Serum	• Linearity range 3 - 5000 ng/mL • Recoveries 88.56 - 100.59% • RSDs < 8.7%	(91)
Voltammetry	• NA	• Food stuffs	• Linearity range 0.45 µM - 0.8 mM, r^2 = 0.9990 (±0.014) • LOD 0.14 µM	(92)
Voltammetry	• NA • NM	• Pharmaceutical preparation (tablets)	• Linearity range 2.7 µM - 2.4 mM • LOD 0.27 - 0.33 µM	(93)

3. Capillary electrophoresis

Electrophoretic separation technique is based on mobility differences of the analytes in an electric field. When the voltage is applied, the charged species move toward the electrode of opposite charge. The velocities of the migrating species also depend on the size and mass-to-charge ratio of species and their environmental. Electrophoresis has been performed on a support medium such as a semisolid slab gel, paper or cellulose acetate. Capillary electrophoresis (CE) (Figure 2.3) has emerged as an alternative, which the capillary wall provides the mechanical stability for the carrier electrolyte (94). Fused silica capillaries employed in CE typically have internal diameters (i.d.) of 20 to 100 µm with outer diameter (o.d.) of 375 µm, lengths from 20 to 100 cm and are externally coated with polymeric polyimide, which imparts flexibility to the capillary that would be very fragile (95). CE incorporates all of eletcrophoretic modes that are performed in the capillary. These are capillary zone electrophoresis (CZE), micellar electrokinetic chromatography (MEKC), capillary electrochromatography (CEC), capillary gel electrophoresis (CGE), and non-aqueous CE (NACE). Furthermore, CE has been coupled to a wide variety of detection scheme including optical (absorbance and fluorescence), electrochemical detection and mass spectrometry (MS).

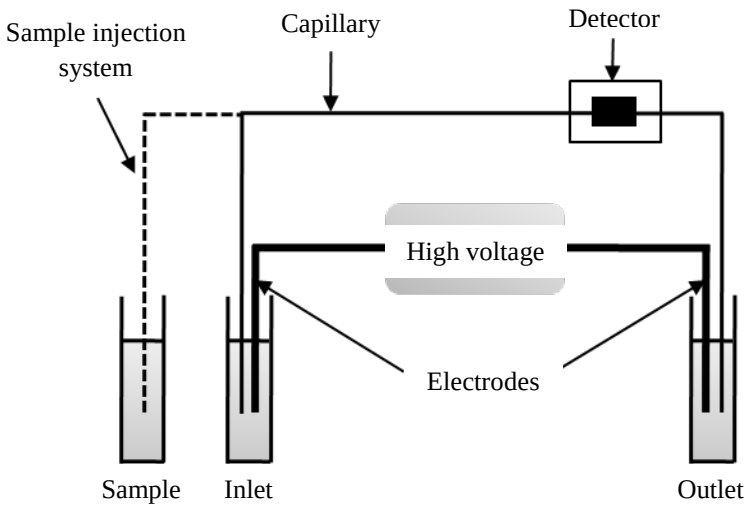

Figure 2.3 Typical CE instrumentation

3.1 Principle of CE

The CE separation is based on the different ion velocities in background electrolyte (BGE) under an applied electric field. The electric field (E) is given by equation (2.1). The migration velocity of a particular species depends on its mobility and the electric field which can be calculated by given equation (2.2).

$$E = V/L \quad (2.1)$$

Where V = the voltage applied

L = the capillary length

$$v = \mu_e E = \mu_e V/L \quad (2.2)$$

Where v = ion velocity

μ_e = electrophoretic mobility

E = applied electric field (volts/cm)

At the constant applied electric field (E), the ion mobility is influenced by electrophoretic mobility of ions (94).

3.1.1 Electrophoretic mobility

The migration of charge species under an applied electrical field is characterized by its electrophoretic mobility (μ_e) which has units of $cm^2sec^{-1}V^{-1}$.

μ_e of a charge species can be approximated from the Dabye-Huckel-Henry theory (94),

$$\mu_e = q/6\pi\eta r \quad (2.3)$$

Where q = the charge on the particle

η = the viscosity of the BGE

r = the Strokes' radius of the particle

From equation (2.3), the electrophoretic mobility depends on charge density, viscosity of electrolyte and ion radius. In the presence of an electroosmotic flow (EOF) mobility, an apparent mobility (μ_{app}) is a sum of μ_e and the mobility of EOF (μ_{eo}) which can be calculated by the equation (2.4) and (2.5).

$$\mu_{app} = \mu_e + \mu_{eo} \quad (2.4)$$

The μ_{eo} can be measured using a neutral marker that moves at a velocity equal to the EOF.

$$\mu_{app} = lL/\ tV \quad (2.5)$$

Where l = effective capillary length (cm)

L = total capillary length (cm)

t = the migration time (s)

V = the applied voltage (volt)

3.1.2 Electroosmotic flow (EOF)

EOF occurs in fused silica capillaries because silanol groups (SiOH) at the inner surface of the capillary dissociate when in contact with an electrolyte solution. The ionized silanol groups (SiO^-) impart a layer of negative charge to the capillary wall attract hydrated cations from the electrolyte solution and then arranged into two layer (Figure 2.4). The ionic layer has a positive charge density that decreases exponentially as the distance from the wall increases. The double layer formed closet to the surface is termed the Stern layer and is static. A more diffuse layer form distal to Stern layer is termed the outer Helmholtz plane (OHP). Cations in the OHP carry water which led to the net movement toward the cathode under an applied field. This EOF or bulk flow has a flat flow resulting in the low dispersion of sample zone due to the uniform distribution of the electrical force along the capillary and acts as a pumping mechanism to propel all molecules (cationic, neutral and anionic) in the direction of the detector with separation eventually being determined by differences in the electrophoretic migration of the individual analytes. Neutral analytes migrate with EOF, cations migrate faster and anions migrate slower than EOF therefore it is useful for characterization of sample component. The EOF is dependent on a number of parameters including pH and ionic strength. An increase in EOF is led by increasing of pH, however, the increase of the ionic strength undergoes a decrease of EOF (96).

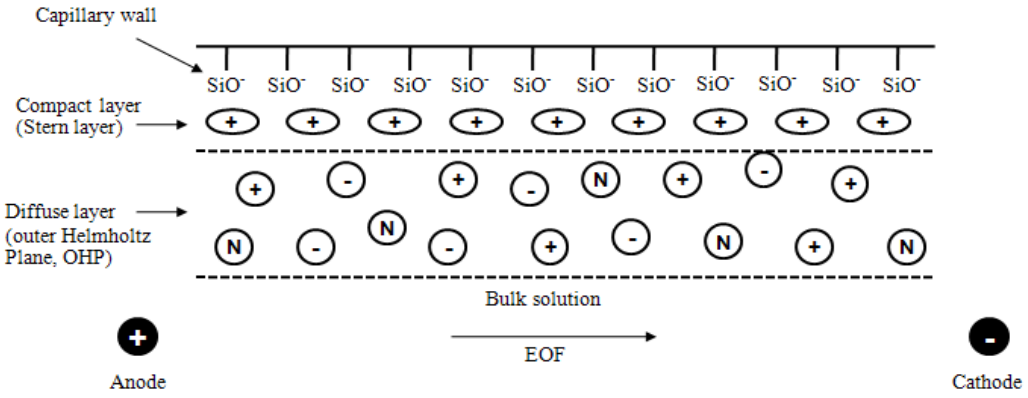

Figure 2.4 Electrical double layer at the ionized silica capillary wall and illustration of EOF

3.2 Separation modes in CE

3.2.1 Capillary zone electrophoresis (CZE)

CZE also known as free-solution CE (FSCE), is the most simple and widely used mode in CE. The separation mechanism is based on differences in the charge-to-mass ratio of the analytes and relies principally on the pH controlled dissociation of acidic groups or the protonation of basic functions on the solute. Analytes migrate in the discrete zone with the differences in their electrophoretic mobilities. Neutral analytes are carried along by the EOF with un resolved peak but cations and anions can be separated from EOF with the higher and lower mobilities than EOF (94).

3.2.2 Capillary gel electrophoresis (CGE)

CGE is the adaptation of traditional gel electrophoresis into the capillary using gel or viscous polymers to create a molecular sieve. This allows analytes having similar charge-to-mass ratios to be resolved by size. Large molecules are restricted and their velocities reduced but small molecules can pass through the pores. This technique is commonly employed in the separation of macromolecules such as proteins and nucleic acids (94).

3.2.3 Capillary isoelectric focusing (cIEF)

cIEF allows amphoteric molecules, such as peptides and proteins, to be separated by electrophoresis in a pH gradient which is generated between the cathode and anode by the use of carrier ampholytes. Analyte will migrate

to a point where its net charge is zero. At the analyte isoelectric point (pI), migration stops and the sample is focused into a tight zone. This technique is commonly employed in protein characterization as a mechanism to determine a protein's isoelectric point (94, 96).

3.2.4 Capillary isotachophoresis (cITP)

cITP is a focusing technique based on the migration of the sample components between leading and terminating electrolytes. During electrophoresis separation, analytes having mobilities intermediate to those of the leading and terminating electrolytes stack into discrete zones. All analytes migrate in order of a decreasing mobility and a decreasing stepwise of conductivity versus time is recorded. The length of the analyte zone is a quantitative parameter relating to the concentration of analyte. The height of the step is qualitative parameter which is characteristic of the analyte and it is directly proportional to analyte mobility. cITP is used as a mode of separation for anions or cations, but not both simultaneously (94, 97).

3.2.5 Micellar electrokinetic chromatography (MEKC)

MEKC is similar to CZE which is performed with an addition of surfactants (micelles) at a higher concentration than its critical micelle concentration (CMC) to an electrophoretic medium. Analyte distribute between the micelle and the surrounding aqueous phase and has an apparent charge, which can be subject to electrophoretic separation. The migration velocity of the neutral analyte in MEKC depends on what portion of the analyte is incorporated into the micelle. Micelles work as pseudo-stationary phase corresponding to the stationary phase in chromatography (98-99). Hence, MEKC is an effective alternative to LC technique and have become capable technique to analyze samples containing mixtures of charged and neutral analytes (99).

3.2.6 Microemulsion electrokinetic chromatography (MEEKC)

MEEKC is similar to MEKC except microemulsion is used as a pseudo-stationary phase instead of micelle. The separation of analytes is based on both their partition with microemulsion droplets and electrophoretic mobilities. The microemulsion droplets are usually formed by sonicating immicible organic solvent (heptanes or octane) with water. Surfactant is added at relatively high concentration to

stabilize the emulsion. This allows the separation of both hydrophilic and hydrophobic compounds and is used effectively as generic method to analyze a broad range of pharmaceuticals (100).

3.2.7 Non-aqueous CE (NACE)

NACE involves the separation of analytes in a medium composed of organic solvents. The physical and chemical properties of organic solvent are very different from each other and from water allowing the important characteristics of separations to be controlled on a wider scale than with water alone. The viscosity and dielectric constants of organic solvents affect both analyte mobility and the level of EOF. Solvent properties affect the acid-base behavior of analytes with pK_a values can differ up to many orders of magnitude. The use of non-aqueous medium allows enormous variations in electrophoretic mobilities and separations are not possible in aqueous CE can be performed with excellent selectivites. A further benefit of NACE is the increased solubility of hydrophobic compounds which extends the applicability of CE. Moreover, non-aqueous solvents are also fully compatible and even sometimes more appropriate than water, with most of the detectors hyphenated with CE (101).

3.2.8 Capillary electrochromatography (CEC)

CEC is a hybrid separation method that couples the high separation efficiency of CZE with HPLC and uses an electric field acting as electropump rather than pressure to propel the mobile phase through a packed stationary phase. Because there is minimal backpressure, it is possible to use small-diameter packings and achieve very high efficiencies. The separation mechanism is based on both the electrophoretic mobility of the analytes and the nature of the packing material. Its most useful application appears to be in the form of on-line analyte concentration that can be used to concentrate a given sample prior to separation by CZE (94).

3.3 Detection in CE

3.3.1 Absorbance detection

Ultraviolet (UV)/visible (Vis) absorbance detectors are the most widely used detector types for CE. The detector response is based on the light

absorption of substances at the wavelength of light source and classified in two region of UV (190-350 nm) and Vis (350-700 nm) detectors (94). Non-UV/Vis absorbing analytes must be derivatized with some chormophores prior detection or employed indirect absorbance detection. The sensitivity of absorbance detection in CE is limited by the optical path length which is restricted by the capillary inner diameter. The extension of the detection region of the capillary to a bubble cell has been utilized to improve detection limit in a narrow bore fused silica capillaries (96) (Figure 2.5).

3.3.2 Fluorescence detection

Fluorescence detection is the most sensitive detection mode available for CE. In fluorescence, analyte molecules absorp a photon, and a fraction of the electronically excited molecules emit a photon upon returning to the ground state. A good fluorophore needs a high absorbtivity at the excitation wavelength (λ_{ex}). After the molecule is excited, it is possible to return to a ground state by a nonradiative process, forming a nonfluorescent product or emitting photon (fluorescence). Only one of which produces fluorescence is measured. The analytical utilities of fluorophore are the absorptivity, fluorescence quantum yield and photostability. The molecule with higher absorptivity gives a more probability excited at a given illumination intensity. The fluorescence quantum yield is the ratio of the emit photons to the excited molecules, therefore good fluorophore exhibits the high fluorescence quantum yield. The analytes do not exhibit a native fluorescence have to derivatize with some types of fluorophore or an alternative is to perform indirect fluorescence detection (102-103).

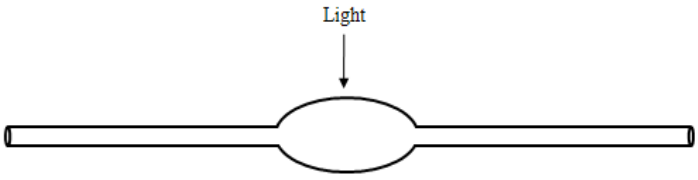

Figure 2.5 The extended path length of a narrow bore fused silica capillary

3.3.3 Electrochemical detection

Capacitively coupled contactless conductivity detection (C^4D) has introduced as an alternative detection method in CE. This is due to its universality for the detection of small inorganic ions as well as organic and biochemical species

(104). Two electrodes are placed around a fused-silica capillary in a certain distance from each other and an oscillation frequency is applied in the range between 20 and 900 kHz. Conductivity changes of the electrolyte in the detection gap between the electrodes inside the capillary using suitable amplifier electronics can be measured. Nevertheless, the detection signal is obtained longitudinal dimension along the capillary (105). C^4D is non-destructive measurement and can be combined with other detectors for simultaneous measurements including photometric and fluorometric detections. The combination of detector is competent to detect the complicated components or mixtures containing analytes with multiple properties (106-108).

3.3.4 Mass spectrometry (MS) detection

CE coupled to MS detection provides a powerful system for the analysis of complex mixtures and it enables applications in characterization, identification and quantitation. MS detection offers great advantages including independence of a chromo- or fluorophore, lower LOD than UV, the structural information and resolve of co-migrating peaks using the information of the mass as second dimension. The separation electrolyte for hyphenation with MS has to be volatile thus non-aqueous solvents are generally well-suited and add another parameter to modify selectivity. Additionally MS/MS can be used for structure elucidation or for additional selectivity in order to gain sensitivity by reducing the chemical noise. Selectivity can also be further increased by applying high-resolution MS with accurate mass determination (109-110).

CHAPTER III
MATERIALS AND METHODS

1 Materials

Table 3.1 List of chemicals and reagents

Name	Grade	Source/Supplier
(-)-Nicotine	RS	Riedel-de Haën (Seelze, Germany) Fluka (Buchs, Switzerland) Sigma (St. Louis Missouri, USA)
(-)-Cotinine	RS	Fluka (Buchs, Switzerland)
Nicotinic acid	RS	Sigma-Aldrich (St. Louis Missouri, USA)
Nicotinamide	RS	Sigma-Aldrich (St. Louis Missouri, USA)
Triprolidine	RS	Sigma-Aldrich (St. Louis Missouri, USA)
Nicotine gum	-	Millimed Co., Ltd. (Samutprakarn,
Multivitamin tablet	-	Anglo-French Drugs & Industries Ltd.
Nicotinic acid tablet	-	Interthai Pharmaceutical Manufacturing Ltd. (Bangkok, Thailand)
30% Hydrogen peroxide	AR	Sigma-Aldrich (St. Louis Missouri, USA)
Sodium acetate	AR	Sigma-Aldrich (St. Louis Missouri, USA)
Methanol	AR	Labscan Asia (Bangkok, Thailand)
Anhydrous citric acid	AR	Riedel-de Haën (Seelze, Germany)
Sodium dihydrogen phosphate dihydrate	AR	Sigma-Aldrich (St. Louis Missouri, USA)
85% Phosphoric acid	AR	Sigma-Aldrich (St. Louis Missouri, USA)

Table 3.1 (continued) List of chemicals and reagents

Name	Grade	Source/Supplier
Hydrochloric acid	AR	Fluka (Buchs, Switzerland)
Sodium hydroxide	AR	Mallinckrodt Baker (Xalostoc, Mexico)
Sterile water for irrigation	-	Thai Otsuka (Samutsakorn, Thailand)
Buffer pH 4.0	-	Ajaxchemical (Sydney, Australia)
Buffer pH 7.0	-	Ajaxchemical (Sydney, Australia)

Table 3.2 List of instruments

Instrument	Source/Supplier
Capillary electrophoresis (^{3D} CE)	Agilent Technologies (Waldbronn, Germany)
Capillary; i.d. 50 μm, o.d. 375	Polymicro Technologies (Arizona, USA)
Capillary; i.d. 50 μm, o.d. 375 μm (extended path length)	Polymicro Technologies (Arizona, USA)
Spectrophotometer	Shidmadzu UV-160A (Japan)
10 mm Square Quartz Cell with Lid	Labomed (California, USA)
Autopipette	Gilson Pipetman (Middleton, USA)
pH meter	Consort model C830 (Turnhout, Belgium)
Analytical balance	Sartorius model AE 160 (Goettingen, Germany)
Diposable syringe 3mL	Nipro (Ayuddhaya, Thailand)
13-mm syringe filters nylon 0.2 μm	Vertical Chromatography (Bangkok, Thailand)
Centrifuge	Labfuge 200 (Heraeus, Germany)
Ultrasonic sonicator	Sithiporn Associates (Bangkok, Thailand)

2 Capillary zone electrophoresis-diode array detection (CZE-DAD) method

CZE was performed on a Hewlett-Packard instrument (^{3D} CE) system (model G1600A) and controlled by PC through Agilent ChemStation Plus software version A.08 (G1601A). The detector measured in the range of 190-600 nm (wavelength accuracy ± 2 nm) was a diode array detector, which was consisted of a deuterium. The regulation of high voltage was varied in a range of 0-30 kV (current 0-300 μA, power 0-6 W). The temperature control the capillary tube was varied from 5 to 60 °C (± 1 °C). The injection systems could be achieved by 1) applying pressure to sample vials (hydrostatic injection) and 2) applying voltage (electromigration injection).

The separation of the biologically active pyridines using a fused-silica capillary tube with a total length (L_{total}) of 64.5 cm, an effective length (L_{eff}) of 56 cm, an inner diameter (i.d.) of 50 μm (extended pathlength) and an outer diameter (o.d.) of 375 μm. The pre-conditioning procedure for a new capillary, for daily uses, between runs and storage was described in Table 3.3.

The separation conditions were optimized by varying the background electrolyte (BGE) types, pHs and concentrations, applied voltage and injection time. Standard solutions were injected into the anodic capillary inlet using 50 mbar pressures. The detection was performed using a diode-array detector at a wavelength of 260 nm with a bandwidth 6 nm.

Table 3.3 The capillary conditioning procedures for the separation of biologically active pyridines

	Conditioning Step	Time (min)
New capillary		
1) Rinse	1 N NaOH	10
2) Rinse	0.1 N NaOH	10
3) Rinse	Deionized water	10
4) Rinse	BGE	10
Daily condition before use		
1) Rinse	1 N NaOH	5
2) Rinse	0.1 N NaOH	5
3) Rinse	Deionized water	5
4) Rinse	BGE	5
Between run		
1) Rinse	0.1 N NaOH	2
2) Rinse	Deionized water	2
3) Rinse	BGE	3
Daily storage		
1) Rinse	1 N NaOH	5
2) Rinse	Deionized water	5
3) Rinse	0.1 N NaOH	5
4) Rinse	Deionized water	5
Storage		
1) Rinse	1 N NaOH	10
2) Rinse	Deionized water	10
3) Rinse	0.1 N NaOH	10
4) Rinse	Deionized water	10
5) Rinse	Air	15

2.1 Stock and working standard solutions preparation

Stock standard solutions of NIC, COT, NA, NM, and TRI (used as internal standard, I.S.) were prepared separately by transferring an accurate weight equivalent to 10.0 mg of each standard in a 10-mL volumetric flask. Water was added and adjusted to volume to obtain the final concentration of 1,000 μg/mL. All stock standard solutions were kept in a refrigerator (at 4-8 °C).

Series of working standard solutions were prepared by transferring an aliquot of the standard stock solution into volumetric flasks and diluted with water. NIC, COT, NA, NM, and TRI were prepared in a range of 3.2 – 1,000, 2.5-160, 3-200, 2-200 and 100 μg/mL, respectively. All solutions were filtered through a 0.2-μm membrane and degassed for 10 minutes prior injection.

2.2 BGE preparation

Citrate buffer was prepared by transferring citric acid and sodium citrate equivalent to 150 mM (1.40 g of anhydrous citric acid and 0.05 g of sodium citrate) into a 50-mL volumetric flask. Then, 40 mL of water was added and swirled. The solution was adjusted to volume with water. BGE were adjusted to the desired pH by adding 1 M hydrochloric acid or 1 M sodium hydroxide, filtered through a 0.2 μm membrane filter and degassed for 10 min prior introduced to CE instrument.

Sodium dihydrogen phosphate buffer was prepared by transferring sodium dihydrogen phosphate dihydrate equivalent to 15, 20, 25 and 30 mM (0.117, 0.156, 0.195 and 0.234 g) into each 50-mL volumetric flask. Then, 40 mL of water was added and swirled. The solution was adjusted to volume by water. BGEs were adjusted to the desired pH by adding 85% phosphoric acid or 1 M NaOH, filtered through a 0.2 μm membrane filter and degassed for 10 min prior introduced to CE instrument.

2.3 Sample preparation

The extraction procedure of NIC gum was modified from Chiu and co-workes (1). An accurately weighed NIC gum was cut into six pieces and transferred to a 15-mL centrifuged tube. The contents of the gum was added in 10 mL of methanol containing 100 ug/mL of I.S. and mixed at 65°C for 40 min. After cooling to room

temperature, the mixture was sonicated for 15 min and then centrifuged for 10 min at 6000 rpm. The resulting clear liquid was evaporated and reconstituted with 10 mL of deionized water. The extract was filtered through a 0.2 mm nylon membrane before CE analysis.

Ten tablets of NM tablet (multivitamin tablet) were crushed and finely powdered by a mortar and pestle. Powder equivalent to 25 mg of NM and about 50 mL of water were transferred into a 250- mL volumetric flask, heated until no more dissolve and adjusted to volume by water. Ten ml of the solution was transferred into a 100- mL volumetric flask and diluted with water to obtain the final concentration of 10 µg/mL (9). The solution was filtered through a 0.2-µm membrane filter and degassed 10 min prior injected into CE instrument.

Twenty tablets of NA tablet were crushed to fine powder by a mortar and pestle. Powder equivalent to 500 mg of NA and about 50 mL of water were transferred into a 100- mL volumetric flask, heated for 30 min, sonicated for 2 min, shaked by mechanical means for 15 min, cooled to room temperature and adjusted to volume by water and mixed. One mL of this solution was transferred into a 100- mL volumetric flask and diluted with water to obtain the final concentration of 50 µg/mL (9). The solution was filtered through a 0.2-µm membrane filter and degassed 10 min prior injected into CE instrument.

Stability of NIC was studied under stress conditions by thermal and oxidative degradations. Nicotine gum was cut into small pieces and transferred to tubes, which was then exposed to air and put on a water bath with controlled temperature at 90˚C. The samples were maintained under degrading conditions for 6 h (8). Another degrading condition was examined by keeping nicotine gum in 10% H_2O_2 for 6 h at room temperature. NIC samples from both degrading conditions were extracted by the procedure described above.

2.4 Optimization

Preliminary experiment for the analysis of four biologically active pyridines; NIC, COT, NA and NM by CZE was performed by the modified condition from Lochmann and co-workers (30). The separation was carried out in 150 mM citric acid, pH 3.6; capillary: 70 cm (50 cm to detector) x 50 μm i.d.; 23 kV and detection: UV 260 nm.

Further optimization was performed in a fused silica capillary tube with L_{total} of 64.5 cm, L_{eff} of 56 cm and i.d. of 50 μm (extended pathlength). The investigated chemical and instrumental factors are shown in Table 3.4.

Table 3.4 Investigated chemical and instrumental factors

Factor	Range
Types of BGEs	Citric acid vs sodium dihydrogen phosphate
pH of BGEs	2.1-3.5
BGE concentration	15-30 mM
Applied voltage	20-30 kV
Injection time	5-20 s

Optimum condition was determined from analytical parameters. These parameters included, migration time (< 10.0 min), resolution (> 1.5), tailing factor (close to 1.0) and number of theoretical plate (> 5,000), which can be calculated by the following equation:

$$R_s = \frac{2(t_2 - t_1)}{w_1 + w_2} \quad (3.1)$$

Where R_s = Resolution

t_x = Migration time of analyte x

w_x = Baseline peak width (in time) of analyte x

$$TF = \frac{w_{0.05}}{2f} \quad (3.2)$$

Where TF = Tailing factor

$w_{0.05}$ = Width of peak at 5 % of peak height

f = Width of line from leading edge of peak to the intercept of a perpendicular line dropped from the peak maximum to the base

$$N = 5.54\left(\frac{t}{w_{0.5}}\right)^2 \quad (3.3)$$

Where N = Number of theoretical plates

t = Migration time of analyte

$w_{0.5}$ = Temporal peak width at half height

2.5 Method validation

The optimum CZE condition was validated by the following procedures.

2.5.1 Linearity

Calibration curves of the investigated analytes were established for five different concentrations (n = 3) on three different days in the range of 3.2-1,000 µg/mL, 8-160 µg/mL, 10-200 µg/mL and 10-200 µg/mL for NIC, NM, COT and NA, respectively. The calibration curves were plotted between peak area, peak area ratio, peak height or peak height ratio against concentrations. Linear regression, coefficient of determination (r^2) and the percent relative standard deviations (%RSDs) of slope and intercept were calculated by Microsoft Excel®.

2.5.2 Precision

2.5.2.1 Injection precision

Injection precision was determined by repetitive injection (n = 10) at the middle point concentration of the calibration curve of the investigated pyridines.

2.5.2.2 Intra-day precision

Intra-day precision was determined on three different concentration (n = 3) of each biologically active pyridines analyzed within one day.

2.5.2.3 Inter-day precision

Inter-day precision was performed by determining three different concentrations (n = 3) of each biologically active pyridines on six different days.

All precision data was assessed from the %RSDs of migration time, peak area, peak area ratio, peak height and peak height ratio of individual biologically active pyridine, which was determined from the following equation:

$$\%\text{RSDs} = \frac{\text{SD}}{\overline{\text{X}}} \times 100 \qquad (3.4)$$

Where: SD = the standard deviation of the mean value

$\overline{\text{X}}$ = the mean value

2.5.3 Limit of detection (LOD) and limit of quantitation (LOQ)

Limit of detection (LOD) is the lowest amount of an analyte in a sample that can be detected, typically with acceptable signal to noise ratio (S/N) of 3. Limit of quantitation (LOQ) is a characteristics of quantitative assays. It is the lowest amount of analyte in the sample that can be determined with acceptable precision and recovery with a S/N of 10.

LODs and LOQs of each biologically active pyridines were determined by serial diluting the concentration of the standard solution of the investigated pyridines at S/N of 3 and 10, respectively (n = 3).

2.5.4 Recovery

Recovery of the method of was performed using standard addition method by spiking 80-120 % of the standard into the sample containing 200 µg/mL of NIC, 10 µg/mL of NM and 50 µg/mL of NA (n = 3). Percent recoveries were calculated by the following equation:

$$\%\text{Recovery} = \frac{X_{found}}{X_{add}} \times 100 \qquad (3.5)$$

Where: X_{found} = the concentration of standard found in the spiked sample

X_{add} = the concentration of standard added

2.5.5 Robustness

Chemical parameter (i.e. pH) and physical parameters (i.e. injection time and voltage) were evaluated for the robustness test. The variation around the nominal value of pH (2.1±0.2) and injection time (10 s ±1), results in a change of injection volume from 15 nL to 13.5 and 16.5 nL, were performed. Voltage was varied from -16.67% (25 kV) to –10% (27 kV) of the optimal value.

2.6 Applications

The developed and validated CE method was applied for the determination of NIC, NM and NA content in pharmaceutical formulations and the degraded products of NIC under the stress conditions. Two different brands of NIC chewing gums, two different brands of NM in multivitamin tablet, one brands of NA tablet and one brand of combined formulation of NA and NM in multivitamin tablet were prepared and injected into CE instrument. Results were reported as percent label amount. This method was also used for monitoring NIC gum stability under thermal (90 ˚C) and oxidative (10% H_2O_2) degradation.

CHAPTER IV
RESULTS AND DISCUSSION

1. Optimization

1.1 Effects of types of BGE

CZE was developed for the separation of the analytes using TRI as an appropriate I.S. since it was well separated from NIC, COT, NM and NA under all investigated conditions. Initial separation of the analytes was performed in 150 mM citric acid (30) and 25 mM sodium dihydrogen phosphate pH 2.5 (33) (Figure 4.1). Figure 4.2 shows the effects of the types of BGEs on the analytical parameters. All analytes and TRI were well separated ($R_s > 2.0$) in both BGE with a migration order of NIC, TRI, NM, COT and NA, respectively. However, the separation efficiency ($R_s > 5.9$ and $N > 69,207$) was superior in sodium dihydrogen phosphate buffer and also peaks of NM and NA were tailing ($TF > 1.5$) in citric acid buffer. Therefore, sodium dihydrogen phosphate buffer was selected for further optimization since it provided the better peak shape and the S/N from this buffer was 1.3-fold higher than in citric acid buffer.

1.2 Effects of pH of BGE

Varying pH from 2.1 to 3.5 greatly influenced migration time and peak shape of NA (Figure 4.3). From pH 2.1 to 2.9, migration times of NIC, NM and COT remained almost constant within 8 min, but that of NA increased from 9.6 to 25.2 min. These results are in good agreement with those reported by Marsh *et al*. (31) and Terekhova *et al.* (32), which confirms that NIC, COT, and NM were in their protonated forms at low pH. However, NA existed as zwitterions at pH 3.5 and as a mixture of cations and zwitterions at lower pH (32), resulting in an asymmetric peak ($TF = 0.7$). Moreover, separation efficiency of all analytes significantly dropped at pH greater than 2.5. For example, N dropped from 264,928 to 75,428 for NIC, from

133,667 to 38,274 for NM, from 89,512 to 24,811 for COT, and from 69,207 to 20,848 for NA when pH increased from 2.5 to 2.9. At pH 3.5, COT and protonated NA co-migrated ($R_s = 0$). Although the highest resolution was obtained at pH 2.5 ($R_s > 5.9$), pH 2.1 was chosen since it offered the lowest RSD of t_r (< 0.37%) within 10 min (comparing to 17 min at pH 2.5) (Figure 4.4).

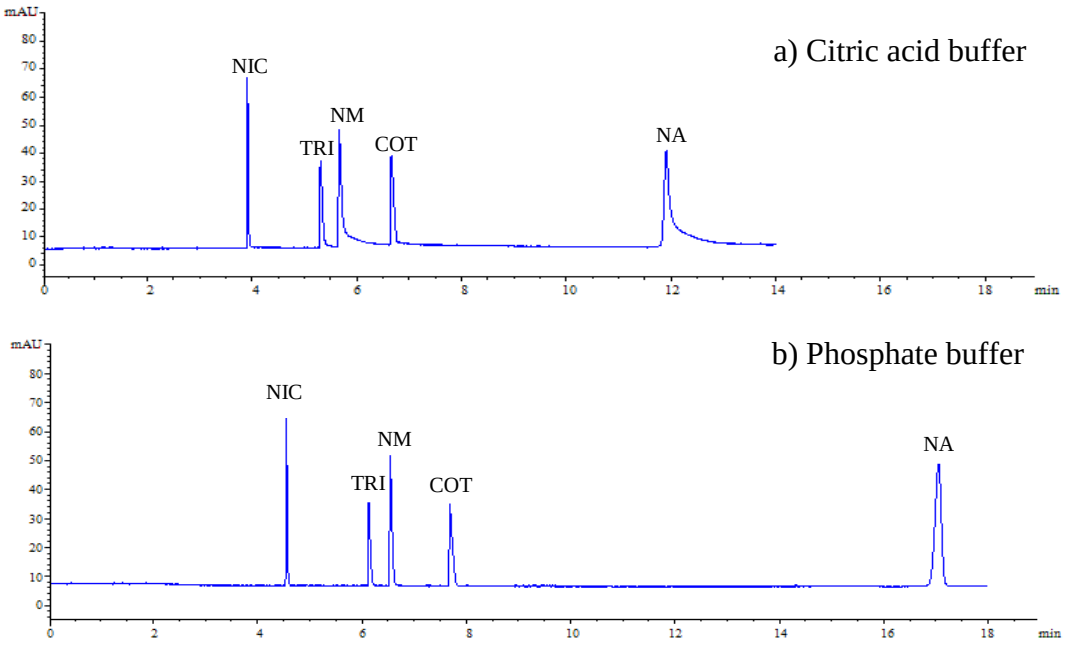

Figure 4.1 Effects of types of BGEs on the separation of the investigated pyridines. Conditions: a) 150 mM citric acid pH 2.5 and b) 25 mM sodium dihydrogen phosphate pH 2.5; capillary 64.5 cm total length (8.5 cm to the detector), 50 µm i.d. (extended pathlegth); hydrodynamic injection at 50 mbar for 10 s; temperature 25 °C; voltage 30kV; detection by UV absorbance at 260 nm. Peak identification: NIC, nicotine; TRI, triprolidine; NM, nicotinamide; COT, cotinine; NA, nicotinic acid.

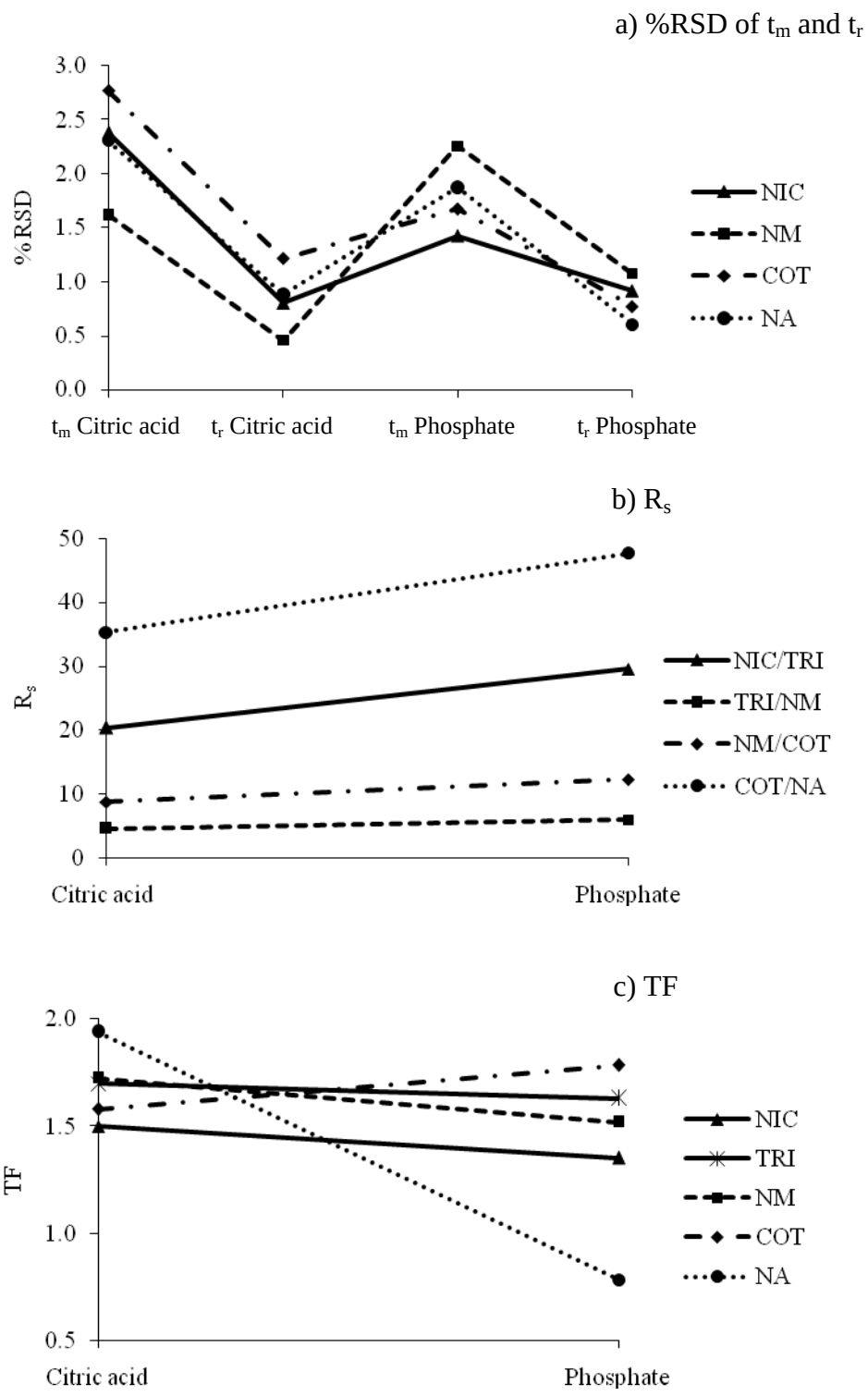

Figure 4.2 Effects of types of BGEs on analytical parameters of the investigated pyridines, a) % relative standard deviation (%RSD) of migration time (t_m) and relative migration time (t_r) calculated from $t_m/t_{I.S.}$, b) resolution (R_s), c) tailing factor (TF) and d) number of theoretical plates (N).

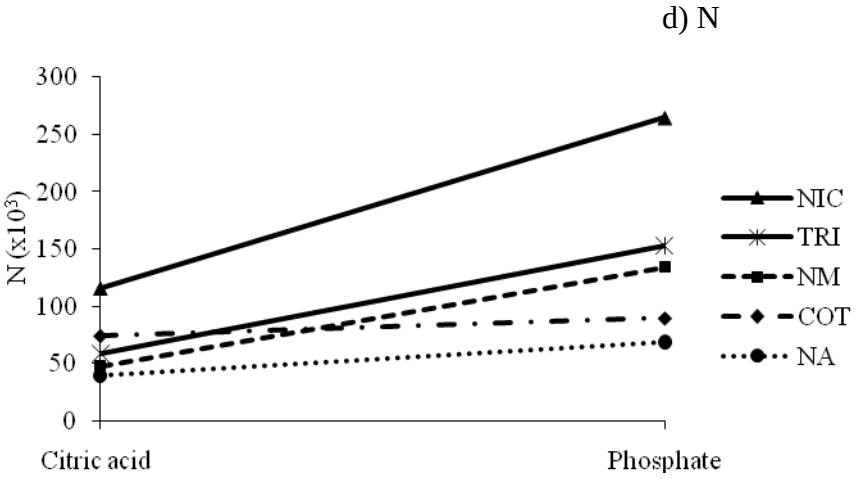

Figure 4.2 (continued) Effects of types of BGEs on analytical parameters of the investigated pyridines, a) % relative standard deviation (%RSD) of migration time (t_m) and relative migration time (t_r) calculated from $t_m/t_{I.S.}$, b) resolution (R_s), c) tailing factor (TF) and d) number of theoretical plates (N).

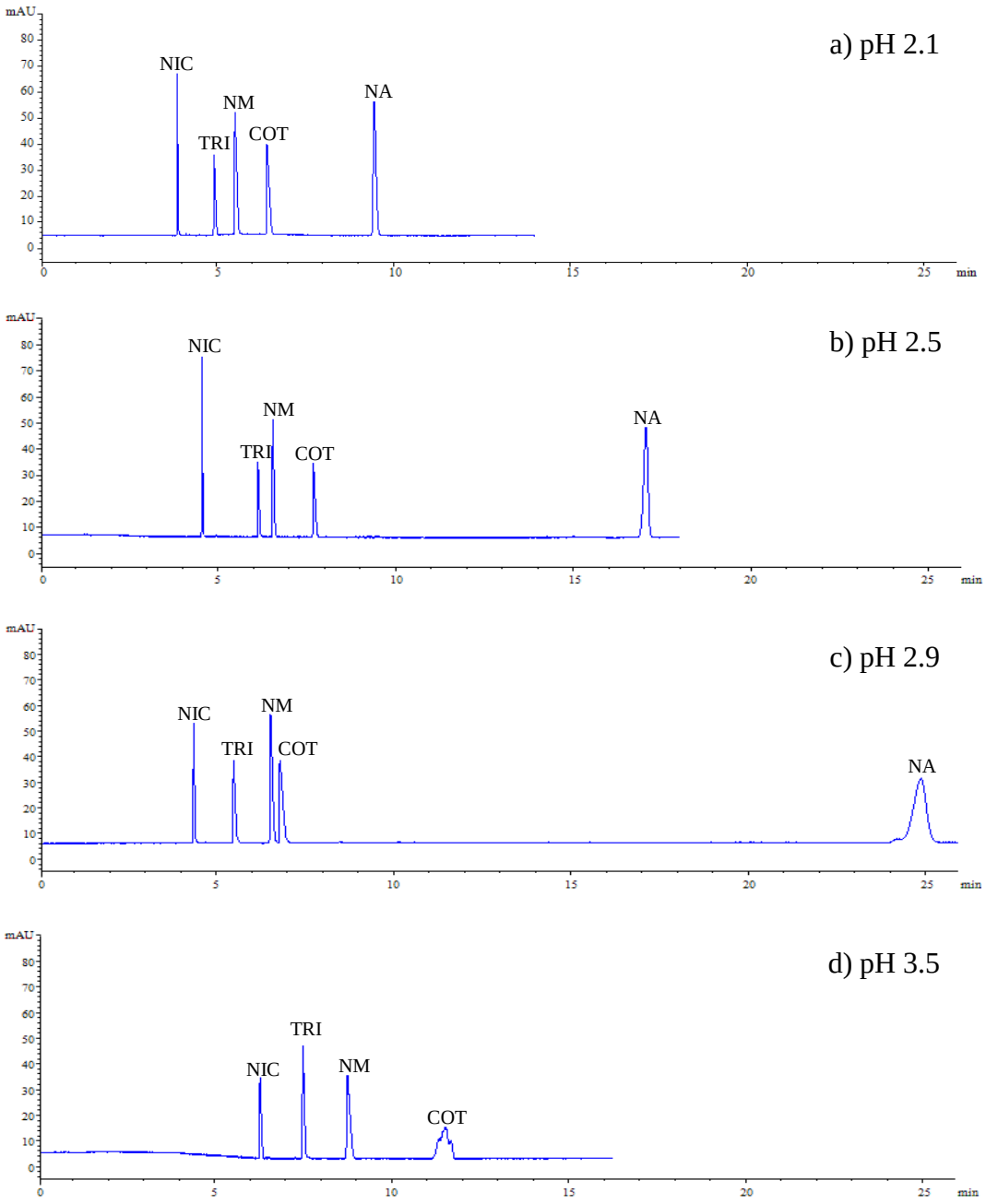

Figure 4.3 Effects of pHs of BGEs on the separation of the investigated pyridines. Conditions: 25 mM sodium dihydrogen phosphate pH a) 2.1, b) 2.5, c) 2.9 and d) 3.5; capillary 64.5 cm total length (8.5 cm to the detector), 50 µm i.d. (extended pathlength); hydrodynamic injection at 50 mbar for 10 s; temperature 25 °C; voltage 30kV; detection by UV absorbance at 260 nm. Peak identification: NIC, nicotine; TRI, triprolidine; NM, nicotinamide; COT, cotinine; NA, nicotinic acid.

a) %RSD of t_m and t_r

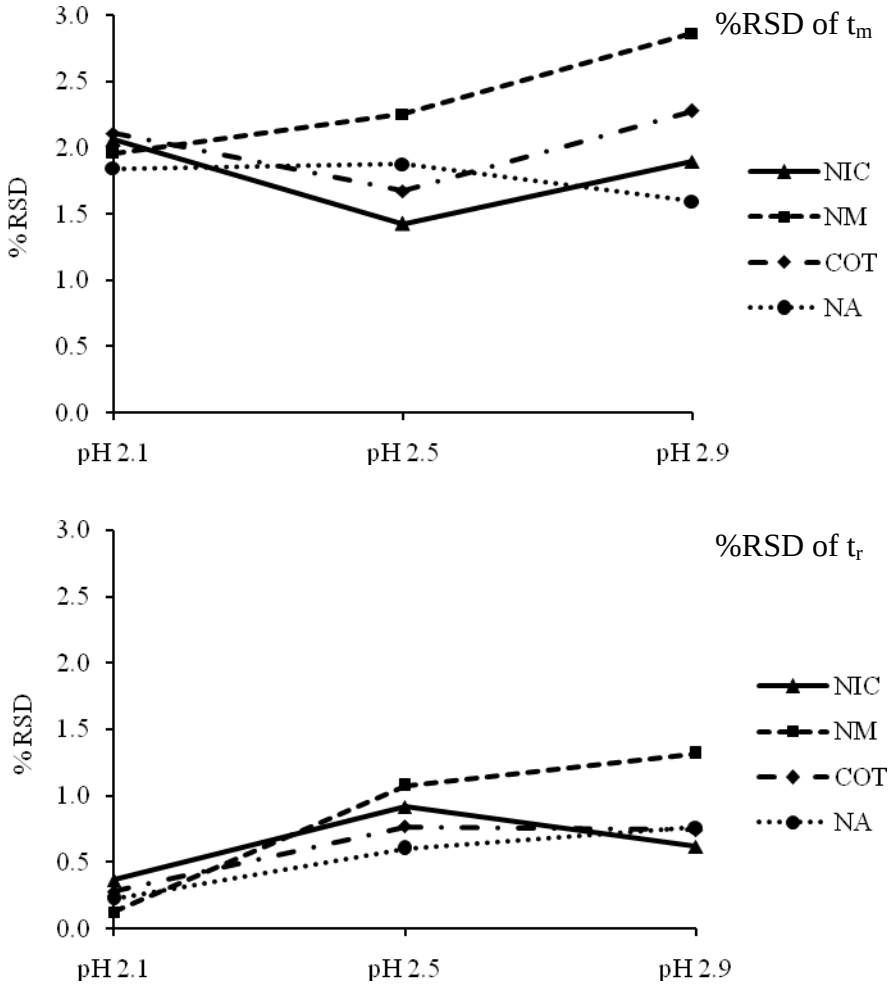

Figure 4.4 Effects of pHs of BGEs on analytical parameters of the investigated pyridines, a) % relative standard deviation (%RSD) of migration time (t_m) and relative migration time (t_r) calculated from $t_m/t_{I.S.}$, b) resolution (R_s), c) tailing factor (TF) and d) number of theoretical plates (N).

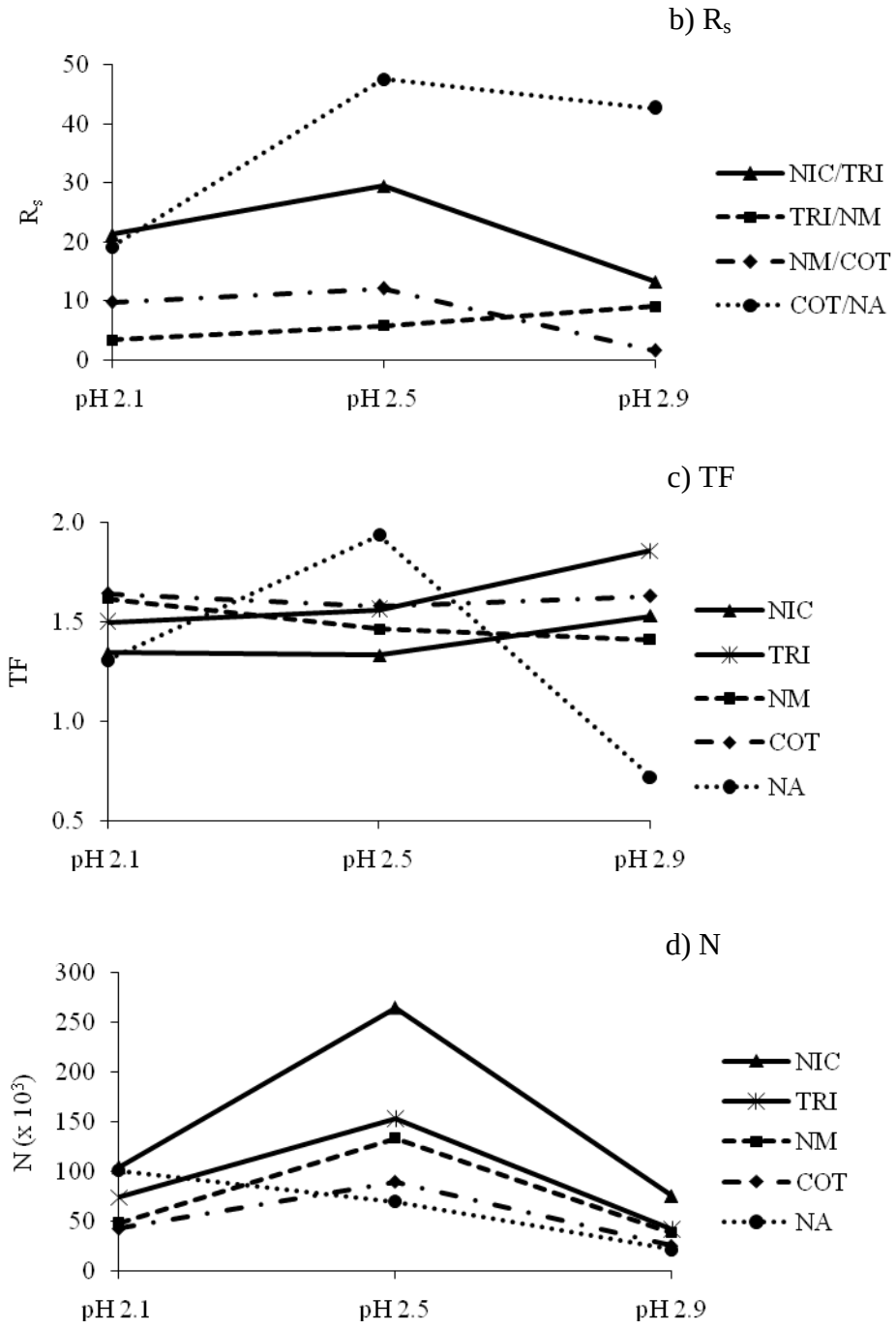

Figure 4.4 (continued) Effects of pHs of BGEs on analytical parameters of the investigated pyridines, a) % relative standard deviation (%RSD) of migration time (t_m) and relative migration time (t_r) calculated from $t_m/t_{I.S.}$, b) resolution (R_s), c) tailing factor (TF) and d) number of theoretical plates (N).

1.3 Effects of BGE concentrations

Results from effects of BGE concentrations revealed that increasing of sodium dihydrogen phosphate buffer (pH 2.1) concentrations from 15 to 30 mM increased migration time from 8.3 to 13.5 min (Figure 4.5). Increased resolution was also observed due to reduction of EOF. However, increasing the BGE concentration to 30 mM increased the RSDs of t_r because of the high current causing elevated temperature and peak dispersion. Phosphate buffer at 25 mM was optimal since it gave the lowest RSD of t_r for most analytes (< 0.37%) and highest N for NA (Figure 4.6).

1.4 Effects of applied voltage and the injection time

Increasing of voltage from 20 to 30 kV decreased the migration time from 22.8 to 9.6 min due to the enhanced EOF velocity (Figure 4.7). At the lowest voltage (20 kV), most peaks were broad with lower S/N (Figure 4.8). Voltage of 30 kV was selected since it gave shortest t_m (9.6 min).

The amount of sample loading depended on the injection time when the injection pressure was constant (50 mbar). The sample loading effects (50 mbar for 5-20 s) showed that 10 s was appropriate because loading time of 5 s provided peaks with lower sensitivity, whereas at injection times of 15 and 20 s, NA peak was highly skew and broad (TF = 1.7) with significant drops of separation efficiency of most analytes (Figure 4.9-4.10).

The optimized condition for the separation of the analytes was in 25 mM sodium dihydrogen phosphate buffer pH 2.1 with the migration order of NIC, TRI (I.S.), NM, COT and NA, respectively (Figure 4.9b). The separation was performed using a fused-silica capillary tube with L_{total} of 64.5 cm, L_{eff} of 56.0 cm and i.d. of 50 μm (extended pathlength). Hydrodynamic injection was at 50 mbar for 10 s, the temperature and applied voltage were 25 $^{\circ}$C and +30 kV. The detection wavelength was 260 nm.

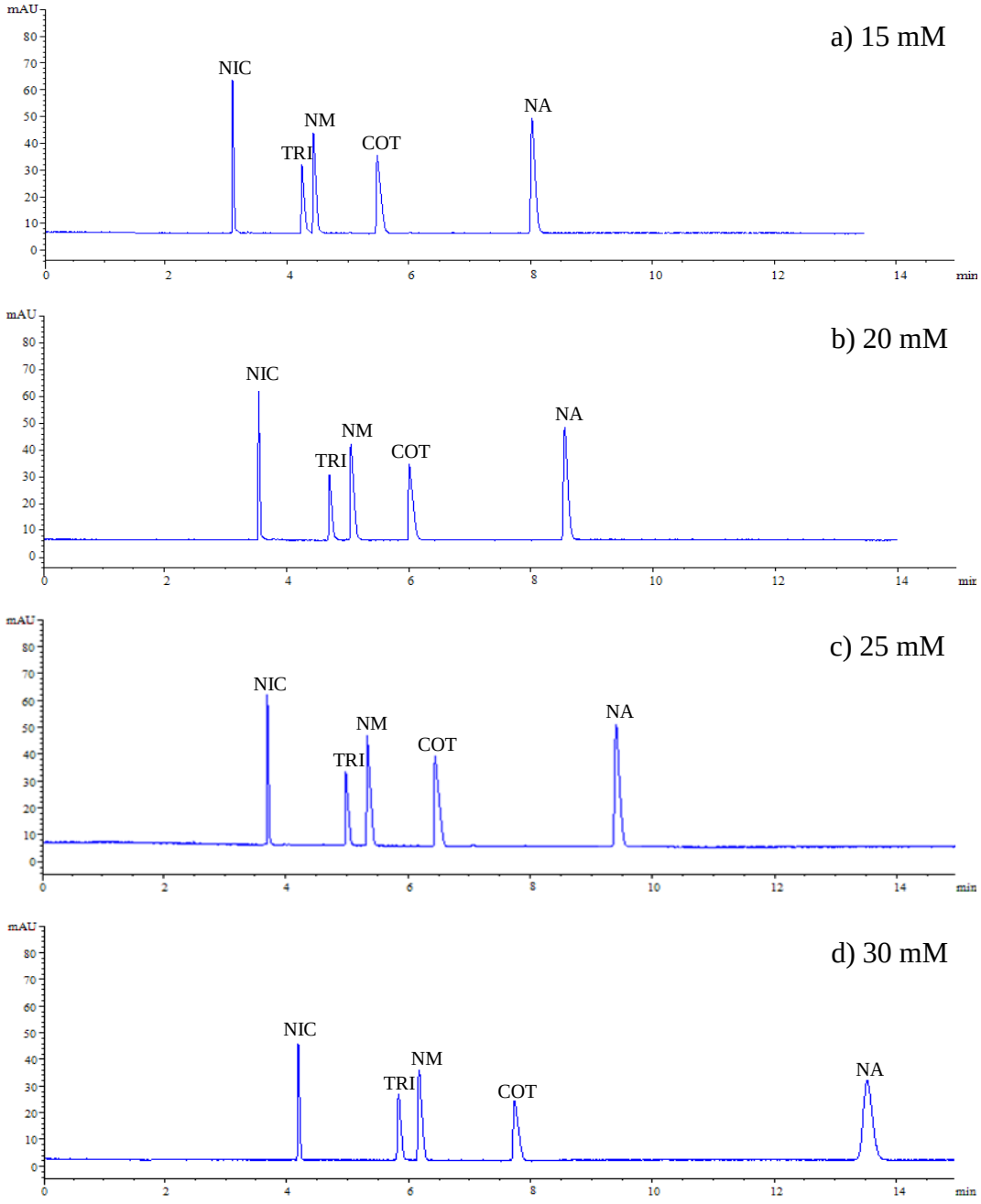

Figure 4.5 Effects of concentrations of BGEs on the separation of the investigated pyridines. Conditions: sodium dihydrogen phosphate pH 2.1 at the concentration of a) 15 mM, b) 20 mM, c) 25 mM and d) 30 mM; capillary 64.5 cm total length (8.5 cm to the detector), 50 µm i.d. (extended pathlength); hydrodynamic injection at 50 mbar for 10 s; temperature 25 °C; voltage 30kV; detection by UV absorbance at 260 nm. Peak identification: NIC, nicotine; TRI, triprolidine; NM, nicotinamide; COT, cotinine; NA, nicotinic acid.

a) %RSD of t_m and t_r

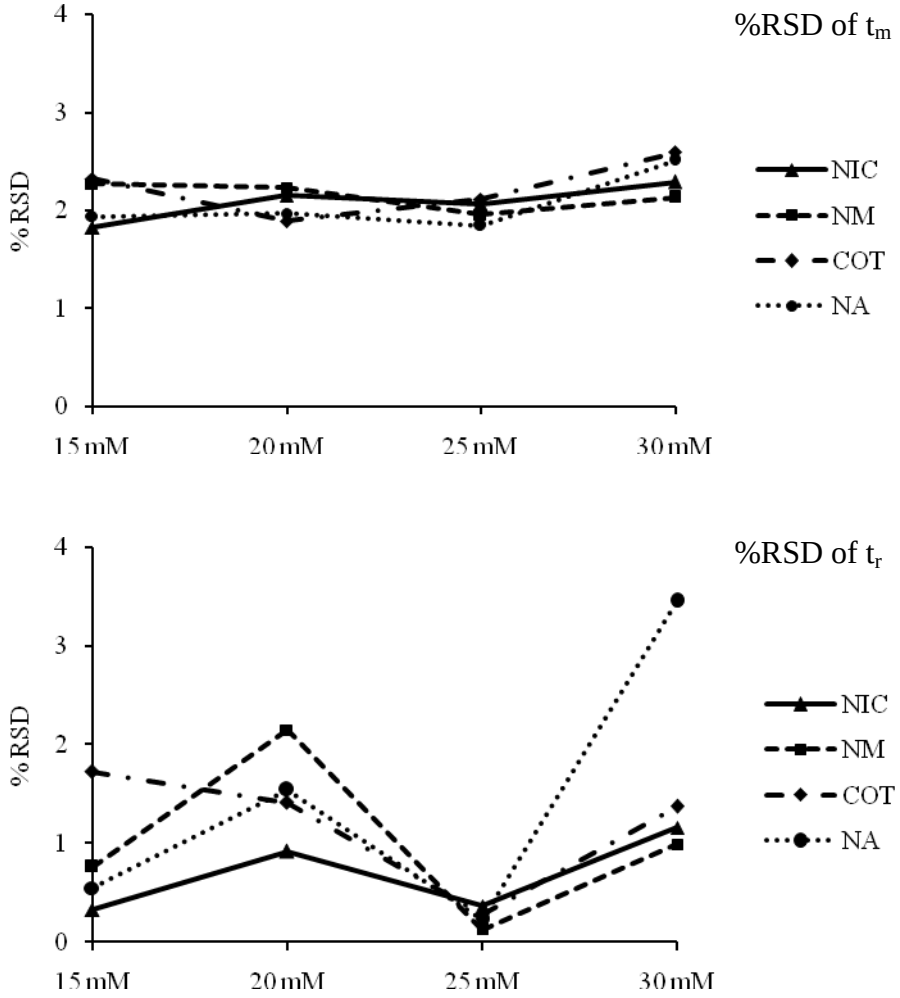

Figure 4.6 Effects of concentrations of BGEs on analytical parameters of the investigated pyridines, a) % relative standard deviation (%RSD) of migration time (t_m) and relative migration time (t_r) calculated from $t_m/t_{I.S.}$, b) resolution (R_s), c) tailing factor (TF) and d) number of theoretical plates (N).

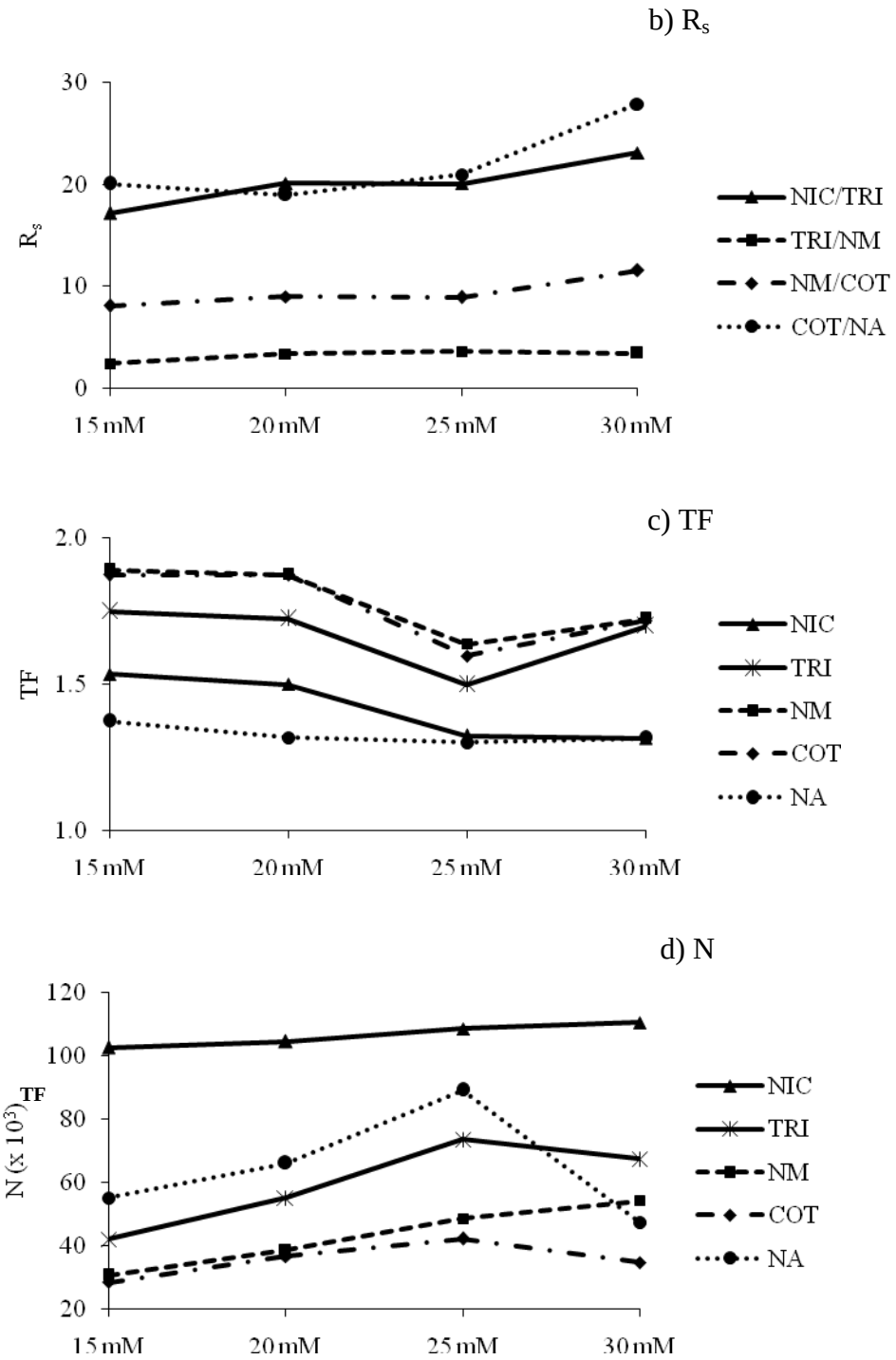

Figure 4.6 (continued) Effects of concentrations of BGEs on analytical parameters of the investigated pyridines, a) % relative standard deviation (%RSD) of migration time (t_m) and relative migration time (t_r) calculated from $t_m/t_{I.S.}$, b) resolution (R_s), c) tailing factor (TF) and d) number of theoretical plates (N).

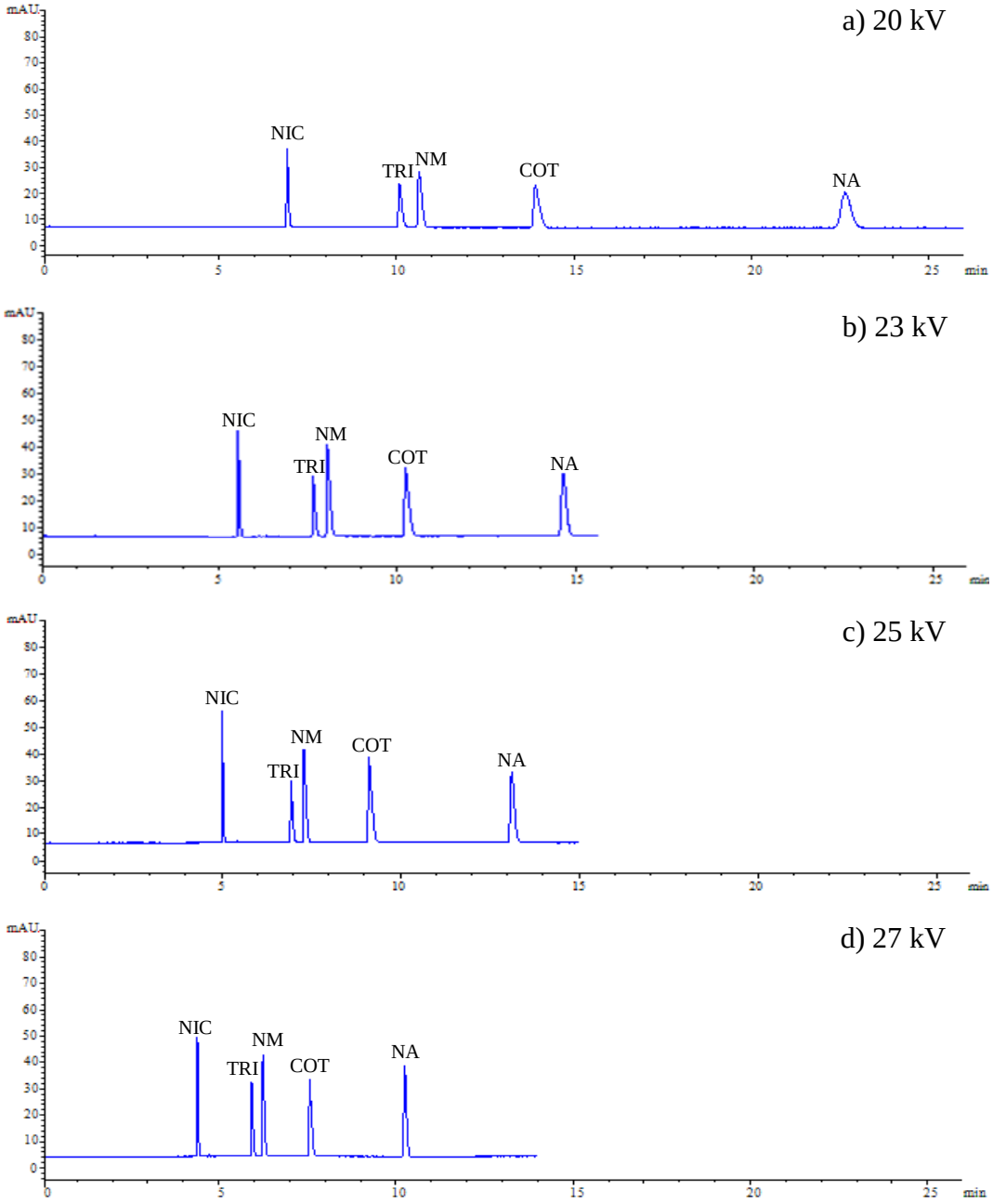

Figure 4.7 Effects of applied voltage on the separation of the investigated pyridines. Conditions: 25 mM sodium dihydrogen phosphate pH 2.1; capillary 64.5 cm total length (8.5 cm to the detector), 50 µm i.d. (extended pathlength); hydrodynamic injection at 50 mbar for 10 s; temperature 25 °C; voltage a) 20 kV, b) 23 kV, c) 25 kV, d) 27 kV and e) 30 kV; detection by UV absorbance at 260 nm. Peak identification: NIC, nicotine; TRI, triprolidine; NM, nicotinamide; COT, cotinine; NA, nicotinic acid.

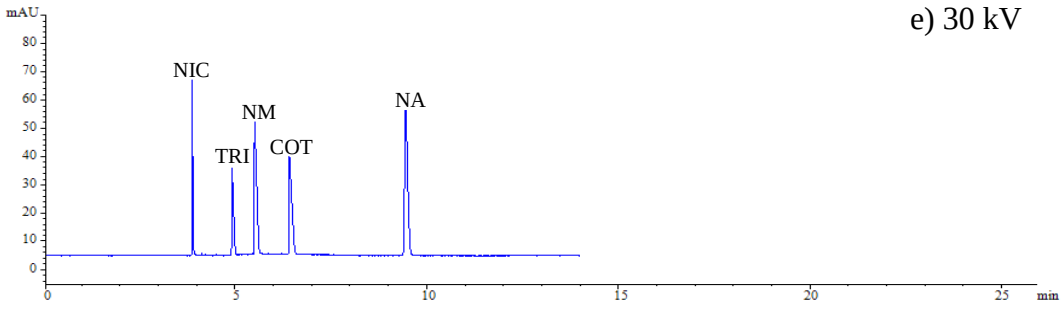

Figure 4.7 (continued) Effects of applied voltage on the separation of the investigated pyridines. Conditions: 25 mM sodium dihydrogen phosphate pH 2.1; capillary 64.5 cm total length (8.5 cm to the detector), 50 µm i.d. (extended pathlength); hydrodynamic injection at 50 mbar for 10 s; temperature 25 °C; voltage a) 20 kV, b) 23 kV, c) 25 kV, d) 27 kV and e) 30 kV; detection by UV absorbance at 260 nm. Peak identification: NIC, nicotine; TRI, triprolidine; NM, nicotinamide; COT, cotinine; NA, nicotinic acid.

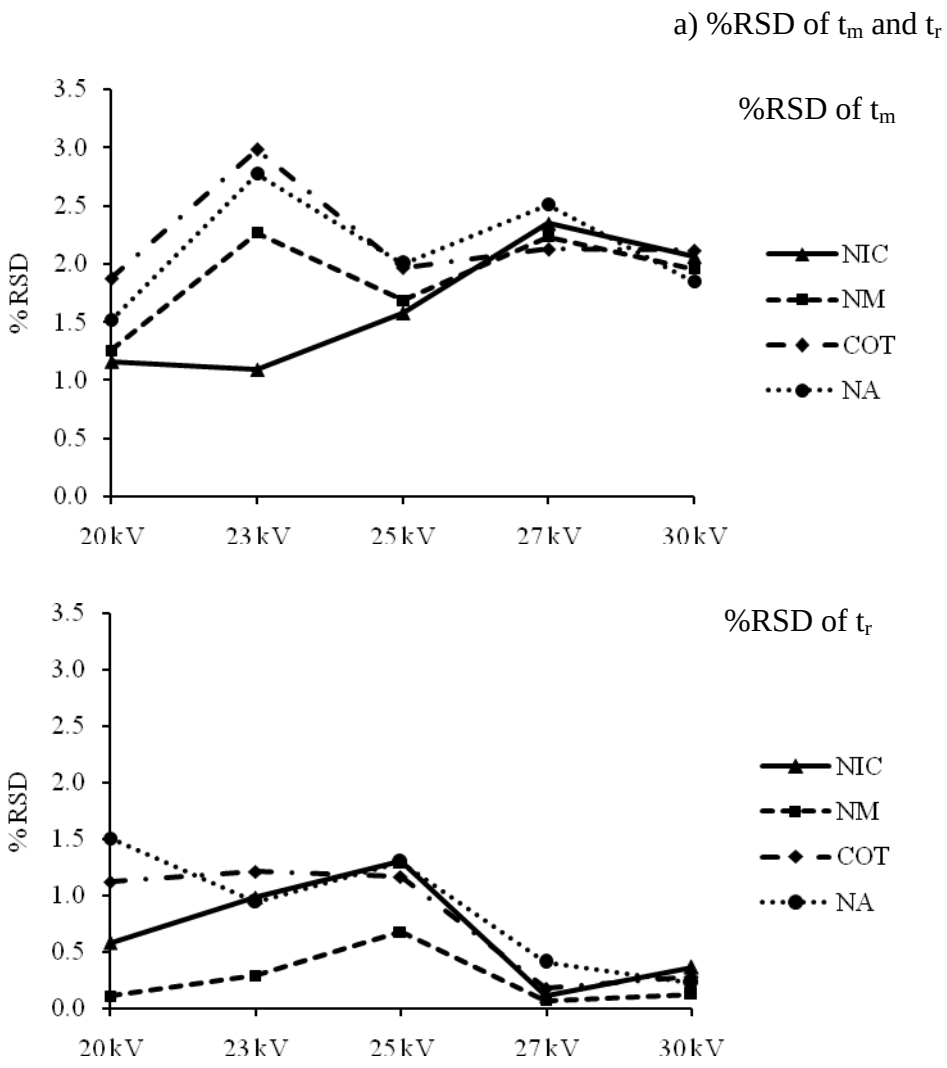

Figure 4.8 Effects of applied voltage on analytical parameters of the investigated pyridines, a) % relative standard deviation (%RSD) of migration time (t_m) and relative migration time (t_r) calculated from $t_m/t_{I.S.}$, b) resolution (R_s), c) tailing factor (TF) and d) number of theoretical plates (N).

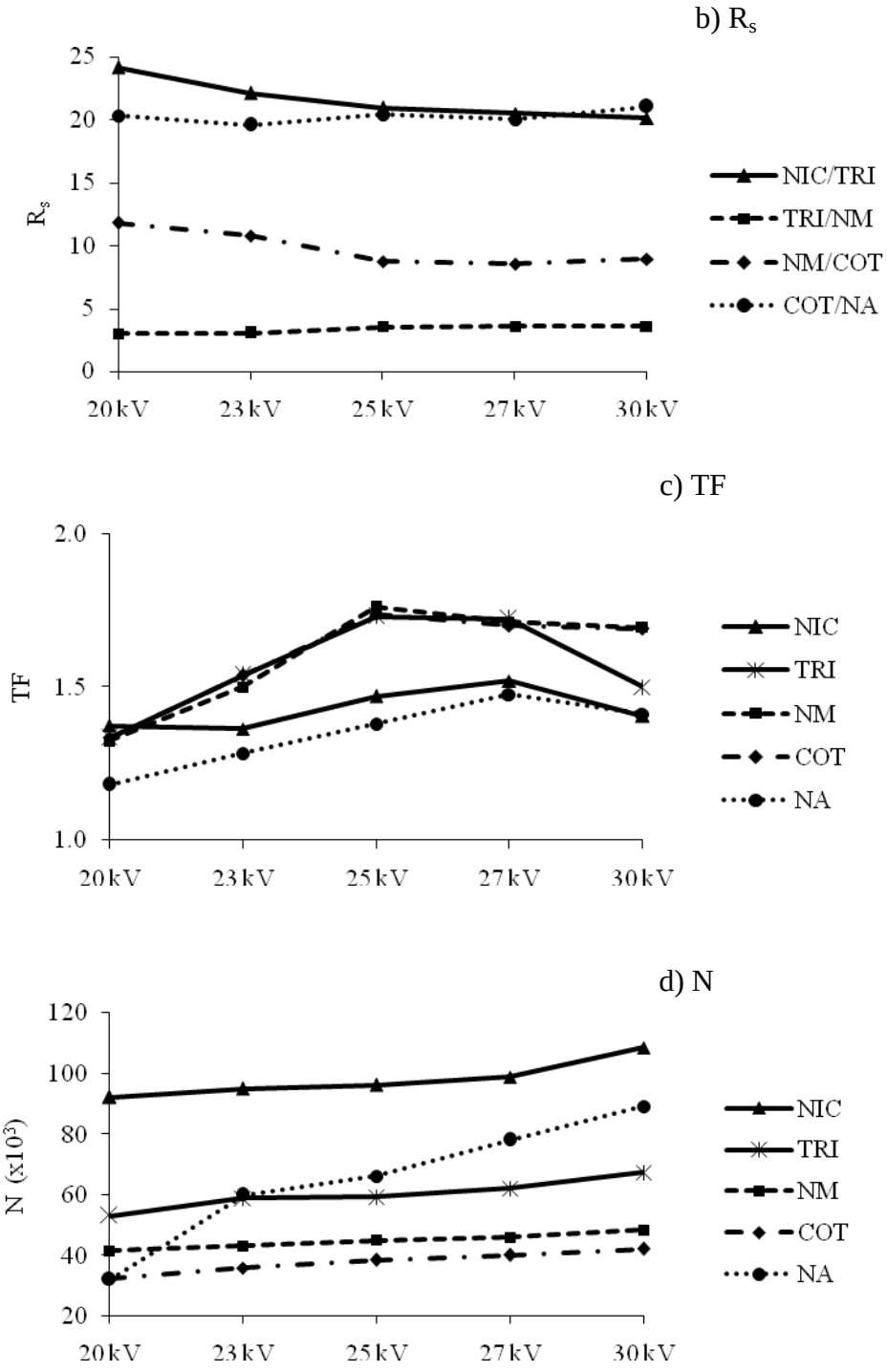

Figure 4.8 (continued) Effects of applied voltage on analytical parameters of the investigated pyridines, a) % relative standard deviation (%RSD) of migration time (t_m) and relative migration time (t_r) calculated from $t_m/t_{I.S.}$, b) resolution (R_s), c) tailing factor (TF) and d) number of theoretical plates (N).

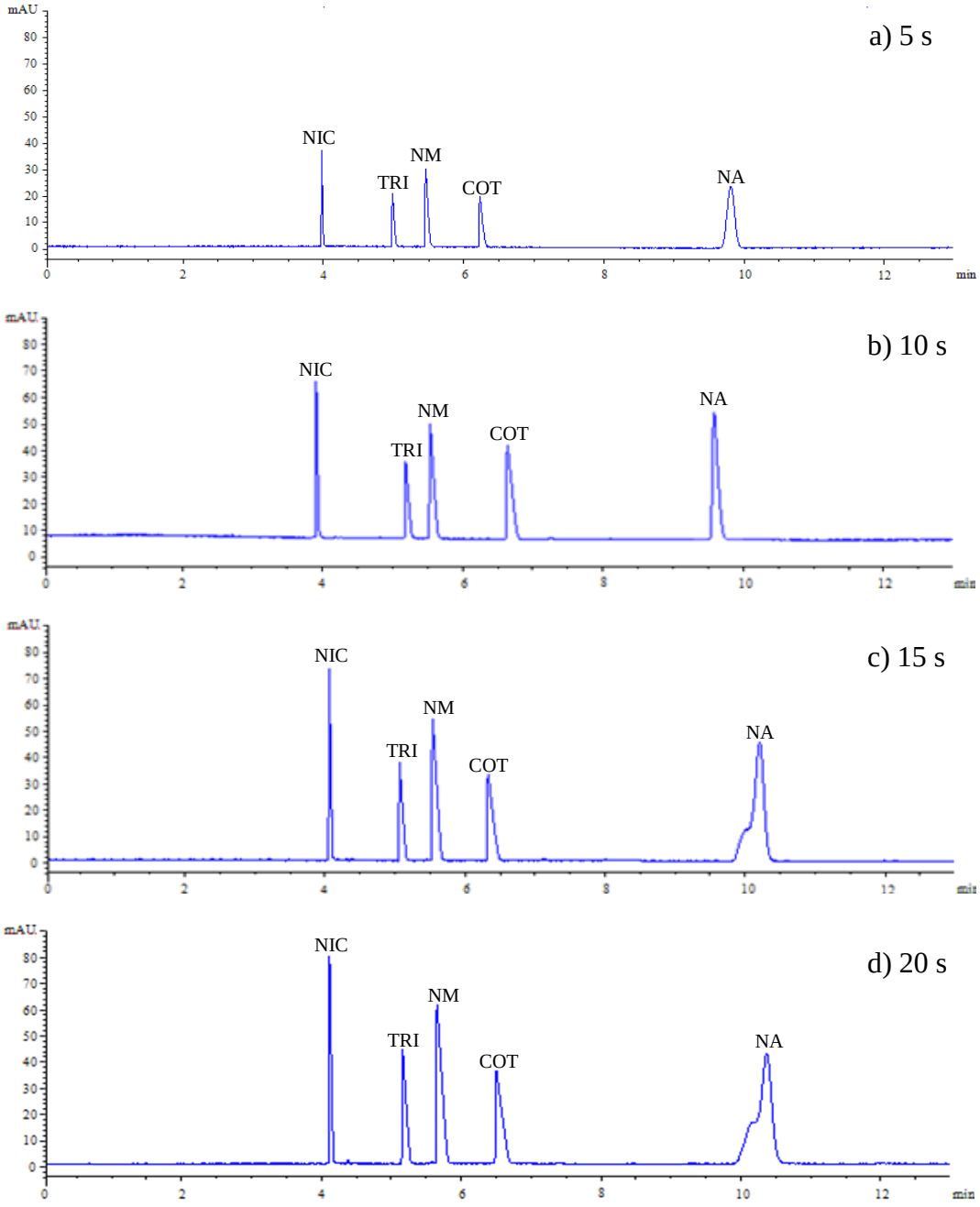

Figure 4.9 Effects of injection time on the separation of the investigated pyridines. Conditions: 25 mM sodium dihydrogen phosphate pH 2.1; capillary 64.5 cm total length (8.5 cm to the detector), 50 µm i.d. (extended pathlength); hydrodynamic injection at 50 mbar for a) 5 s, b) 10 s, c) 15 s and d) 20 s; temperature 25 °C; voltage 30 kV; detection by UV absorbance at 260 nm. Peak identification: NIC, nicotine; TRI, triprolidine; NM, nicotinamide; COT, cotinine; NA, nicotinic acid.

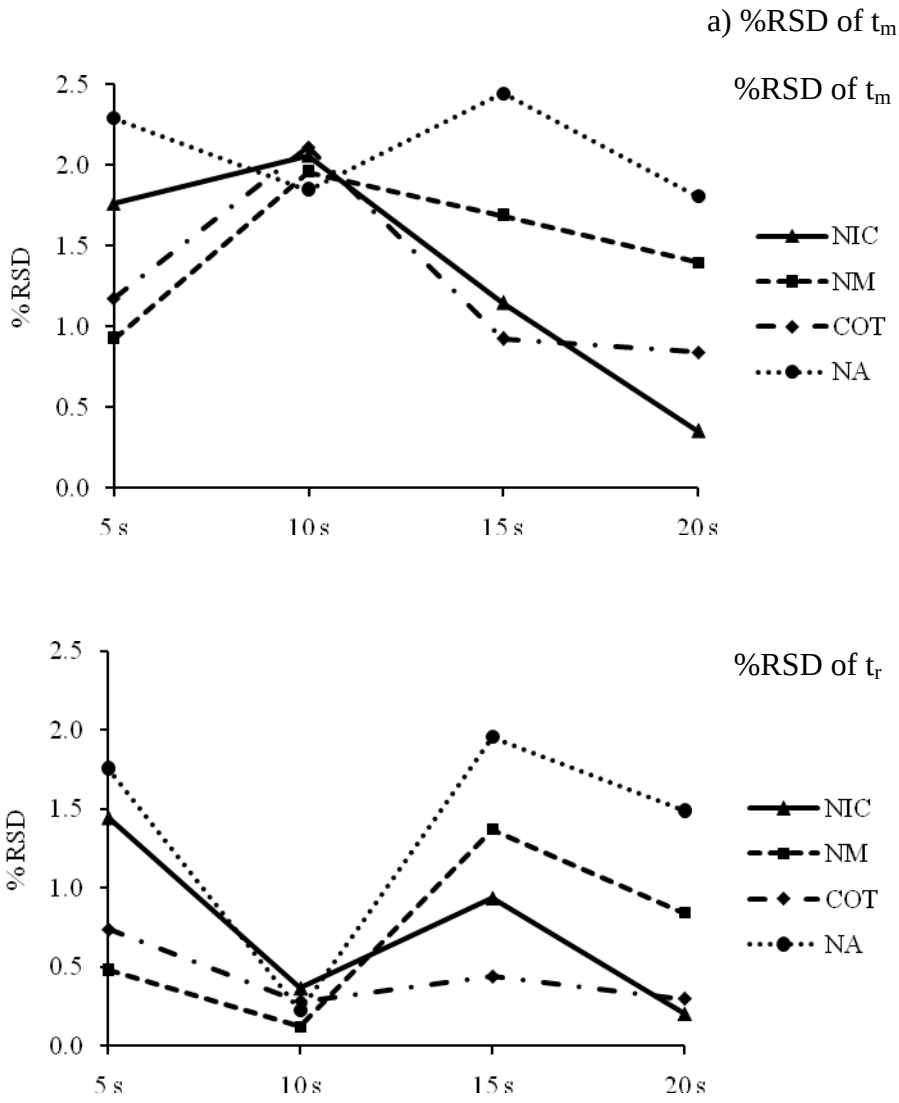

Figure 4.10 Effects of injection time on analytical parameters of the investigated pyridines, a) % relative standard deviation (%RSD) of migration time (t_m) and relative migration time (t_r) calculated from $t_m/t_{I.S.}$, b) resolution (R_s), c) tailing factor (TF) and d) number of theoretical plates (N).

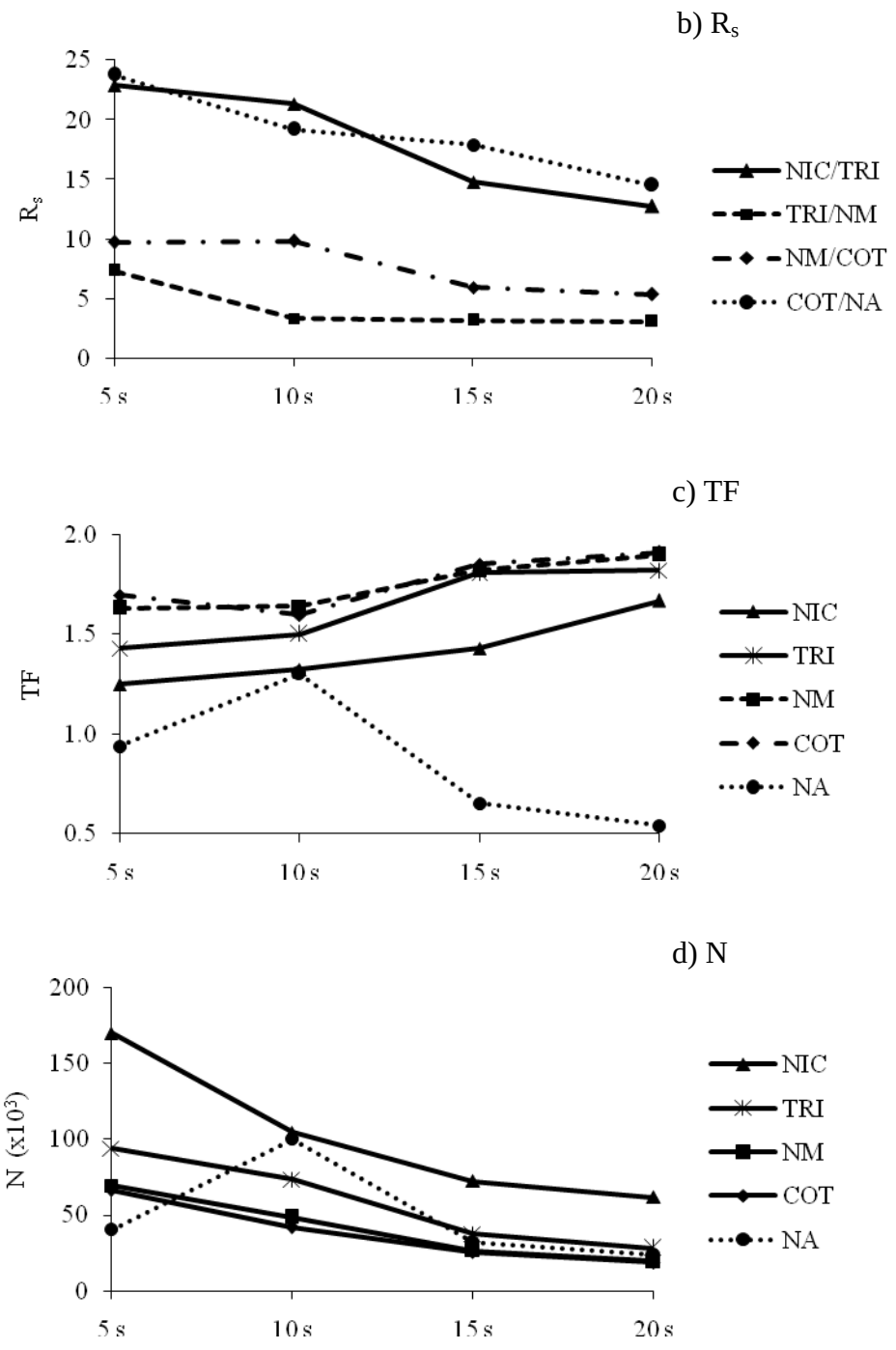

Figure 4.10 (continued) Effects of injection time on analytical parameters of the investigated pyridines, a) % relative standard deviation (%RSD) of migration time (t_m) and relative migration time (t_r) calculated from $t_m/t_{I.S.}$, b) resolution (R_s), c) tailing factor (TF) and d) number of theoretical plates (N).

2. Method validation

The optimized CZE condition for the separation of NIC, NM, COT and NA was validated in terms of linearity, precision, recoveries, LOD, LOQ and robustness.

2.1 Linearity

The calibration curves of NIC, NM, COT and NA were established by triplicate injections of five different concentrations of the working standard solutions. From Table 4.1, the calibration curves were plotted from the concentration vs peak area and peak area ratio. Detector response was linear with r^2 between 0.9970-0.9998 in ranges of 50-600 µg/mL for NIC, 8-160 µg/mL for NM and 10-200 µg/mL for COT and NA.

2.2 Precision

Precision of the optimized CZE condition was evaluated from intra-day, inter-day and injection precision. Table 4.2 shows the precision of the method. %RSDs of t_m and peak area of analytes decreased when they were corrected with t_m and peak area of I.S. For intra-day precision, %RSDs of t_r and peak area ratio were less than 1.75 and 2.16, respectively. For inter-day precision, the %RSD of t_r and peak area ratio were less than 2.24 and 2.10, respectively. The %RSD of injection precision of t_r and peak area ratio were less than 1.82 and 1.86, respectively.

Table 4.1 Slope, y-intercept, standard error of slope and intercept and coefficient of determination of NIC, NM, COT and NA

Analyte	Range (µg/mL)	Calibration curve*	Slope	y-intercept	Standard error of mean		r^2
					slope	intercept	
NIC	3.2-1,000	a	1.0619	4.6619	0.0016	0.2277	0.9998
		b	0.0107	0.0395	0.0000	0.0024	0.9999
NM	8-160	a	1.3511	1.7137	0.0028	0.0011	0.9991
		b	0.0136	0.0207	0.0001	0.0002	0.9993
COT	10-200	a	1.1878	- 0.2422	0.0028	0.0037	0.9970
		b	0.0122	- 0.0129	0.0000	0.0001	0.9982
NA	10-200	a	3.9258	-15.7310	0.0112	0.2072	0.9978
		b	0.0396	- 0.1640	0.0004	0.0013	0.9983

*a: concentration vs peak area, b: concentration vs peak area ratio

Table 4.2 Precision of NIC, NM, COT and NA presented as %RSDs

	Concentration (µg/mL)	Intra-day				Inter-day				Injection			
		t_m	t_r	area	area ratio	t_m	t_r	area	area ratio	t_m	t_r	area	area ratio
NIC	3.2	1.03	0.23	1.02	0.61	2.52	1.99	2.49	1.84	-	-	-	-
	400	1.59	1.26	1.69	0.66	2.31	2.08	1.21	1.05	2.80	1.82	1.23	0.58
	1,000	1.37	1.04	1.46	0.60	1.81	1.59	1.33	1.14	-	-	-	-
NM	8	1.54	0.96	3.42	2.16	2.58	2.24	2.42	2.10	-	-	-	-
	80	2.06	1.20	1.42	0.48	2.28	1.94	1.39	1.08	2.74	1.55	2.07	1.86
	160	1.49	0.62	0.64	0.57	1.41	1.23	1.46	1.13	-	-	-	-
COT	10	3.25	1.49	2.67	1.60	1.84	1.50	2.02	1.80	-	-	-	-
	100	2.23	1.23	1.84	1.30	1.88	1.16	0.99	0.47	2.13	1.78	1.61	1.32
	200	2.11	1.75	1.40	0.87	1.54	1.27	2.03	1.70	-	-	-	-
NA	10	1.30	0.38	2.20	0.91	1.39	1.33	1.48	0.83	-	-	-	-
	100	2.48	1.52	1.89	0.79	1.64	1.41	1.63	1.38	2.24	1.66	1.95	1.66
	200	2.13	1.51	1.44	0.60	1.09	0.62	1.07	0.71	-	-	-	-

*%RSD = percent relative standard deviation, t_m = migration time, t_r = relative migration time calculated from $t_m/t_{I.S.}$

2.3 Limit of detection (LOD) and limit of quantitation (LOQ)

LOD and LOQ of analytes were the concentration that can be determined with acceptable precision and recovery at the signal to noise ratio (S/N) of 3 and 10, respectively. Figure 4.11-4.14 and Table 4.3 shows LODs and LOQs of NIC, NM, COT and NA. LOQs of analytes were around three times (2.8-3.3 times) greater than LODs.

Table 4.3 LODs and LOQs of NIC, NM, COT and NA

Analyte	LOD (µg/mL)	LOQ (µg/mL)
NIC	1	3.2 (0.89)
NM	2.5	8 (1.80)
COT	3	10 (1.28)
NA	2	5.5 (1.80)

*numbers in parentheses represent %RSDs (percent relative standard deviation), LOD = limit of detection, LOQ = limit of quantitation

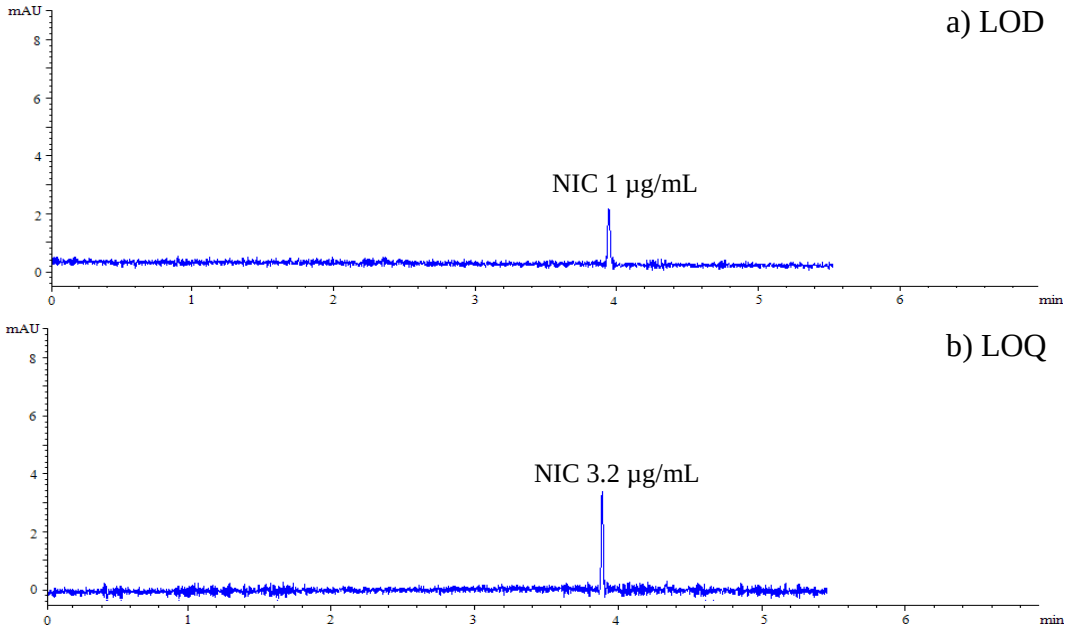

Figure 4.11 Electropherograms of nicotine (NIC) at limit of detection (LOD) and limit of quantitation (LOQ) levels. CE conditions see Figure 4.9b.

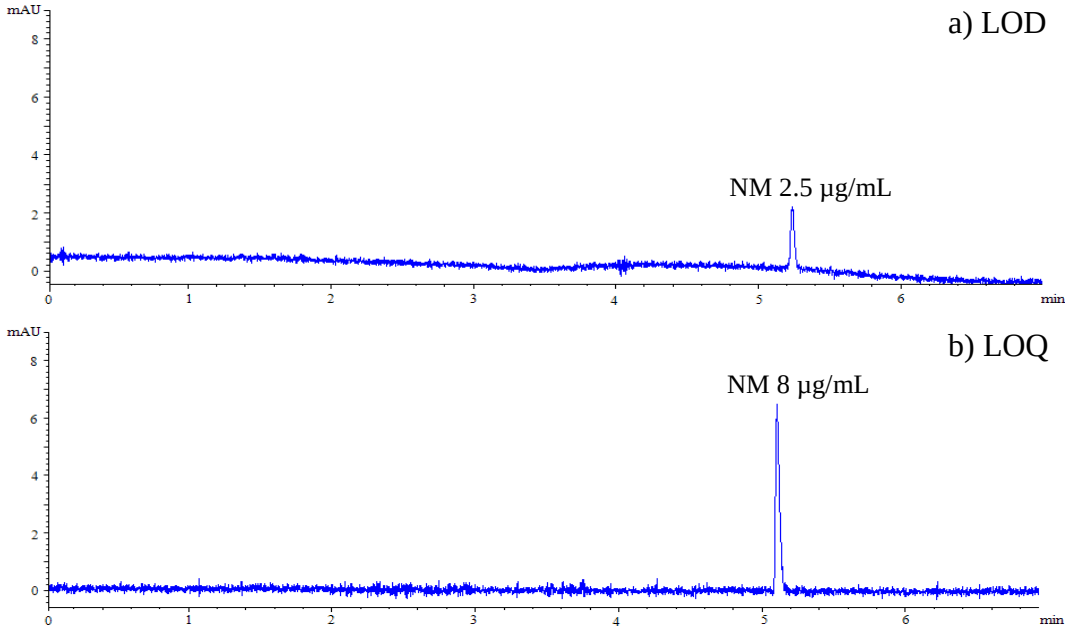

Figure 4.12 Electropherograms of nicotinamide (NM) at limit of detection (LOD) and limit of quantitation (LOQ) levels. CE conditions see Figure 4.9b.

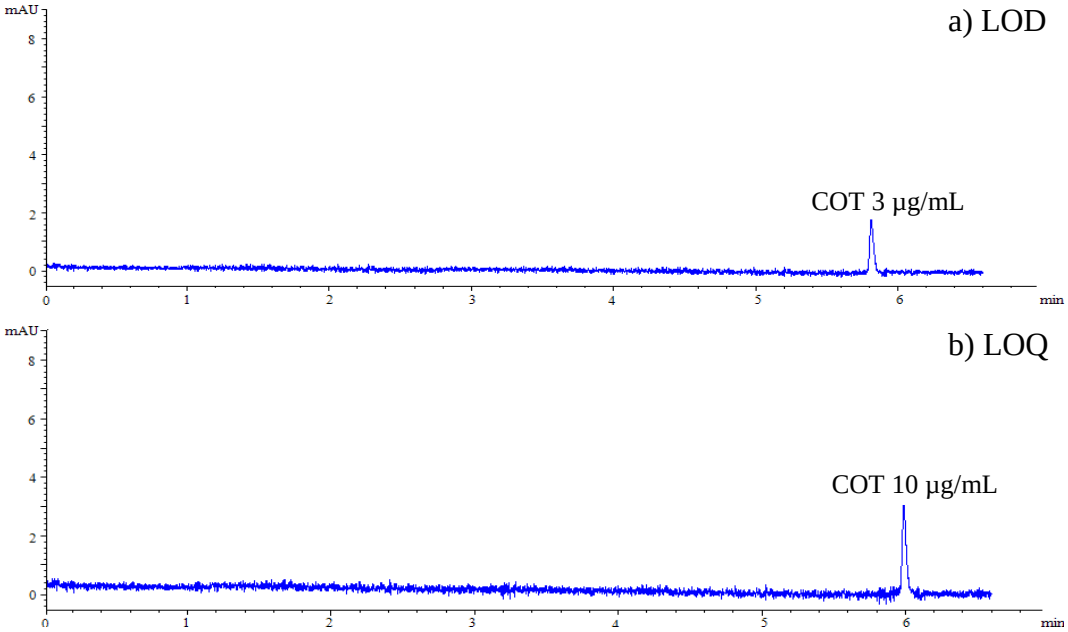

Figure 4.13 Electropherograms of cotinine (COT) at limit of detection (LOD) and limit of quantitation (LOQ) levels. CE conditions see Figure 4.9b.

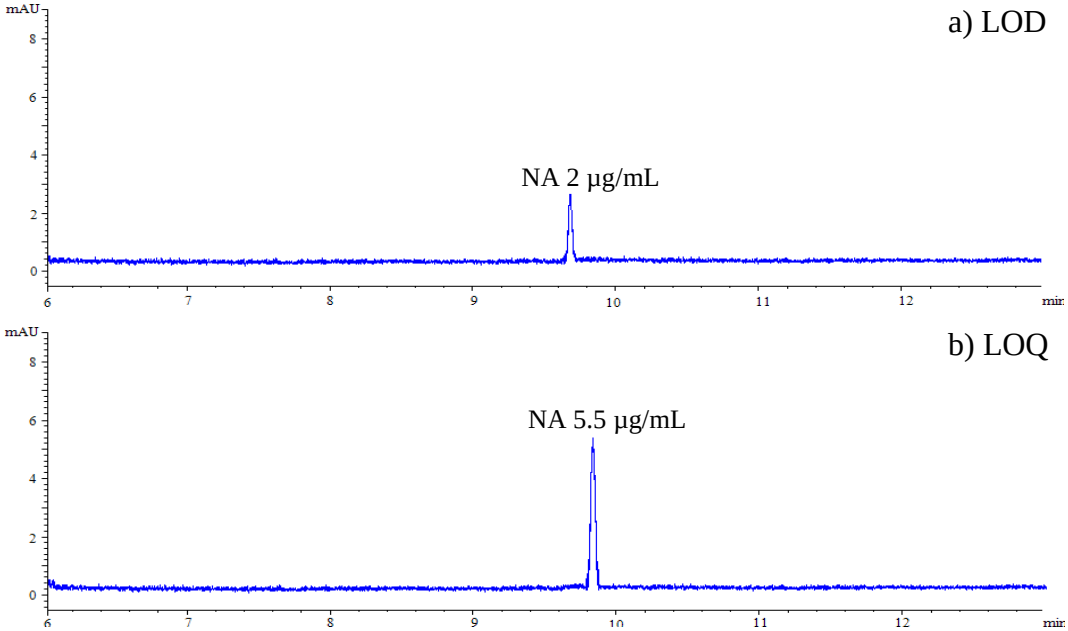

Figure 4.14 Electropherograms of nicotinic acid (NA) at limit of detection (LOD) and limit of quantitation (LOQ) levels. CE conditions see Figure 4.9b.

2.4 Recovery

Recovery was performed by the standard addition method by spiking NIC, NM and NA in the range 80-120% of assay concentration to pharmaceutical samples. Table 4.4 show recoveries of NIC, NM and NA. Percent recoveries of NIC, NM and NA were found in a range of 95.4-97.2%, 98.2-101.5% and 100.4-102.4%, respectively.

Table 4.4 Recovery data

	% Recovery				
%Add	80	100	120	average	%RSD (n = 3)
NIC	95.4	96.6	97.2	96.4	0.98
NM	98.2	100.5	101.5	100.1	1.66
NA	100.4	102.4	102.0	101.6	1.06

*%RSD = percent relative standard deviation

2.5 Robustness

Robustness data were obtained by varying the optimum CE condition around the nominal value of pH (2.1±0.2), injection time (10 s ±1) and voltages (25, 27 and 30 kV). Data revealed that t_r, and R_s were not significantly affected despite of the varied pH of the BGE, separating voltage and injection time (Table 4.5).

Table 4.5 Robustness data

	pH				Voltage (kV)				Injection time (s)			
	1.9	2.1	2.3	%RSD	25	27	30	%RSD	9	10	11	%RSD
t_r												
NIC	0.78	0.75	0.75	2.28	0.74	0.74	0.75	0.78	0.76	0.75	0.79	2.72
NM	1.09	1.07	1.08	0.93	1.07	1.05	1.07	1.09	1.06	1.07	1.07	0.54
COT	1.26	1.29	1.28	1.20	1.30	1.27	1.29	1.19	1.27	1.29	1.26	1.20
NA	1.93	1.87	1.93	1.81	1.86	1.84	1.87	0.82	1.91	1.87	1.91	1.22
R_s												
NIC/TRI	19.9	20.1	20.8	2.33	20.9	20.5	20.1	1.95	21.1	20.1	19.9	3.16
TRI/NM	3.5	3.6	3.6	1.62	3.50	3.6	3.6	1.62	3.6	3.6	3.5	1.62
NM/COT	8.6	8.9	8.7	1.75	8.7	8.5	8.9	2.30	9.0	8.9	8.6	2.36
COT/NA	21.9	21.0	22.4	3.26	20.4	20.0	21.0	2.46	21.3	21.0	20.1	3.00

*%RSD = percent relative standard deviation, t_r = relative migration time calculated from $t_m/t_{I.S.}$, R_s = resolution

3. Applications

The developed and validated method was applied for the determination of NIC, NM, COT and NA in pharmaceutical formulations containing single and combined analytes in formulations and in stress test of a product. The method was applied to determine NIC in three different lots of NIC gum, NM in two different lots of vitamin B complex tablets, NA in one lot of NA tablets and NM and NA in one lot of multivitamin tablets. BGE and water (sample solvent) did not interfere the CE separation since no extra peaks were observed during the analysis. Relative migration times of the analytes in sample solutions do not differ from those of the standards (0.75, 1.07, 1.29 and 1.87 for NIC, NM, COT and NA, respectively) (Table 4.6). The internal standard plays a roles on precision enhancement. In sample solutions, data shows that RSDs calculated from relative migration times (1.93%) were smaller than those calculated from migration times (3.21%). Figure 4.15 shows typical electropherograms of NIC, NM and NA in various products. Percent label amounts of the tested samples were within 99.1-104.3% (RSD < 1.95%), which were within the USP limits (Table 4.6).

Table 4.6 Assay data*

	Brand	t_r (min, n = 9)	% Labeled amount (n = 3)	USP 31 limit
NIC (2 mg/gum)	A	0.75 (1.23)	103.3 (1.03)	90.0-120.0
NIC (2 mg/gum)	B	0.75 (1.69)	102.9 (0.79)	
NIC (4 mg/ gum)	B	0.76 (1.87)	100.9 (1.01)	
NM (15 mg/tablet)	C	1.09 (1.56)	101.4 (1.30)	90.0-110.0
NM (20 mg/tablet)	D	1.08 (1.21)	100.2 (1.52)	
NA (50 mg/tablet)	E	1.84 (1.43)	99.1 (1.03)	90.0-110.0
NM, NA (45 and 15 mg/tablet, respectively)	F	1.08 (1.85), 1.93 (1.42)	104.3 (1.86), 103.7 (1.95)	

* numbers in parentheses represent %RSDs (percent relative standard deviation), t_r = relative migration time calculated from $t_m/t_{I.S.}$

Additionally, the validated method could be applied for determination of COT in force degradation of NIC gum. The degradant (COT) was well separated from the major peak (NIC). Small amounts of COT (1.48% w/w) was found in the thermal degradation (90 °C, 6 h) of NIC gum sample and no other peaks were observed within 10 min (Figure 4.15b).

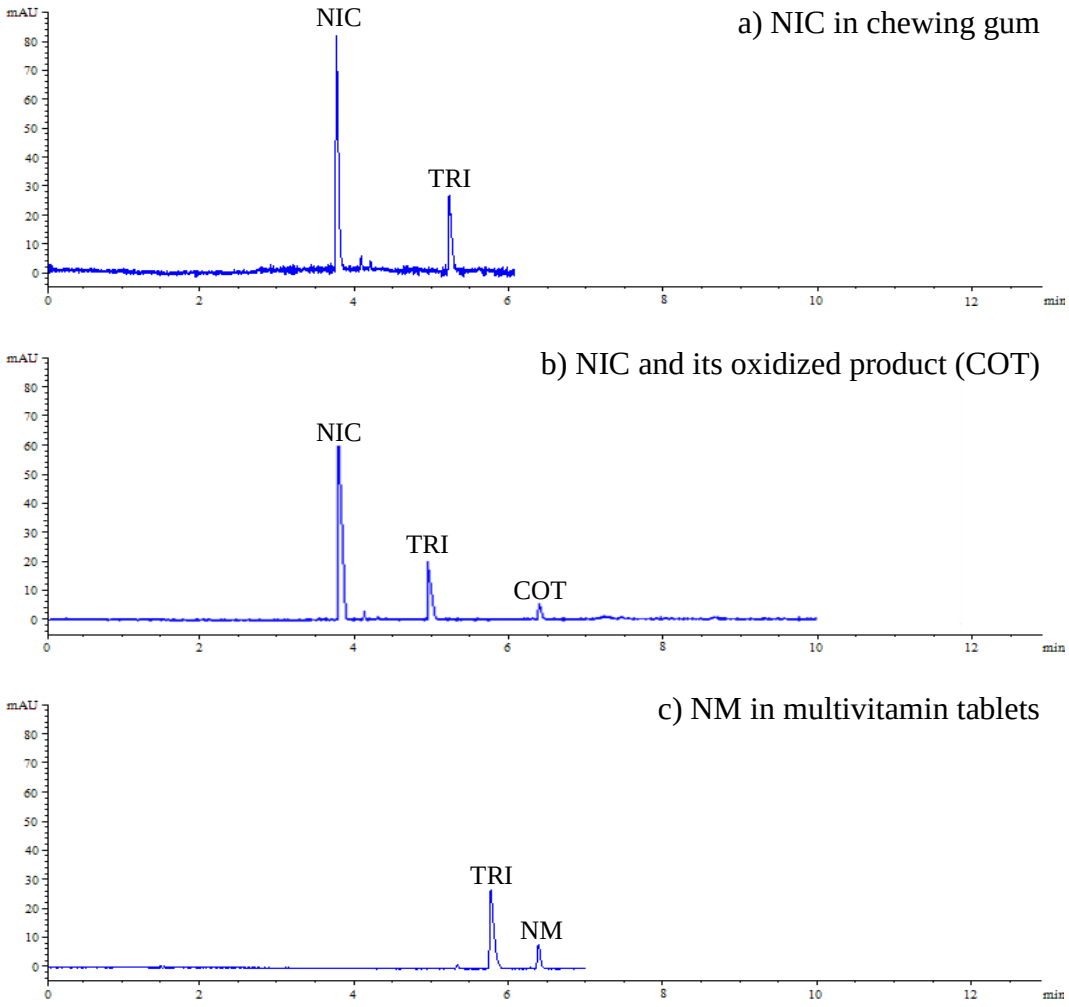

Figure 4.15 Electropherograms of a) NIC in chewing gum b) NIC and its oxidized product (COT) from stress test c) NM in multivitamin tablets d) NA in tablets and e) NM and NA in multivitamin tablets. Conditions: 25 mM sodium dihydrogen phosphate pH 2.1; capillary 64.5 cm total length (8.5 cm to the detector), 50 µm i.d. (extended pathlength); hydrodynamic injection at 50 mbar for 10 s; temperature 25 °C; voltage 30 kV; detection by UV absorbance at 260 nm. Peak identification: NIC, nicotine; TRI, triprolidine; NM, nicotinamide; COT, cotinine; NA, nicotinic acid.

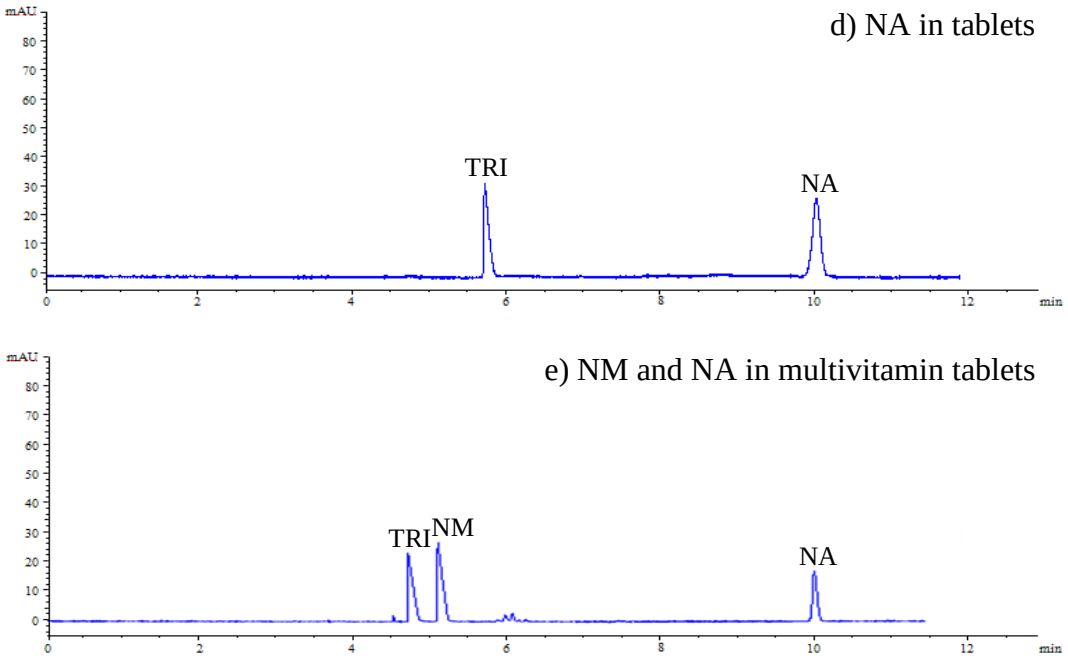

Figure 4.15 (continued) Electropherograms of a) NIC in chewing gum b) NIC and its oxidized product (COT) from stress test c) NM in multivitamin tablets d) NA in tablets and e) NM and NA in multivitamin tablets. Conditions: 25 mM sodium dihydrogen phosphate pH 2.1; capillary 64.5 cm total length (8.5 cm to the detector), 50 µm i.d. (extended pathlength); hydrodynamic injection at 50 mbar for 10 s; temperature 25 °C; voltage 30 kV; detection by UV absorbance at 260 nm. Peak identification: NIC, nicotine; TRI, triprolidine; NM, nicotinamide; COT, cotinine; NA, nicotinic acid.

CHAPTER V
CONCLUSION

CZE method for the simultaneous analysis of NIC, COT, NM and NA in pharmaceutical formulations was established using TRI as an internal standard. Optimization was performed by varying chemical parameters i.e. types of BGEs (citric acid vs sodium dihydrogen phosphate), pH of BGEs (2.1-3.5) and concentration of BGEs (15-30 mM) and instrumental parameters i.e. the applied voltage (20-30 kV) and injection time (5-20 s). The separation of the investigated pyridines was achieved in 10 min in 25 mM sodium dihydrogen phosphate (pH 2.1) using a capillary with a total length of 64.5 cm (8.5 cm to the detector), 50 µm i.d. (extended path length); hydrodynamic injection at 50 mbar for 10 s, temperature of 25 °C, the applied voltage of 30 kV and detection at 260 nm. The optimum condition provided a baseline separation of all compounds with the R_s > 3.60, N > 42,117, TF = 1.31-1.90, %RSD of t_m < 2.24 and %RSD of t_r < 1.18. The optimized CZE condition was validated in term of linearity, precision, recoveries, LOD and LOQ. Calibration curves were established over 3.2-1,000, 8-160, 10-200 and 10-200 µg/mL for NIC, NM, COT and NA, respectively. The good linearity (r^2 = 0.9970-0.9998) was obtained for all analytes. Precision of method was performed by intra-, inter-day and injection precision. The %RSD of t_m and t_r were less than 3.25 and 2.24, respectively and the %RSD of peak area and peak area ratio were less than 3.42 and 2.16, respectively. Recoveries were performed by standard addition method in a range of 80-120% of the assay concentrations. Recoveries of analytes were in the range of 96.4-101.6% with %RSD of 0.98-1.66. The LODs were 1, 2.5, 3 and 2 µg/mL (%RSD 1.79-2.06) and the LOQs were 3.2, 8, 10 and 5.5 µg/mL (%RSD 0.89-1.80) for NIC, NM, COT and NA, respectively. Robustness data obtaining from the variation around the nominal value of pH (2.1±0.2), injection time (10 s ±1) and voltages (25, 27 and 30 kV) revealed that t_r, and R_s were not significantly affected despite of the varied pH of the BGE, separating voltage and injection time. Finally, the validated method was applied for

the determination of NIC, NM, COT (in stress test of NIC gum) and NA in pharmaceutical formulations. The % label amounts of two different brands of NIC chewing gums, two different brands of NM in multivitamin tablet, one brands of NA tablet and one brand of combined formulation of NA and NM in multivitamin tablet were 99.1- 104.3% (%RSD < 1.95), which were within limit of USP. Additionally, this method could be applied for determination of COT in thermal degradation (90 °C, 6 h) of NIC gum. Small amounts of degradant (COT) (1.48% w/w) was found in the NIC gum sample and was well separated from the major peak (NIC).

PART I: REFERENCES

1 Chiu C-W, Liang H-H, Huang H-Y. Analyses of alkaloids in different products by NACE-MS. Electrophoresis. 2007; 28(22): 4220-6.

2 Kataoka H, Inoue R, Yagi K, Saito K. Determination of nicotine, cotinine, and related alkaloids in human urine and saliva by automated in-tube solid-phase microextraction coupled with liquid chromatography-mass spectrometry. J Pharm Biomed Anal. 2009; 49(1): 108-14.

3 Stepanov I, Feuer R, Jensen J, Hatsukami D, Hecht SS. Mass spectrometric quantitation of nicotine, cotinine, and 4-(Methylnitrosamino)-1-(3-Pyridyl)-1-Butanol in Human Toenails. Cancer Epidemiol Biomarkers Prev. 2006; 15(12): 2378-83.

4 Kataoka H, Inoue R, Yagi K, Saito K. Determination of nicotine, cotinine, and related alkaloids in human urine and saliva by automated in-tube solid-phase microextraction coupled with liquid chromatography–mass spectrometry. J Pharm Biomed Anal. 2009; 49: 108-14.

5 Chang Y-L, Tsai P-L, Chou Y-C, Tien J-H, Tsai T-H. Simultaneous determination of nicotine and its metabolite, cotinine, in rat blood and brain tissue using microdialysis coupled with liquid chromatography: Pharmacokinetic application. J Chromatogr A. 2005; 1088: 152-7.

6 Tambwekar KR, Kakariya RB, Garg S. A validated high performance liquid chromatographic method for analysis of nicotine in pure form and from formulations. J Pharm Biomed Anal. 2003;32:441-50.

7 Tricker AR. Biomarkers derived from nicotine and its metabolites: A review*. Beiträge zur Tabakforschung international/contributions to tobacco research. 2006; 22 (3).

8 Hădărugă D, Hădărugă N, Butnaru G, Tatu C, Gruia A. Bioactive microparticles (10): thermal and oxidative stability of nicotine and its complex with β-cyclodextrin. J Incl Phenom Macro Chem. 2010; 68(1): 155-64.

9 The United State Pharmacopeial Convention. USP 31 NF 26, Rockville: The Board of Trustees; 2008.

10 British Pharmacopoeia Commission British Pharmacopoeia. The Stationery Office, London; 2008.

11 Chen Z, Chen Y. Aqueous room temperature ionic liquids as green mobile phases for liquid chromatographic analysis of nicotine and cotinine in serum. Anal Lett. 2010; 43(3): 393-405.

12 Miller EI, Norris H-RK, Rollins DE, Tiffany ST, Wilkins DG. A novel validated procedure for the determination of nicotine, eight nicotine metabolites and two minor tobacco alkaloids in human plasma or urine by solid-phase extraction coupled with liquid chromatography-electrospray ionization-tandem mass spectrometry. J Chromatogr B. 2010; 878(9-10): 725-37.

13 Yue B, Kushnir MM, Urry FM, Rockwood AL. Quantitation of nicotine, its metabolites, and other related alkaloids in urine, serum, and plasma using LC-MS-MS clinical applications of mass spectrometry: Meth Mol Biol. 2010; 603: 389-98.

14 Shakleya DM, Huestis MA. Simultaneous and sensitive measurement of nicotine, cotinine, trans-3'-hydroxycotinine and norcotinine in human plasma by liquid chromatography-tandem mass spectrometry. J Chromatogr B. 2009; 877(29): 3537-42.

15 Aresta A, Palmisano F, Zambonin CG. Simultaneous determination of caffeine, theobromine, theophylline, paraxanthine and nicotine in human milk by liquid chromatography with diode array UV detection. Food Chem. 2005; 93(1): 177-81.

16 Shakleya D, Huestis M. Simultaneous quantification of nicotine, opioids, cocaine, and metabolites in human fetal postmortem brain by liquid chromatography tandem mass spectrometry. Anal Bioanal Chem. 2009; 393(8): 1957-65.

17 Yang X-L, Luo M-B, Ding J-H. Rapid determination of nicotine in saliva by liquid phase microextraction-high performance liquid chromatography. Chinese J Anal Chem. 2007; 35(2): 171-5.

18 Yang J, Hu Y, Cai J-B, Zhu X-L, Su Q-D. A new molecularly imprinted polymer for selective extraction of cotinine from urine samples by solid-phase extraction. Anal Bioanal Chem. 2006; 384(3): 761-8.

19 Shrivas K, Patel DK. Liquid-phase microextraction combined with gas chromatography mass spectrometry for rapid determination of nicotine in one-drop of nightshades vegetables and commercial food products. Food Chem. 2010; 122(1): 314-8.

20 Cai J, Liu B, Lin P, Su Q. Fast analysis of nicotine related alkaloids in tobacco and cigarette smoke by megabore capillary gas chromatography. J Chromatogr A. 2003; 1017(1-2): 187-93.

21 Brcic Karaconji I, Skender L, Karacic Vl. Determination of nicotine and cotinine in urine by headspace solid phase microextraction gas chromatography with mass spectrometric detection. Ljubljana, Acta Chim Slov; 2007; 54: 74-78.

22 Kim I, Darwin WD, Huestis MA. Simultaneous determination of nicotine, cotinine, norcotinine, and trans-3'-hydroxycotinine in human oral fluid using solid phase extraction and gas chromatography-mass spectrometry. J Chromatog B. 2005; 814(2): 233-40.

23 Man CN, Ismail S, Harn GL, Lajis R, Awang R. Determination of hair nicotine by gas chromatography-mass spectrometry. J Chromatogr B. 2009; 877(3): 339-42.

24 Toraño JS, van Kan HJM. Simultaneous determination of the tobacco smoke uptake parameters nicotine, cotinine and thiocyanate in urine, saliva and hair, using gas chromatography-mass spectrometry for characterisation of smoking status of recently exposed subjects. Analyst. 2003; 128(7): 838-43.

25 Sheng LQ, Ding L, Tong HW, Yong GP, Zhou XZ, Liu SM. Determination of nicotine-related alkaloids in tobacco and cigarette smoke by GC-FID. Chromatographia. 2005; 62(1): 63-8.

26 Shen J, Shao X. Determination of tobacco alkaloids by gas chromatography-mass spectrometry using cloud point extraction as a preconcentration step. Anal Chim Acta. 2006; 561(1-2): 83-7.

27 Baidoo EEK, Clench MR, Smith RF, Tetler LW. Determination of nicotine and its metabolites in urine by solid-phase extraction and sample stacking capillary electrophoresis-mass spectrometry. J Chromatogr B. 2003; 796: 303-13.

28 Chang P-L, Lee K-H, Hu C-C, Chang H-T. CE with sequential light-emitting diode-induced fluorescence and electro-chemiluminescence detections for the determination of amino acids and alkaloids. Electrophoresis. 2007; 28(7): 1092-9.

29 Kodama S, Morikawa A, Nakagomi K, Yamamoto A, Sato A, Suzuki K, et al. Enantioseparation of nicotine alkaloids in cigarettes by CE using sulfated β-CD as a chiral selector and a capillary coated with amino groups. Electrophoresis. 2009; 30(2): 349-56.

30 Lochmann H, Bazzanella A, Kropsch S, Bächmann K. Determination of tobacco alkaloids in single plant cells by capillary electrophoresis. J Chromatogr A. 2001; 917: 311-7.

31 Marsh A, Clark BJ, Altria KD. Orthogonal separations of nicotine and nicotine-related alkaloids by various capillary electrophoretic modes. Electrophoresis. 2004; 25: 1270-8.

32 Terekhova IV, Scriba GKE. Study on complex formation of biologically active pyridine derivatives with cyclodextrins by capillary electrophoresis. J Pharm Biomed Anal. 2007; 45(4): 688-93.

33 Ralapati S. Capillary electrophoresis as an analytical tool for monitoring nicotine in ATF regulated tobacco products. J Chromatogr B. 1997; 695: 117-29.

34 Trenerry VC. The application of capillary electrophoresis to the analysis of vitamins in food and beverages. Electrophoresis 2001; 22: 1468-78.

35 Keung TP, Lixuan Z. Quantitative analysis of nicotinic acid, nicotinamide and 3-cyanopyridine in industrial effluent by high performance liquid chromatography. Front Chem China. 2007; 2(3): 270–3.

36. Shen HC, Colletti SL. Novel patent publications on high-affinity nicotinic acid receptor agonists. Expert Opin Ther Pat. 2009; 19(7): 957-67.

37 Rosenson RS. Antiatherothrombotic effects of nicotinic acid. Atherosclerosis. 2003; 171(1): 87-96.

38 Szafarz M, Lomnicka M, Sternak M, Chlopicki S, Szymura-Oleksiak J. Simultaneous determination of nicotinic acid and its four metabolites in rat plasma using high performance liquid chromatography with tandem mass spectrometric detection (LC/MS/MS). J Chromatogr B. 2010; 878(11-12): 895-902.

39 Guyton JR, Simmons PD. Flushing and other dermatologic adverse events associated with extended-release niacin therapy. J Clin Lipid. 2009; 3(2): 101-8.

40 Jain KS, Kathiravan MK, Somani RS, Shishoo CJ. The biology and chemistry of hyperlipidemia. Bioor Med Chem. 2007; 15(14): 4674-99.

41 Esteve-Romero JS, Monferrer-Pons L, Ramis-Ramos G, Garcia-Alvarez-Coque MC. Enhanced spectrophotometric determination of nicotinic acid in a sodium dodecyl sulphate micellar medium. Talanta. 1995; 42(5): 737-45.

42 Wang X, Yang N, Wan Q. Cyclic voltammetric response of nicotinic acid and nicotinamide on a polycrystalline gold electrode. Electrochim Acta. 2006; 52: 361-8.

43 Lang R, Wahl A, Skurk T, Yagar EF, Schmiech L, Eggers R, et al. Development of a hydrophilic liquid interaction chromatography-high-performance liquid chromatography-tandem mass spectrometry based stable isotope dilution analysis and pharmacokinetic studies on bioactive pyridines in human plasma and urine after coffee consumption. Anal Chem. 2010; 82(4): 1486-97.

44 Almagro I, Andres M, Vera S. Determination of water-soluble vitamins in pharmaceutical preparations by reversed-phase high-performance liquid chromatography with a mobile phase containing sodium dodecylsulphate and *n*-propanol. Chromatographia. 2002; 55(3): 185-8.

45 Catz P, Shinn W, Kapetanovic IM, Kim H, Kim M, Jacobson EL, et al. Simultaneous determination of myristyl nicotinate, nicotinic acid, and nicotinamide in rabbit plasma by liquid chromatography-tandem mass spectrometry using methyl ethyl ketone as a deproteinization solvent. J Chromatogr B. 2005; 829(1-2): 123-35.

46 Pfuhl P, Kärcher U, Häring N, Baumeister A, Tawab MA, Schubert-Zsilavecz M. Simultaneous determination of niacin, niacinamide and nicotinuric acid in human plasma. J Pharm Biomed Anal. 2005; 36(5): 1045-52.

47 Gomis DB, González LL, Álvarez DG. Micellar electrokinetic capillary chromatography analysis of water-soluble vitamins. Anal Chim Acta. 1999; 396(1): 55-60.

48 Iwaki M, Murakami E, Kakehi K. Chromatographic and capillary electrophoretic methods for the analysis of nicotinic acid and its metabolites. J Chromatogr B: Biomed Sci Appl. 2000; 747(1-2): 229-40.

49 Su SC, Chou SS, Hwang DF, Chang PC, Liu CH. Capillary zone electrophoresis and micellar electrokinetic capillary chromatography for determining water-soluble vitamins in commercial capsules and tablets. J Food Sci. 2001; 66(1): 10-4.

50 Stolker AAM, Niesing W, Hogendoorn EA, Bisoen Rambali A, Vleeming W. Determination of nicotine and cotinine in rat plasma by liquid chromatography-tandem mass spectrometry. J Chromatogr A. 2003; 1020(1): 35-43.

51 Gorrod JW, III PJ. Analytical determination of nicotine and related compounds and their metabolites. Amsterdam: Elsevier; 1999.

52 Yildiz D. Nicotine, its metabolism and an overview of its biological effects. Toxicon. 2004; 43(6): 619-32.

53 Capella-Peiro M-E, Carda-Broch S, Monferrer-Pons L, Esteve-Romero J. Micellar liquid chromatographic determination of nicotinic acid and nicotinamide after precolumn König reaction derivatization. Anal Chima Acta. 2004; 517(1-2): 81-7.

54 Findlay JWA, Butz RF, Sailstad JM, Warren JT, Welch RM. Pseudoephedrine and triprolidine in plasma and breast milk of nursing mothers. Br J Clin Pharmacol, (1984). 1984; 18: 901-6.

55 Meger M, Meger-Kossien I, Schuler-Metz A, Janket D, Scherer G. Simultaneous determination of nicotine and eight nicotine metabolites in urine of smokers using liquid chromatography-tandem mass spectrometry. J Chromatogr B. 2002; 778(1-2): 251-61.

56 Benowitz NL, Jacob P, Fong I, Gupta S. Nicotine metabolic profile in man: comparison of cigarette smoking and transdermal nicotine. J Pharmacol Exp Ther. 1994; 268(1): 296-303.

57 Tricker AR. Nicotine metabolism, human drug metabolism polymorphisms, and smoking behaviour. Toxicology. 2003; 183(1-3): 151-73.

58 Karačonji IB, Skender L, Karačić V. Determination of nicotine and cotinine in urine by headspace solid phase microextraction gas chromatography with mass spectrometric detection. Acta Chim Slov. 2007;54:74-8.

59 Kardani F, Daneshfar A, Sahrai R. Determination of nicotine, anabasine, and cotinine in urine and saliva samples using single-drop microextraction. J Chromatogr B. 2010; 878(28): 2857-62.

60 Hegaard HK, Kjærgaard H, Møller LF, Wachmann H, Ottesen B. Determination of a saliva cotinine cut-off to distinguish pregnant smokers from pregnant non-smokers. Acta Obstet Gynecol Scand. 2007; 86(4): 401-6.

61 Yakovleva E, Belotserkovskaya V, Skrypnik O. A gas-chromatographic study of the retention of reaction components in the catalytic oxidation of β-picoline to nicotinic acid. Anal Chem. 2008; 63(9): 863-6.

62 Lafay F, Vulliet E, Flament-Waton M-M. Contribution of microextraction in packed sorbent for the analysis of cotinine in human urine by GC–MS. Anal Bioanal Chem. 2010; 396(2): 937-41.

63 Musshoff F, Rosendahl W, Madea B. Determination of nicotine in hair samples of pre-Columbian mummies. Forensic Sci Int. 2009; 185(1-3): 84-8.

64 Pieraccini G, Furlanetto S, Orlandini S, Bartolucci G, Giannini I, Pinzauti S, et al. Identification and determination of mainstream and sidestream smoke components in different brands and types of cigarettes by means of solid-phase microextraction-gas chromatography-mass spectrometry. J Chromatogr A. 2008; 1180(1-2): 138-50.

65 Welerowicz T, Śliwka K, Buszewski B. HPLC analysis of cotinine in urine after SPE with a cholesterol-modified adsorbent. Chromatographia. 2007; 66(1): 63-70.

66 Pietsch J, Gunther J, Henle T, DreBler J. Simultaneous determination of thirteen plant alkaloids in a human specimen by SPE and HPLC. J Sep Sci. 2008; 13: 2410-6.

67 Chin-Chen M-L, Rambla-Alegre M, Durgavanshi A, Bose D, Esteve-Romero J. Rapid and sensitive determination of nicotine in formulations and biological fluid using micellar liquid chromatography with electrochemical detection. J Chromatogr B. 2010; 878(26): 2397-402.

68 Malkawi AH, Al-Ghananeem AM, de Leon J, Crooks PA. Nicotine exposure can be detected in cerebrospinal fluid of active and passive smokers. J Pharm Biomed Anal. 2009; 49(1): 129-32.

69 Baumann F, Regenthal R, Burgos-Guerrero IL, Hegerl U, Preiss R. Determination of nicotine and cotinine in human serum by means of LC/MS. J Chromatogr B. 2010; 878(1): 107-11.

70 Kim I, Huestis MA. A validated method for the determination of nicotine, cotinine, trans-3′-hydroxycotinine, and norcotinine in human plasma using solid-phase extraction and liquid chromatography-atmospheric pressure chemical ionization-mass spectrometry. J Mass Spec. 2006; 41(6): 815-21.

71 Fan Z, Xie F, Xia Q, Wang S, Ding L, Liu H. Simultaneous determination of nicotine and its nine metabolites in human urine by LC–MS–MS. Chromatographia. 2008; 68: 623–7.

72 Marclay F, Saugy M. Determination of nicotine and nicotine metabolites in urine by hydrophilic interaction chromatography-tandem mass spectrometry: Potential use of smokeless tobacco products by ice hockey players. J Chromatogr A. 2010; 1217(48): 7528-38.

73 Jacob III P, Yu L, Duan M, Ramos L, Yturralde O, Benowitz NL. Determination of the nicotine metabolites cotinine and trans-3'-hydroxycotinine in biologic fluids of smokers and non-smokers using liquid chromatography-tandem mass spectrometry: Biomarkers for tobacco smoke exposure and for phenotyping cytochrome P450 2A6 activity. J Chromatogr B. 2011; 879(3-4): 267-76.

74 Concheiro M, Gray T, Shakleya D, Huestis M. High-throughput simultaneous analysis of buprenorphine, methadone, cocaine, opiates, nicotine, and metabolites in oral fluid by liquid chromatography tandem mass spectrometry. Anal Bioanal Chem. 2010; 398(2): 915-24.

75 Fukuwatari T, Shibata K. Urinary water soluble vitamins and their metabolite contents as nutritional markers for evaluating intakes in young Japanese women. J Nutr Sci Vitaminol. 2008; 54: 223-9.

76 Vidovic S, Stojanovic B, Veljkovic J, Prazic-Arsic L, Roglic G, Manojlovi D. Simultaneous determination of some water-soluble vitamins and preservatives in multivitamin syrup by validated stability-indicating high-performance liquid chromatography method. J Chromatogr A. 2008; 1202: 155-62.

77 Cheng Z, Wang Y, Xu H, Jia Z, Li H, Hu R. Observation of nicotinic acid in nicorandil samples and simultaneous determination of nicorandil and its three degradation products in raw drug and tablet form by high performance liquid chromatography. J Anal Chem. 2009; 64(10): 1059-65.

78 Zafra-Gomez A, Garballo A, Morales JC, Garcia-Ayuso LE. Simultaneous determination of eight water-soluble vitamins in supplemented foods by liquid chromatography. J Agric Food Chem. 2006; 54(13): 4531-6.

79 Karatapanis AE, Fiamegos YC, Stalikas CD. HILIC separation and quantitation of water-soluble vitamins using diol column. J Sep Sci. 2009; 32(7): 909-17.

80 Paternoster T, Vrhovsek U, Pertot I, Duffy B, Gessler C, Mattivi F. Determination and confirmation of nicotinic acid and its analogues and derivates in pear and apple blossoms using high-performance liquid chromatography−diode array−electrospray ionization mass spectrometry. J Agri Food Chem. 2009; 57(21): 10038-43.

81 Chen Z, Chen B, Yao S. High-performance liquid chromatography/ electrospray ionization-mass spectrometry for simultaneous determination of taurine and 10 water-soluble vitamins in multivitamin tablets. Anal Chim Acta. 2006; 569(1-2): 169-75.

82 Mallett DN, Dayal S, Dear GJ, Pateman AJ. The determination of nicotinic acid in plasma by mixed-mode liquid chromatography-tandem mass spectrometry following ion exchange solid phase extraction. J Pharm Biomed Anal. 2006;4 1(2): 510-6.

83 Lang R, Yagar EF, Eggers R, Hofmann T. Quantitative investigation of trigonelline, nicotinic acid, and nicotinamide in foods, urine, and plasma by means of LC-MS/MS and stable isotope dilution analysis. J Agri Food Chem. 2008; 56(23): 11114-21.

84 Jia L, Liu Y, Du Y, Xing D. Pressurized capillary electrochromatographic analysis of water-soluble vitamins by combining with on-line concentration technique. J Chromatogr A. 2007; 1154(1-2): 416-22.

85 Marszałł MP, Markuszewski MJ, Kaliszan R. Separation of nicotinic acid and its structural isomers using 1-ethyl-3-methylimidazolium ionic liquid as a buffer additive by capillary electrophoresis. J Pharm Biomed Anal. 2006; 41: 329–32.

86 Figueiredo EC, de Oliveira DM, de Siqueira MEPB, Arruda MAZ. On-line molecularly imprinted solid-phase extraction for the selective spectrophotometric determination of nicotine in the urine of smokers. Anal Chim Acta. 2009; 635(1): 102-7.

87 Zhou Y, Yu H, Zhang L, Xu H, Wu L, Sun J, et al. A new spectrofluorometric method for the determination of nicotine base on the inclusion interaction of methylene blue and cucurbit[7]uril. Microchim Acta. 2009; 164: 63–8.

88 Lin MS, Wang JS, Lai CH. Electrochemiluminescent determination of nicotine based on tri(2,2'-bipyridyl) ruthenium (II) complex through flow injection analysis. Electrochim Acta. 2008;5 3(26): 7775-80.

89 Zhaoyang W, Xiaolei Z, Yunhui Y, Guoli S, Ruqin Y. A sensitive nicotine sensor based on molecularly imprinted electropolymer of o-aminophenol. Front Chem China 2006; 2: 183−7.

90 Levent A, Yardim Y, Senturk Z. Voltammetric behavior of nicotine at pencil graphite electrode and its enhancement determination in the presence of anionic surfactant. Electrochim Acta. 2009; 55(1): 190-5.

91 Wielkoszynski T, Tyrpien K, Szumska M. The enzyme-linked immunosorbent assay (ELISA) method for nicotine metabolites determination in biological fluids. J Pharm Biomed Anal. 2009; 49(5): 1256-60.

92 Yang N, Wang X. Thin self-assembled monolayer for voltammetrically monitoring nicotinic acid in food. Colloids Surf B. 2008; 61(2): 277-81.

93 Wang X, Yang N, Wan Q. Cyclic voltammetric response of nicotinic acid and nicotinamide on a polycrystalline gold electrode. Electrochim Acta. 2006; 52(1): 361-8.

94 Weston A, Brown PR. HPLC and CE Principles and Practice. Utah: Academic Press; 1997.

95 Tagliaroa F, Manettoa G, Crivellentea F, Smithb FP. A brief introduction to capillary electrophoresis. Forensic Sci Int. 1998; 92: 75-88.

96 Leaders JP, editor. Handbook of capillary electrophoresis. Florida: CRC Press Inc.; 1994.

97 Janasek D, Schilling M, Franzke J, Manz A. Isotachophoresis in Free-Flow Using a Miniaturized Device. Anal Chem. 2006; 78(11): 3815-9.

98 Silva M. MEKC: An update focusing on practical aspects. Electrophoresis. 2007; 28(1-2): 174-92.

99 Silva M. Micellar electrokinetic chromatography: Methodological and instrumental advances focused on practical aspects. Electrophoresis. 2009; 30(1): 50-64.

100 Marsh A, Clark B, Broderick M, Power J, Donegan S, Altria K. Recent advances in microemulsion electrokinetic chromatography. Electrophoresis. 2004; 25(23-24): 3970-80.

101 Geiser L, Veuthey J-L. Nonaqueous capillary electrophoresis in pharmaceutical analysis. Electrophoresis. 2007; 28(1-2): 45-57.

102 Zhang L, Wang R, Yu Y, Zhang Y. Capillary electrophoresis with laser-induced fluorescence and pre-column derivatization for the analysis of illicit drugs. J Chromatogr B. 2007; 857(1): 130-5.

103 Wang W, Tang J, Wang S, Zhou L, Hu Z. Method development for the determination of coumarin compounds by capillary electrophoresis with indirect laser-induced fluorescence detection. J Chromatogr A. 2007; 1148(1): 108-14.

104 Kubán P, Hauser PC. A review of the recent achievements in capacitively coupled contactless conductivity detection. Anal Chim Acta. 2008; 607(1): 15-29.

105 Zemann AJ. Capacitively coupled contactless conductivity detection in capillary electrophoresis. Electrophoresis. 2003; 24(12-13): 2125-37.

106 Zikmundová J, Tuma P, Opekar F. A dual spectrophotometric/contactless conductivity detector for CE determination of incompletely separated amino acids. J Sep Sci. 2008; 31(2): 353-5.

107 Li X, Tong Y-L, Liu C, Li O-L, Yang X-J, Chen Z-G. Dual detection methods for microchip and conventional capillary electrophoreses. Chinese J Anal Chemistry. 2009; 37(10): 1547-54.

108 Ryvolová Mt, Preisler J, Foret Fe, Hauser PC, Krásenský P, Paull B, et al. Combined contactless conductometric, photometric, and fluorimetric single point detector for capillary separation methods. Anal Chem. 2010; 82(1): 129-35.

109 Ohnesorge J, Neusüß C, Wätzig H. Quantitation in capillary electrophoresis-mass spectrometry. Electrophoresis. 2005; 26(21): 3973-87.

110 Klampfl CW. Recent advances in the application of capillary electrophoresis with mass spectrometric detection. Electrophoresis. 2006; 27(1): 3-34.

PART II: THE POTENTIAL OF MICROCHIP CAPILLARY ELECTROPHORESIS ON MICROORGANISM DETECTION

CHAPTER VI
INTRODUCTION

The emergence of microfluidics and lab-on-a-chip technology has generated much interest in analytical chemistry over recent years. The first applications were those of electrophoretic separations, primarily because of the simplicity of using voltages to control fluid and analyte movement within these devices. The improvement of throughput for many samples, particularly in the biological and life sciences that revolve around the use of electrophoresis is also needed. Moving to the microfluidic platform results in separations that can be achieved in shorter time of analysis than that previously being achieved in conventional CE instrumentation and there are now a number of examples illustrating the benefits in moving to the microchip platform (1-4). In order to conduct research in microfluidics, it is necessary to have access to analytical microchips and also to have the instrumentation to use these microchips. Early researchers had to make their own microchips from plastics and glass, piecing together instrumentation to make an appropriate detection system (5-12). However, the commercial suppliers present an alternative route to mainstream researches and there are now a number of commercial avenues to microchip sources, with both standard and customized designs available, as well as those that also provide the necessary equipment to perform simple electrophoretic separations.

One of the commercial consumer-grade instrument from the Agilent 2100 Bioanalyzer (Agilent Technologies, Waldbronn, Germany) using relatively simple chips, through to the products from Caliper LifeSciences. Generally, this system is sold as kits with fixed methods and little flexibility, which approaches for a variety of voltage-driven separation techniques, addressing separation of DNA, RNA and protein samples. However, this work aimed to evaluate performances of the commercial microchip CE instrument and its DNA chips for orienting this instrument as a generic CE platform with high throughput analysis. The main limitation in this regard is the

method of detection, with the Bioanalyzer featuring a 634/38 nm laser for laser induced fluorescence (LIF) detection with emission collected at 685/22 nm (13-14) and the short separation length, with 14 mm from injection to the detector. Therefore, several structurally related fluorescent basic blue dyes (*i.e.* methylene blue (MB), nile blue A perchlorate (NB), toluidine blue (TB) and brilliant cesyl blue (BC)), were selected as test analytes to develop appropriate microchip condition for the separation of basic dyes. Non-aqueous CE (NACE) was optimized by varying types and concentrations of BGEs, BGE solvents and water contents in the BGE. The optimal NACE separation of fluorescent dyes was achieved in 80 mM NH_4OAc, 870 mM acetic acid in DMSO using DNA chip with separation length of 14 mm, injection/separation voltage 1,400/1,500 V and temperature of 25°C. The optimized NACE condition was validated in term of linearity, precision, LOD and LOQ.

Detection of microbial contamination especially pathogenic microorganisms is critical to ensure the safety and quality in food/beverage, pharmaceutical and medical industries (15-16). Conventional culture methods are widely used for bacterial enumeration; however, for accurate enumeration of bacterial numbers, epifluorescence microscopy and flow cytometry have been used to detect various fluorescent dyes stained cells (17-21). Although epifluorescennce microscopic observation provides color and cell shape information, individual differences may rise due to human error (22). It is also laborious and time consuming. Flow cytometry is an effective alternative to traditional methods of cell detection, since the procedure offers rapid, sensitive, and reliable quantification of individual cells. However, flow cytometer is relatively expensive and require complicated maintenance and skilled operators. On-chip flow cytometry can be an interesting promise due to its miniaturization and automation feasibility (23). This study investigated the on-chip flow cytometry for the cell enumeration of bacteria and fungi with appropriate fluorescent staining. Nile blue (NB) was used as a fluorescent stain for *E. coli, B. subtilis, M. luteus, S. aureus, C. albicans* and *L. fungicola*. The optimization of NB concentration for cell staining was investigated on the on-chip flow cytometry to ensure complete cell staining. Then, analyses of single microorganism were carried out in 1 mg/mL CTAB in 1 mM Tris/0.33 mM citric acid, pH 7.0 using 5 mg/mL SB3-10 as blocking agent, separation length 14 mm, injection/separation voltage -1,000/-

1,000 V and temperature of 25°C. The developed method provided the simple, cheap, rapid and efficient microbial analysis which would be useful for contamination testing.

However, separations of a mixture containing *E. coli*, *S. aureus* and *C. albicans* had to be re-optimized by varying pHs of BGEs and amount of PEO in TBE buffer. The optimal condition was achieved in 3.94 mM Tris, 0.56 mM boric acid and 0.013 mM Na_2EDTA pH 10.5 containing 0.025% PEO, separation length 14 mm, injection/separation voltage 1,000/1,000 V and temperature of 25°C. This condition was also applied for the separation of Gram positive bacteria such as *B. subtilis*, *M. luteus* and *S. aureus*.

CHAPTER VII
LITERATURE REVIEW

1. Microchip capillary electrophoresis

Recently, microfluidics has generated the enormous interest of researches in analytical sciences as a novel approach to high speed separation, increase sample processing throughput, high separation efficiencies, integration of sample preparation steps into the device and small reagent and sample consumption (24). The first applications were those of electrophoretic separations, primarily because of the simplicity of using voltages to control fluid and analyte movement within these devices. The improvement of throughput for many samples has been rapidly adapted to a variety of applications those are environmental, industrial and particularly the biological and life science applications. Moving to the microfluidic platform results in separations that can be achieved in shorter time of analysis than that previously being achieved in conventional CE instrumentation and there are now a number of examples illustrating the benefits in moving to the microchip platform (1-4). In order to conduct research in microfluidics, it is necessary to have access to analytical microchips and also to have the instrumentation to use these microchips. Microchip CE separations have been performed in a variety of materials *i.e.* glass and polymer. Several characteristics of material allow it to serve as a suitable substrate for microchip CE applications and these are listed below (24).

- The substrate should supports a stable EOF because it affects the apparent mobility. If the EOF is not stable, changes in apparent mobilities provide irreproducible results and makes difficulty in peak identification by migration time.

- Most detection is based on optical schemes thus, the substrate is necessary to provide a good optical clarity at the monitoring wavelengths. The substrate material must possess small extinction coefficients at those wavelengths in UV absorption detection. For fluorescence detection, the excitation wavelength must not produce large backgrounds.

- The device requires the microfabrication of channels with μm dimensions. Therefore, the material should provide accessibility to a variety of microfabrication technologies to make high reproducibility and the required dimensions and aspect ratios. In addition, the fabrication should produce fairly smooth sidewalls.

- The substrate materials may require chemical modification of its surface to modify or suppress the EOF or establish a stationary phase (capillary electrochromatography, CEC). Therefore, stable and diverse modification chemistries must be supported by the intended substrate material.

- The microchip CE separation may require the use of either an aqueous, organic or mixed organic/aqueous electrolyte. Therefore, the substrate must be compatible with the background electrolyte due to a good wettability with a wide range of electrolytes and not providing deformation. Additionally, the substrate should possess good thermal conductivity and lead to minimize Joule heating when operated at high electric field strengths (24).

CE chip are mainly fabricated using various glass sustrates, from inexpensive soda lime glass to high quality quartz because they are similar to fused silica that uses in conventional CE. Also, the favorable optically transparent properties of glass and quartz substrates offer the detection of analytes using a variety of optical readout modes such as absorbance (UV-Vis), LIF, electrochemiluminescence, or refractive index. Its surface chemistry is reasonably well-characterized, compatible with most solvents, stable in high temperature applications due to its high glass transition temperature (Table 7.1). The most significant drawbacks associated with using glass as a substrate is the requirement for a cleanroom-based fabrication facilities. Fabrication for glass substrate are usually generated using standard photolithographic technologies (25-26).

Polymer microchips has generated attention due to the use of replication based microtechnologies with the ability to manufacture inexpensive devices in large numbers, hence being disposable. A additional attractive is the wide range of available plastic materials (*e.g.* polyethylenephthalate (PETG), poly(dimethylsiloxane) (PDMS), polymethyl methacrylate (PMMA), polyimide (PI), polystyrene, polyvinylchloride and polycarbonate), which allows the manufacturer to choose

materials' properties suitable for their specific applications. Methods for the fabrication of polymer microchips include laser ablation, injection molding, silicone ruber casting and hot embossing (26-27)

Table 7.1 Comparison of glass and polymers properties (25, 27)*

Property	Glass	PDMS	PMMA	PI
Polymer type	NA	Elatomeric	Thermoplastic	Thermoplastic
Glass temperature (°C)	525	-120	106	285
Useful temperature range (°C)	≤ 500	-40 to 50	-70 to 100	-73 to 240
Thermal conductivity (W/mK)	1.2	0.17 to 0.3	0.186	0.2
Visible transmittance (%)	> 90	91	92	87
Surface charge (native)	Yes	Weak	Yes	No
Chemical resistance				
Acid	Excellent	Fair-good	Good	Fair-good
Solvent	Excellent	Poor	Poor	Fair
Alkali	Excellent	Poor-fair	Excellent	Fair-good

*PDMS = poly(dimethylsiloxane), PMMA = polymethyl methacrylate, PI = polyimide

Sample introduction in microchip CE differs from conventional CE. Integrated sample injection is typically used to produce the small sample size (measured in pL) required for microchip CE. The integrated injectors are usually either cross channel injector (single T injector), form by intersection the sample to sample waste reservoirs or twin T injector where the two arms of the sample to sample waste channel are offset to form a larger injector region (Figure 7.1). Injection volume is defined by electrokinetic injection of short injection plugs. Band broadending of plug injection can occur from leakage around the intersection. The leakage has been attributed to diffusive and convective phenomena. This leakage can be reduced by

using the pinched mode in which the buffers from two adjacent channels are flowed by application of electrical bias to shape the plug (26). Sample leakage can cause peak tailing. To avoid this, the buffer is pushed back into the sample channel and analyte waste channel by applying a push-back voltage. This can be applied for a short duration to provide a clean cut of the injection plug. In the case of repetitive injection/separation, the loading time for a subsequent injection should be long enough to compensate for the location of the sample front pushed back in the previous separation (28).

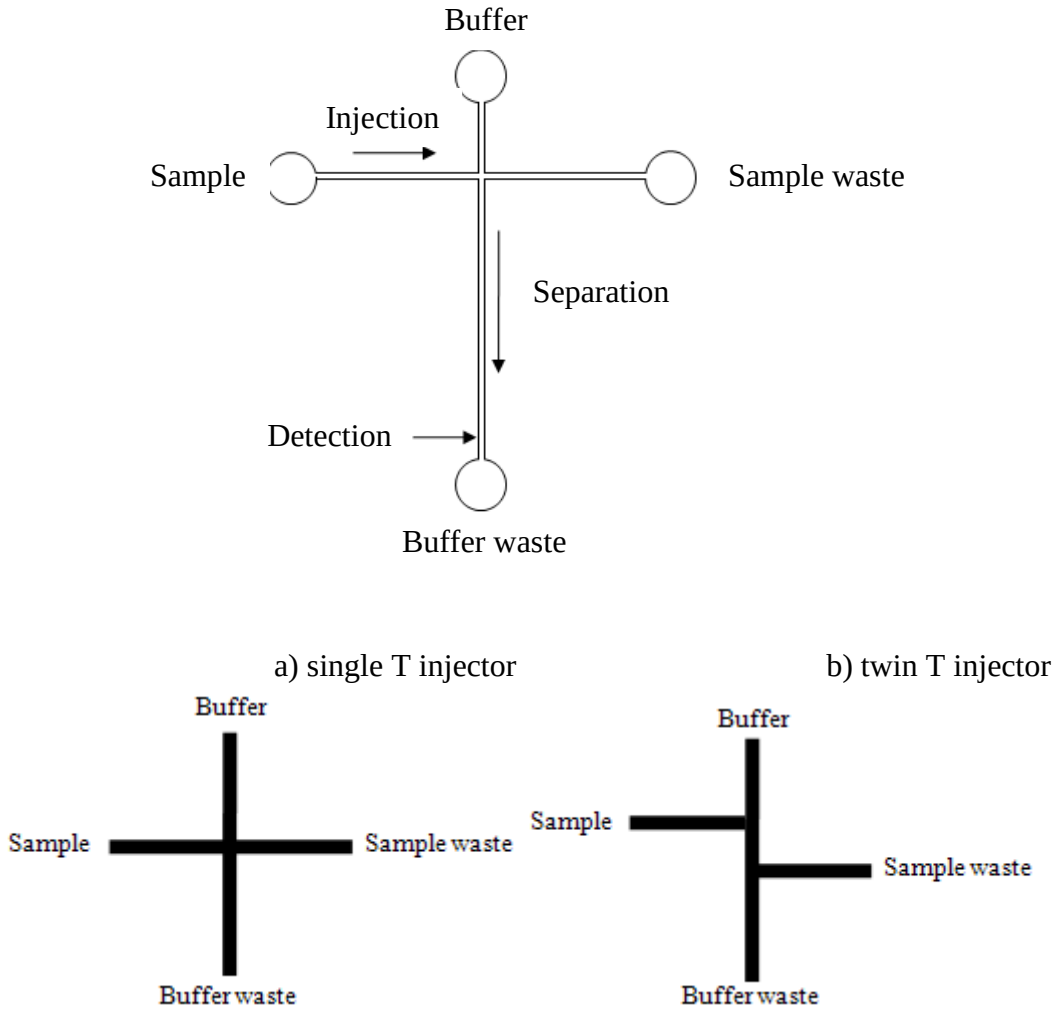

Figure 7.1 Microchip CE schematic with two injector configurations: a) single T (cross) injector and b) twin T injector.

Although worldwide researchers have been made efforts to develop their own microchips from glass and plastics, piecing together instrumentation to make an appropriate detection system (5-12), commercial suppliers present an alternative route to mainstream researches and there are now a number of commercial avenues to microchip sources, with both standard and customized designs available, as well as those that also provide the necessary equipment to perform simple electrophoretic separations.

2. Fluorescent stained microorganism detection

Dyes are commonly used to provide colour for various products including medications, foods, clothing, and paint and ink components (13). Dye analysis has considerable applications in numerous industries, as well as being important in environmental, forensic science and life science in particular microbiological area. Moreover, molecular methods for early diagnosis of malignant disease have been considerably improved by employing fluorescence. Additionally in analytical chemistry field, the dyes are widely used to derivatize substances of interest prior determination with fluorescence detection because only few biogenic substances and microorganisms show adequate inherent fluorescence.

Basic dyes are positively charged and used to bind negatively charged tissues or cell components. Their primary mechanism of cell staining is ionic bonding. Basic dyes have amino groups or alkylamino groups as their auxochromes and consequently have overall positive charges. These dyes, possessing strong absorption and fluorescence bands in the red region, are classified as oxazine (*i.e.* nile blue (NB) and brilliant cresyl blue (BC)) and thiazine (*i.e.* methylene blue (MB) and toluidine blue (TB)) (Figure 7.2). Oxazine dyes containing polar chromophores are an important group of laser dyes frequently used as an active medium in tuning lasers. However, their spectral behavior and laser properties are strongly influenced by the solvent properties and they have also been established to be a solvatochromic dye because of its highly sensitivity to surrounding (29). Recently, the interest in long-wavelength emission fluorescent dyes has increased remarkably, since this spectral region exhibits minimal interference especially from biological samples (30-32).

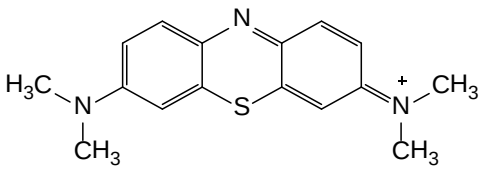

Methylene blue (MB)

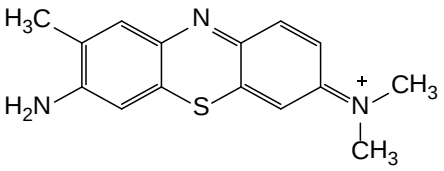

Toluidine blue (TB)

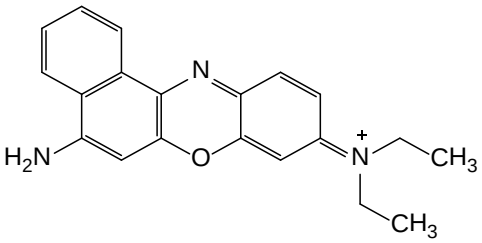

Nile blue (NB)

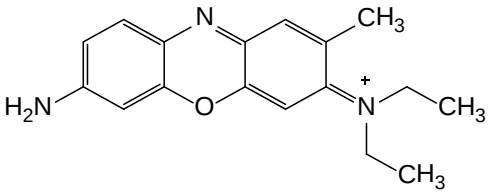

Brilliant Cresyl blue (BC)

Figure 7.2 Structures of methylene blue, toluidine blue, nile blue and brilliant cresyl blue.

Detection of microbial contamination especially pathogenic microorganisms is critical to ensure the safety and quality in food/beverage, pharmaceutical and medical industries (15-16). Conventional culture methods are widely used for bacterial enumeration; however, for accurate enumeration of bacterial numbers, epifluorescence microscopy and flow cytometry have been used to detect various fluorescent dyes stained cells (17-21). Although epifluorescennce microscopic observation provides color and cell shape information, individual differences may rise due to human error (22). It is also laborious and time consuming. Flow cytometry is an effective alternative to traditional methods or cell detection, since the procedure offers rapid, sensitive, and reliable quantification of individual cells. However, flow cytometer is relatively expensive and require complicated maintenance and skilled operators. On-chip flow cytometry can be an interesting promise due to its miniaturization and automation feasibility (23). Furthermore, capillary and microchip electrophoresis could potentially revolutionize certain aspects of microbiology involving diagnosis, profiling of pathogens, environmental analysis, and many other areas (33). Microbes have a surface charge that originates from the ionization of surface molecules and the adsorption of ions from solution. Microbial cell wall and membranes containing

numerous proteins, lipid molecules, lipopolisaccharides which give them characteristic charge. Therefore, cells undergo with their own mobility. Table 7.2 shows capillary and microchip electrophoresis methods that have been reported for the analysis of the microorganisms.

Table 7.2 Capillary and microchip electrophoresis methods for the analysis of the microorganisms

Method	Analyte	Sample	Significant finding	Reference
CZE-UV	• *Lactobacillus delbrueckii* subsp. *Bulgaricus* • *Streptococcus thermophilus*	• Yogurt	• Linearity: $r^2 > 0.99$ • Precision RSDs < 9.3% • Recovery = 91.7 - 106.7% • LOQ 1.0×10^6 CFU/mL	(34)
CZE-UV	• *Micrococcus Lysodeikticus* • *Pseudomonas fluorescens* • *Aerobacter aerogenes*	-	• Total analysis time < 15 min • Investigate migration behavior of bacteria at different storage condition	(35)
CZE-UV	• *Staphylococcus aureus*	-	• Selective isolate *S. aureus* from bacterial mixtures (*Escherichia coli*, *Pseudomonas aeruginosa*, and *Klebsiella pneumoniae*) • LOD = 9.0×10^5 CFU/mL • Linearity: 1.5×10^8 -1.5×10^{10} CFU/mL $y = 35{,}313x + 42{,}977$, $r^2 = 0.99$	(36)

Table 7.2 (continued) Capillary and microchip electrophoresis methods for the analysis of the microorganisms

Method	Analyte	Sample	Significant finding	Reference
CZE-UV	• *Escherichia coli* • *Staphylococcus aureus* • *Helicobacter pylori* • *Proteus valgaris*	• Infected urine	• Linearity (*E. coli* counts) 0.45×10^{9} - 3.0×10^{9} cells/mL, r^2 = 0.9903 • RSDs of t_m = 1.46% to 6.74%	(37)
CE-UV	• *Brevibacterium taipei* • *Corynebacterium acetoacidophilum* • *Escherichia blattae* • *Escherichia coli* • *Candida albicans* • *Bacillus cereus* • *Saccharomyces cerevisiae* • *Spongospora subterranean* • *Rhodoturula*	-	• Analysis of single species of bacteria or fungi • Dicationic ionic liquid competed with CTAB to coat the capillary wall and lowered the risk of lysing the cell.	(38)

Table 7.2 (continued) Capillary and microchip electrophoresis methods for the analysis of the microorganisms

Method	Analyte	Sample	Significant finding	Reference
CZE-UV	• *Micrococcus luteus* • *Neisseria cinerea* • *Pseudomonas fluorescens*	-	• Size and surface charges of *Micrococcus luteus* was strongly dependent on the preparation of the cells. • Separation of *N. cinerea* and *P. fluorescens* could be easily reproduced thus, they will be used for evaluating antibiotic activity.	(39)
CIEF-UV	• *Escherichia coli* • *Candida spp.* (5 species) • *Proteus vulgaris* • *Klebsiela pneumonia* • *Staphylococcus spp.* (2 species) • *Streptococcus agalactiae* • *Enterococcus faecalis*	-	• Linear pH gradient over pH 2.0-5.0 • RSDs < 2.0% • Total analysis time < 25 min	(40)

Table 7.2 (continued) Capillary and microchip electrophoresis methods for the analysis of the microorganisms

Method	Analyte	Sample	Significant finding	Reference
CE-DAD	• *Escherichia coli* • *Helicobacter pylori* • *Serratia marcescens*	• Human urine	• Analysis of single species of bacteria - *Escherichia coli, Helicobacter pylori and Serratia marcescens* • Separation of two bacterial species - *Helicobacter pylori and Serratia marcescens* • RSDs = 2.36 - 2.96	(41)
CZE-DAD	• *Escherichia coli* • *Micrococcus spp.* • *Proteus valgaris* • *Bacillus megaterium* • *Arthobacter globiformis*		• Use of a trimethylchlorosilane-modified over a short distance (8.5 cm) for separation of five species of bacteria • RSDs < 8.1% • N > 4,000,000 plates/m	(42)
CZE-DAD	• *Micrococcus luteus* • *Bacillus subtilis* • *Pseudomonas fluorescens*	-	• High injection volume increased migration time but not affected on peak efficiency	(43)

Table 7.2 (continued) Capillary and microchip electrophoresis methods for the analysis of the microorganisms

Method	Analyte	Sample	Significant finding	Reference
CIEF and CZE-UV and fluorometric detection	• *Aspergillus niger* • *Aspergillus fumigatus* • *Aspergillus flavus* • *Fusarium solani* • *Penicillium chrysogenum*	-	• LOD 10^4 conidia/mL • RSDs < 2.2%	(44)
CZE-LEDIF	• *Edwardsiella tarda*	• Fish fluid	• N > 1,200,000 theoretical plates/m • Linearity 2.5 x 10^6 to 2.0 x 10^7 cells/mL $y = 14.3x - 2.42$, $r^2 = 0.9985$ • LOD 4.2 x 10^4 cells/mL • Recovery 70.0%	(45)
CZE-LIF	• *Lactobacillus acidophilus* • *Bifidobacterium infantis*	• Pill, syrup and powder health products	• Linearity range (*L. acidophilus*) 50-200 cells/nL y = 0.046x-2.51, $r^2 = 0.995$ • Simultaneously monitoring viable and dead cells	(46)

Table 7.2 (continued) Capillary and microchip electrophoresis methods for the analysis of the microorganisms

Method	Analyte	Sample	Significant finding	Reference
CZE-LIF	• *Escherichia coli*	• Contaminated meat	• A combination of immunofluorescent (FAb) staining and CE-LIF • Direct and indirect detection of *E.coli* • Total analysis time (6–8 h) is less than most commercial assay	(47)
CE-LIF	• Ochratoxin A (secondary fungal metabolite)	• Roasted coffee • Corn • Sorghum	• Linearity range 0.005-0.5 ng/µL $y = 662.669x + 0.6408$, $r^2 = 0.999$ • Recoveries = 86-99%	(48)
CE-LIF	• *Brevibacterium taipei* • *Corynebacterium acetoacidophilum* • *Escherichia blattae* • *Candida albicans* • *Bacillus megaterium*	-	• Use of caprylyl sulfobetaine greatly reduced background fluorescence. • Single cell of *B. taipei*, *C. acetoacidophilum*, *E. blattae*, *C. albicans* and *B. megaterium* displayed S/N of 5.5, 5.8, 5.1,8.3 and 6.5, respectively.	(49)
CE-LIF	• *Candida albicans*	• Plasma	• $t_m < 7$ min • LOD = 5 cells/injection	(50)

Table 7.2 (continued) Capillary and microchip electrophoresis methods for the analysis of the microorganisms

Method	Analyte	Sample	Significant finding	Reference
CE-LIF	• *Candida albicans*	• Whole blood	• *in situ* hybridization yielded *Candida*-specific fluorescence • LOD = 2.0 x10^3 (±0.2 x 10^3) CFU/mL • LOQ = 5.2 x10^3 (±0.3 x 10^3) CFU/mL	(51)
CZE-LIF	• Boar sperm	• Semen sample	• Single viability assay < 10 min • Minimum amount of dye to saturate 10^7 sperm was 0.1 nmol for SYBR-14 (living cell, green fluorescence) and 25 nmol for propiodium iodide (dead cell, red fluorescence).	(52)
Multiplex-PCR-CGE-LIF	• *Staphylococcus aureus* • *Listeria monocytogenes* • *Salmonella spp.*	• Artificially inoculated food	• LOD - *S. aureus* 260 cfu/mL - *L. monocytogenes* 79 CFU/mL - *Salmonella spp.* 57 CFU/mL • RSD of t_m < 0.8% • RSD of peak area < 5.8%	(53)

Table 7.2 (continued) Capillary and microchip electrophoresis methods for the analysis of the microorganisms

Method	Analyte	Sample	Significant finding	Reference
PDMS based microchip electrophoresis-LIF	• *Escherichia coli*		• Rapid identification within 2 min • RSDs of t_m < 0.5 • RSDs of peak area < 5% • N > 100,000	(33)

CHAPTER VIII
MATERIALS AND METHODS

1. Materials

Table 8.1 List of chemicals and reagents

Name	Grade	Source/Supplier
Nile blue A perchlorate (NB)	RS	Aldrich (Wisconsin, USA)
Methylene blue (MB)	RS	Aldrich (Wisconsin, USA)
Toluidine blue (TB)	RS	Fluka (Buchs, Switzerland)
Brilliant cresyl blue (BC)	RS	Fluka (Buchs, Switzerland)
Fluorescein	RS	Fluka (Buchs, Switzerland)
Ammonium acetate (NH_4OAc)	AR	Sigma-Aldrich (St. Louis Missouri, USA)
Sodium acetate (NaOAc)	AR	Sigma-Aldrich (St. Louis Missouri, USA)
Calcium nitrate ($Ca(NO_3)_2$)	AR	Aldrich (Wisconsin, USA)
Lithium chloride (LiCl)	AR	Fluka (Buchs, Switzerland)
Cetyltrimethylammonium bromide **(**CTAB)	AR	Fluka (Buchs, Switzerland)
Caprylyl sulfobetaine (SB3-10)	AR	Sigma-Aldrich (St. Louis Missouri, USA)
Poly(ethylene oxide) (PEO, MW 600,000)	AR	Aldrich (Wisconsin, USA)
Tris(hydroxymethyl)aminomethane (Tris)	AR	Sigma-Aldrich (St. Louis Missouri, USA)

Table 8.1 (continued) List of chemicals and reagents

Name	Grade	Source/Supplier
Sodium tetraborate decahydrate	AR	Sigma-Aldrich (St. Louis Missouri, USA)
Ethylenediaminetetraacetic acid disodium salt dihydrate ($Na_2EDTA{\cdot}2H_2O$)	AR	Sigma-Aldrich (St. Louis Missouri, USA)
Acetic acid	AR	Sigma-Aldrich (St. Louis Missouri, USA)
Boric acid	AR	Sigma-Aldrich (St. Louis Missouri, USA)
Citric acid	AR	Riedel-de Haën (Seelze, Germany)
Acetonitrile (ACN)	AR	Sigma-Aldrich (St. Louis Missouri, USA)
Dimethyl sulfoxide (DMSO)	AR	Sigma-Aldrich (St. Louis Missouri, USA)
Dimethylformamide (DMF)	AR	Sigma-Aldrich (St. Louis Missouri, USA)
Methanol (MeOH)	AR	Sigma-Aldrich (St. Louis Missouri, USA)
Hydrochloric acid	AR	Fluka (Buchs, Switzerland)
Sodium hydroxide	AR	Sigma-Aldrich (St. Louis Missouri, USA)
Buffer pH 4.0	-	Fluka (Buchs, Switzerland)
Buffer pH 7.0	-	Fluka (Buchs, Switzerland)

Table 8.2 List of instruments

Instrument	Source/Supplier
The 2100 Bioanalyzer	Agilent Technologies (Waldbronn, Germany)
DNA chip	Caliper Labchip®, Agilent Technologies (Waldbronn, Germany)
The Cell Fluorescence kit	Caliper Labchip®, Agilent Technologies (Waldbronn, Germany)
Spectrophotometer	Perkin-Elmer Lambda 40 UV/VIS Spectrometer (Massachusetts, USA)
Autopipette	Eppendorf Research® (Hamburg, Germany)
pH meter	Thermo Fisher Scientific Orion Model 420A$^+$ (Massachusetts, USA)
Analytical balance (AE 160)	Sartorius (Goettingen, Germany)
25-mm syringe filters with polyvinylidene difluoride (PVDF) membrane 0.2 μm	Whatman® (New Jersey, USA)
Microcentrifuges	VWR™ Galaxy 7D (Leicestershire, UK)
Ultrasonic sonicator	Branson Model 5510 (Connecticut, USA)
Vortexer	IKA® MS3 (North Carolina, USA)
Water purification system	Millipore-Milli-Q system (Massachusetts, USA)

2. Standard fluorescent dye solution, background electrolyte and fluorescent stained microorganism preparations

2.1 Fluorescent dye solution preparations

Stock solutions of MB, TB, NB and BC were prepared at a concentration of 1 mM in acetonitrile (ACN) and diluted as necessary in appropriate background electrolyte (BGE) (see section 2.2). All stock standard solutions were kept at room

temperature and protected from light. Working standard solutions were diluted from the stock solutions to obtain concentrations of 5-28 µM, 10-100 µM, 1.5-50 nM and 10-75 nM for MB, TB, NB and BC, respectively.

2.2 BGE preparations

2.2.1 BGEs for separations of fluorescent dyes

NH_4OAc, monovalent (*i.e.* NaOAc and LiCl) and divalent (*i.e.* $Ca(NO_3)_2$) metal salts were used to prepare BGEs. Electrolytes were prepared by transferring NH_4OAc, NaOAc, LiCl and $Ca(NO_3)_2$ equivalent to 26 - 90 mM NH_4OAc, 26 - 70 mM NaOAc (13), 26 - 70 mM LiCl and 15 - 40 mM $Ca(NO_3)_2$ (e.g. 0.010 - 0.035 g for NH_4OAc, 0.011 - 0.029 g for NaOAc, 0.006 - 0.013 g for LiCl and 0.012 - 0.033 g for $Ca(NO_3)_2$) into each 5-mL volumetric flask. Then, DMSO containing 870 mM acetic acid was added and adjusted to volume.

BGE containing 870 mM acetic acid in different solvents were investigated using DMSO, 60% MeOH and 60% ACN. Additionally, water content in DMSO was optimized.

2.2.2 BGEs for analysis of single microorganism

Stock solution of 10 mM Tris/3.3 mM citric acid was prepared by transferring 0.030 g Tris/0.015g citric acid into a 10-mL volumetric flask and sterile water was added to volume. The solution was adjusted to pH 7.0 using 1 M hydrochloric acid or 1 M sodium hydroxide and diluted to 1 mM Tris/0.33 mM citric acid (solution A). CTAB was added to solution A to obtain concentration of 1 mg/mL CTAB.

For analysis of single microorganism, a blocking agent was required to focus cells in narrow zone. Liquid nutrient broth and SB3-10 were used as blocking agents. Liquid nutrient broth was autoclaved at 121 ˚C and 15 psi for 15 min and SB3-10 was weighed and dissolved in sterile water to obtain concentration of 5 mg/mL (49).

2.2.3 BGEs for separations of microorganism mixtures

Tris-borate-EDTA (TBE) buffer stock solution containing 394 mM Tris, 56 mM boric acid and 1.3 mM EDTA was prepared by transferring 0.477 g Tris, 0.035g boric acid and 0.005 g $Na_2EDTA{\cdot}2H_2O$ into a 10-mL volumetric flask

and sterile water was added to volume. This solution was adjusted to pH 8.5, 9.0, 9.5, 10.5 and 11.0 with 1 M hydrochloric acid or 1 M sodium hydroxide solution and diluted with sterile water to 3.94 mM Tris, 0.56 mM boric acid, 0.013 mM EDTA working solution (solution B). 0.5% PEO was prepared by dissolving 0.025 g of PEO in 5 mL of sterile water and sonicated at ~ 60˚C for 4 h. BGEs containing 0.0125, 0.025 and 0.05% PEO were prepared by diluting 125, 250 and 500 µL, respectively, of 0.5% PEO solution with solution B into each 5-mL volumetric flask (45).

Sterile water was prepared by autoclaving deionized water at 121 ˚C and 15 psi for 15 min. All standard dye solutions and BGEs for both analyses of fluorescent dyes and microorganisms were filtered through a 0.2-µm membrane and degassed for 5 minutes prior uses. BGEs for analysis of microorganisms were freshly prepared.

2.3 Fluorescent stained microorganism preparations

The microorganisms (*i.e.* Gram negative bacteria; *E. coli*, Gram negative bacteria; *B. subtilis, M. luteus, S. aureus* and fungi; *C. albicans*, *L. fungicola*) were grown on agar plates and transferred from a single colony on a plate to a surface of agar slant in a tube. The microbes were incubated until growth was evident then refrigerated the tube. Before analyses, cells were taken with a sterile sterile loop and streaked on an agar plate then incubated overnight. Well-isolated colonies were transferred to a liquid nutrient broth and again incubated overnight. The cells were harvested for uses when the concentration was around 10^8 colony forming unit (CFU)/mL. Estimation of cell numbers was performed using optical density (OD). OD of microbial samples is usually measured at 600 nm and known as OD_{600}. OD_{600} depends on concentrations, species and strains of microbes, growth conditions used, and wavelengths of the light being transmitted. Calibration curves were plotted between OD_{600} against microbial concentration (CFU).

Fluorescent stained microorganism suspensions were freshly prepared by the following procedure. 50 µL of microorganism suspensions was transferred to a centrifuged vial, centrifuged 3000 rpm for 2 min, the excess broth was removed and the microorganisms were washed with 1 mM Tris/0.33 mM citric acid buffer (pH 7.0). Stock solution of NB (1 mM NB in ACN) was diluted to 100 µM with ACN and used

as fluorescent stain. Cells were stained by adding 1.25 - 7.5 µL of the dye solution/50 µL of microbial solution (2.5 - 15 µM of NB) and vortexed to obtain homogeneous cell staining. The cell suspensions were recentrifuged, decanted and finally suspended in 1 mM Tris/0.33 mM citric acid buffer (pH 7.0) with the same volume as the broth that was originally removed. The final concentration of the cells was ~10^8 CFU/mL and used for analyses.

3. Microchip capillary electrophoresis (CE) and on-chip flow cytometry with fluorescence detection methods

Microchip CE separations were performed on the Agilent 2100 Bioanalyzer (Agilent Technologies, Waldbronn, Germany), which was introduced as the first commercially-available product. Generally, this system approached for a variety of voltage-driven separation techniques, addressing separation of DNA, RNA and protein samples. However, other applications using CE methods were achieved in this study using a DNA chip which was a disposable glass chip.

The microchannel design for the DNA chip used in this study is illustrated in Figure 8.1. The microchip featured a separation channel with a total length of approximately 40 mm and with 14 mm from injection to the detector. Width and depth of microchannels were 40 µm and 15 µm, respectively. Microchips were filled and flushed with buffer by manually pipetting into the buffer reservoir and applying vacuum to the buffer waste reservoir using a home-made device consisting of a 3-mL plastic syringe and a piece of pipette tip that fitted tightly into the reservoirs on the top of the chip. All channels of the chip were typically filled with electrolyte by capillary force for 1 min but not over than 5 min in order to prevent the evaporation of electrolyte. Sample reservoirs (up to 12 samples, A1-3, B1-3, C1-3 and D1-3) were filled with 7 µL of sample, while buffer reservoirs were filled with 10 µL of buffer. Electrofluidic control of the microchip was achieved by development of a new script *via* the assay and script developer mode. Injection was achieved by applying voltage (electrokinetic injection). The chip was interfaced a cartridge with 16 electrode pins with the voltage controls. Voltage and temperature were varied in a range of 0 - 1,600 V and 5 - 40 ˚C, respectively. The system is capable of red laser-induced fluorescence

(LIF) and blue light emitting diode-induced fluorescence (LEDIF) detections. The red LIF is featured excitation at 634/38 nm (λ_{ex}) with emission collected at 685/22 nm (λ_{em}) and the blue LEDIF configures the excitation and emission wavelength of 470/25 nm and 525/30 nm, respectively. The detector focused onto the separation channel using fluorescent dye that its λ_{ex} and λ_{ex} matching to each detection. The focusing step was performed prior the operation of CE separations. Data was displayed as electropherograms, which were plots of migration time against fluorescence intensity.

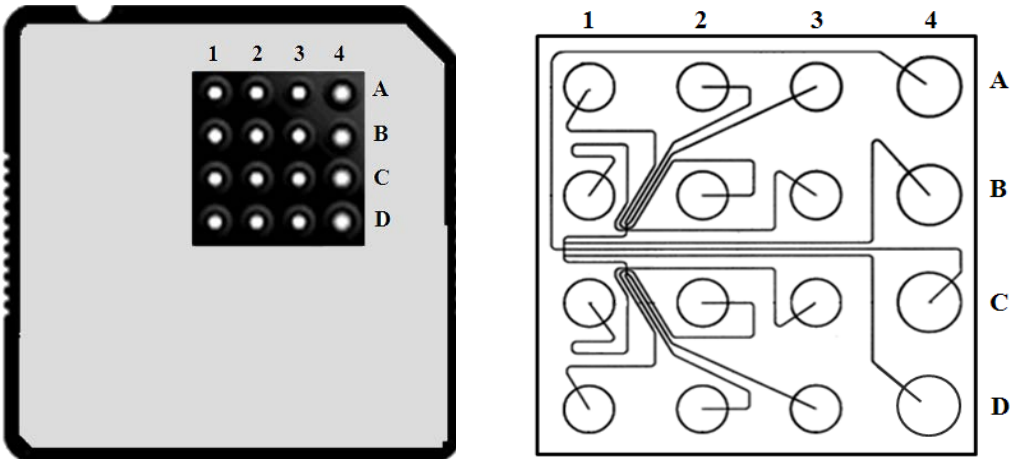

Figure 8.1 Photographs of the DNA chips used in this work. The photograph of the glass chip (right) resemble the microchannel design layout of the chip as it would appear if viewed looking through the plastic cover from the top. Wells A1-3, B1-3, C1-3 and D1-3 were sample reservoirs. Buffer was placed in wells A4 to D4. A4 was inlet buffer well, B4 and D4 were sample waste reservoirs and C4 was buffer waste reservoir.

3.1 Compatibility of the chip

Compatiblity of the DNA chip with organic solvents (*i.e.* ACN, DMF, DMSO and MeOH) was initially investigated. Appearances of the chips after filling the plastic reservoirs with various organic solvents were visually observed. Further experiments were examined on the analysis repeatability with three different chips for ~50 h by analyses of NB in BGE containing 26 mM NH_4OAc and 870 mM acetic acid

in DMSO (13) using injection and separation voltage of 1,400 V at temperature of 25°C.

3.2 Optimization of fluorescent dye separations by chip-based NACE

Non-aqueous CE (NACE) separations of the blue fluorescent dyes was initially carried out in 26 mM NH_4OAc and 870 mM acetic acid in DMSO (13). Further optimization was performed by evaluating effects of types and concentrations of BGE (*i.e.* 26-90 mM NH_4OAc, 26-70 mM NaOAc, 26-70 mM LiCl and 15-40 mM $Ca(NO_3)_2$ with 870 mM acetic acid in DMSO), BGE solvents (*i.e.* MeOH, ACN and DMSO), and water contents in BGE (10-30%). Samples were electrokinetically injected at 1,400 V for 50 s by application of 100 V to the sample waste reservoir and 1,500 V to the sample reservoir. Separation was performed at 1,500 V by application of 100 V to the buffer waste reservoir and 1,600 V to the buffer reservoir. Temperature was set at 25°C and detection was *via* the red LIF detector.

3.3 Method validation of chip-based NACE for separations of fluorescent dyes

The optimum NACE condition was validated by the following procedures.

3.3.1 Linearity

Calibration curves of MB (5-28 µM), TB (10-100 µM), NB (3.1-50 nM) and BC (10-75 nM) were established by analyzing five concentrations of the dyes on three different days (n = 3). The calibration curves were plotted between peak area or peak height against concentrations. Linear regression and coefficient of determination (r^2) were calculated by Microsoft Excel®.

3.3.2 Precision

3.3.2.1 Injection precision

Injection precision was determined by repetitive injection (n = 10) at the middle point concentration of the calibration curve of the investigated dyes.

3.3.2.2 Intra-day precision

Intra-day precision was determined from three different concentrations (n = 3) of each dyes analyzed within one day.

3.3.2.3 Inter-day precision

Inter-day precision was performed by determining three different concentrations (n = 3) of each dyes on six different days.

All precision data was assessed from the %RSDs of migration time, peak area and peak height.

3.3.3 Limit of detection (LOD) and limit of quantitation (LOQ)

Limit of detection (LOD) is the lowest amount of an analyte in a sample that can be detected, typically with acceptable signal to noise ratio (S/N) of 3. Limit of quantitation (LOQ) is a characteristics of quantitative assays. It is the lowest amount of analyte in the sample that can be determined with acceptable precision and recovery with a S/N of 10.

LODs and LOQs of each fluorescent dye were determined by serial diluting the concentration of the standard solution of the investigated dyes at S/N of 3 and 10, respectively (n = 3).

3.4 Optimization of fluorescent staining of micoorganisms using on-chip flow cytometry

Optimization of NB concentration for cell staining was investigated by on-chip flow cytometry. Cells were stained with NB at the concentrations of 2.5-15 µM. The optimal NB concentration for each microorganism was determined from the maximum cell events on a dot plot of the on-chip flow cytometry.

On-chip flow cytometry employed vacuum to move cells through the microfluidic channels of a special cell-fluorescence chip. Fluid flow was controlled by a peristaltic pump and the vacuum was controlled by a pressure sensor (range 0 - 140 mbar), to guarantee a constant flow speed within the microfluidic channels. A special cartridge was used to interface the pressure control with the chip. The system was comprised of two independent fluorescence detections and cells were analyzed on disposable glass chips, while flowing through microfluidic channels. Cells were hydrodynamically focused to a portion of the microfluidic channel before they passed the detector in single cell. Channel dimensions were 25 x 75 µm with rounded shape wells. Cell numbers could be counted up to 2,500 cell events in 4 min. This resulted in sample preparation of 2,000 cells/µL. The glass chip was glued into a plastic holder

as shown in Figure 8.2. In order to test performance of the chip design and detection system, commercially available calibration beads were used. Red and blue fluorescently labeled beads were measured on the microfluidic system.

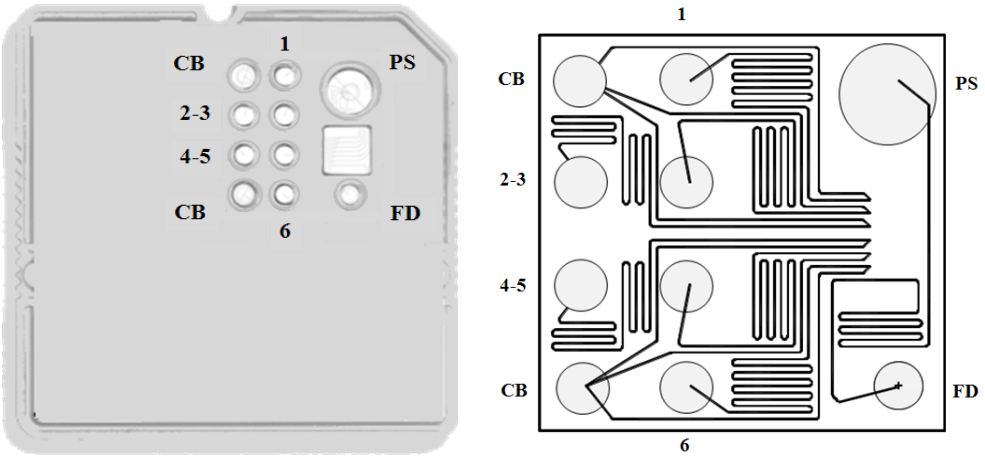

Figure 8.2 The microchannel layout of the cell chip (right), as it would appear if viewed looking through the plastic cover from the top, used for on-chip flow cytometry. PS and FD were priming solution and focusing dye reservoirs, respectively. CB were cell buffer reservoirs and wells 1-6 were sample reservoirs.

Prior analysis, the chip was primed with 10 µL of priming solution (PS, Figure 8.2), which was an aqueous buffer, through a central priming well that fills the channels by capillary forces and left for 1 min. This well also acted as the interface to the instrument's vacuum source. Afterward, 10 µL of focusing dye was added to the focusing well (FD, Figure 8.2). A reference fluorescent dye was used for focusing the optical detection at the beginning of every chip run. Then, 30 µL of cell buffer was filled into each of the two cell buffer wells (CB, Figure 8.2). Finally, 10 µL of the fluorescent stained cells could be loaded into the sample wells (well 1-6, Figure 8.2) up to six cell samples and the total time of analysis was approximately 25 min. Data showed that the cell populations are clearly segregated into distinct groups of two color fluorescence, depending on their staining and fluorescence from one channel does not leak into the other. The measured fluorescence values and event number were displayed as a histogram or dot plot (22-23, 54).

3.5 Analysis of single microorganism

Determination of each microorganism using the nutrient broth and SB3-10 as the blocking agents were evaluated. Spacer method for sample injection was modified from Armstrong and co-workers (Figure 8.3) (49, 55). The microchannels were filled with BGE containing CTAB before the injection of the cell suspensions in 1 mM Tris/0.33 mM citric acid buffer (pH 7.0) was made. Then, a spacer of BGE containing CTAB and the blocking agents (nutrient broth or SB3-10) were injected. The separation voltage was -1,000 V by application of 100 V to buffer reservoir and 1,100 V to buffer waste reservoir.

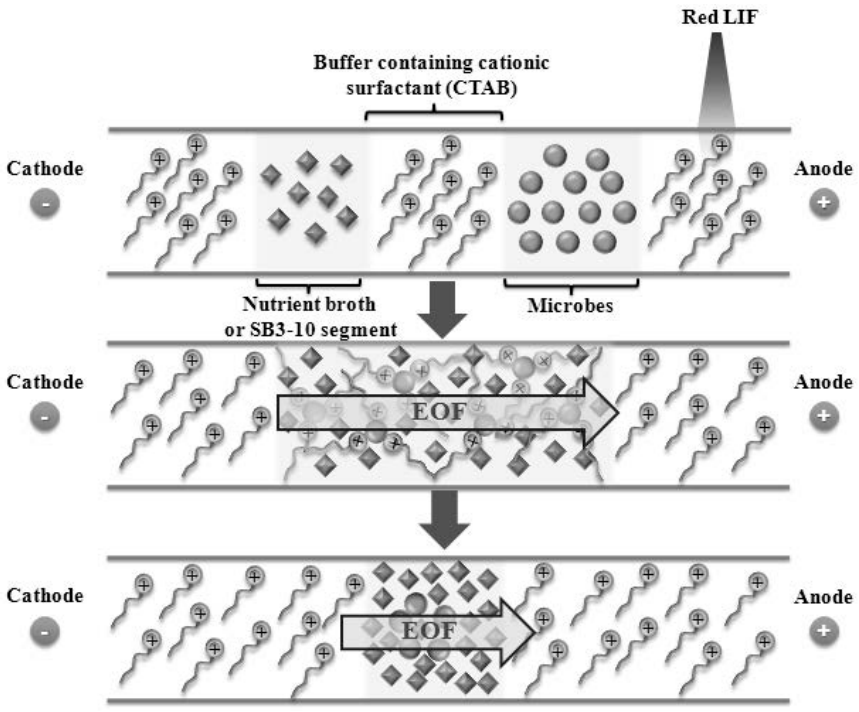

Figure 8.3 The spacer method used for the injection of microorganisms.

3.6 Optimization of microorganism separation

The fluorescent stained microorganism mixture consisted of *E. coli*, *S. aureus* and *C. albicans*, which were selected from Gram negative bacteria, Gram positive bacteria and fungi, respectively. Additionally, *B. subtilis*, *M. luteus* and *S. aureus* were selected to produce the mixture of Gram positive bacteria. Microorganism separation was optimized by varying pH of BGE (8.5 – 11.0) and

amounts of PEO (0.0125 – 0.05%). The separation voltage was 1,000 V by application of 1,100 V to buffer reservoir and 100 V to buffer waste reservoir.

CHAPTER IX
RESULTS AND DISCUSSION

1. Compatibility of the chip

Initially, the compatibility of the microchips with organic solvents (*i.e.* ACN, DMF, DMSO and MeOH) was visually observed. The plastic covering chip was deformed in DMF, while ACN and MeOH were evaporated from the reservoir within a few minutes due to their low boiling point and high vapor pressure (Table 9.1). However, the appearance of the chip reservoir was slightly white in DMSO after 1 h. A closer inspection with a digital camera showed that the white marks caused by a change of the roughness on the plastic surface. Further experiments on repeatability were performed on analysis of NB in BGE containing 26 mM NH_4OAc and 870 mM acetic acid in DMSO with three different chips (1). After 50 h, the migration time (t_m) of NB remained constant (%RSD = 1.37-1.92%, Figure 9.1) and no extra peak was observed, therefore, DMSO was compatible with the chips.

Table 9.1 Physical properties of organic solvents (2)

Solvent	Boiling point (˚C)	Melting point (˚C)	Vapor pressure (21˚C, mmHg)	Absolute viscosity (25˚C, cP)	Solubility in water
Acetonitrile (ACN)	81.6	-44	71	0.38	Miscible
Dimethyl formamide (DMF)	153	-61	3.8	0.82	Miscible
Dimethyl sulfoxide (DMSO)	189	18.5	0.7	2.0	Miscible
Methanol (MeOH)	64	-98	103	0.6	Miscible
Water	100	0	19	0.89	-

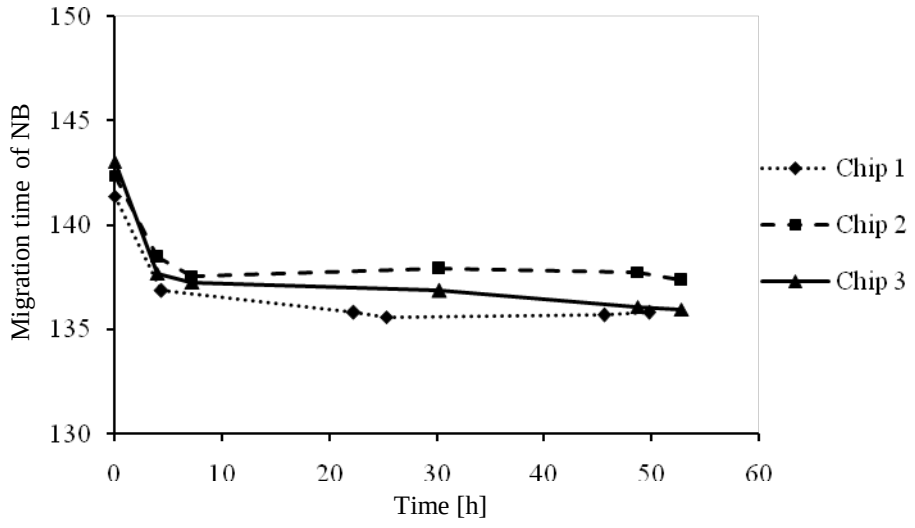

Figure 9.1 Repeatability of NB on microchip CE using three difference chips. Conditions: 26 mM NH_4OAc and 870 mM acetic acid in DMSO; separation length 14 mm; injection/separation voltage 1,400 V; temperature 25°C and red LIF detection with λ_{ex} 634/38 nm and λ_{em} 685/22 nm.

2. Optimization of fluorescent dye separations by chip-based NACE

2.1 Effects of types and concentrations of BGE

Compositions of BGE have significant impacts on CE separation. Both the ionic strength and pH can influence analysis times and separation selectivity due to either acid/base or ion-association equilibria, as well as through influences on the EOF (1). Since non-aqueous solvents were employed, a concept of "relative acidity/basicity" was adopted, in which various alkaline metal salts were added to the electrolyte containing constant amounts of acetic acid to obtain distinct acidity or basicity. Separations of MB, TB, NB and BC were investigated in NH_4OAc, mono- and divalent metal salts (*i.e.* 26-90 mM NH_4OAc, 26-70 mM NaOAc, 26-70 mM LiCl and 15-40 mM $Ca(NO_3)_2$) with 870 mM acetic acid in DMSO. Baseline separations of the dyes were not observed in the initial condition using 26 mM NH_4OAc as BGE. Separation efficiency was improved at higher amounts of NH_4OAc and the optimum condition was achieved at 80 mM NH_4OAc (Figure 9.2).

TB and NB overlapped at low concentrations of NaOAc (26-50 mM). Their resolution was achieved at 60-70 mM NaOAc, however, broad with splitting peak of NB was observed in 70 mM NaOAc (Figure 9.3). Another monovalent metal salt, LiCl electrolyte could not provide the baseline separation of TB and NB but sufficient resolution of MB/TB and NB/BC was obtained at 60 mM LiCl. Lower mobility with similar separation efficiency was found at higher concentrations of LiCl (70 mM). At both concentrations (60 and 70 mM LiCl), splitting peaks of BC were observed (Figure 9.4). Additional peaks of either NB in NaOAc or BC in LiCl might be a structurally related isomer formed during the synthesis of the dye, which remained after subsequent purification steps (1). The splitting peaks of dyes were observed at high pH due to changes in ionization as a result of slight different pK_a.

For the divalent metal salts, the dyes showed multiple peaks with no baseline separation in 15 mM $Ca(NO_3)_2$. Although the baseline separation was improved at higher concentration of $Ca(NO_3)_2$, TB and NB still not completely separated (Figure 9.5).

In comparison of the separation of the basic blue dyes in different BGEs (Figure 9.6), NH_4OAc electrolyte showed the best separation of the dyes in term of the

%RSD of t_m (1.93-2.39%), baseline separation (R_s = 1.02-1.50), peak shapes (TF = 0.73-1.26) and number of theoretical plates (N = 6461.35 – 9803.33) with highest peak intensities.

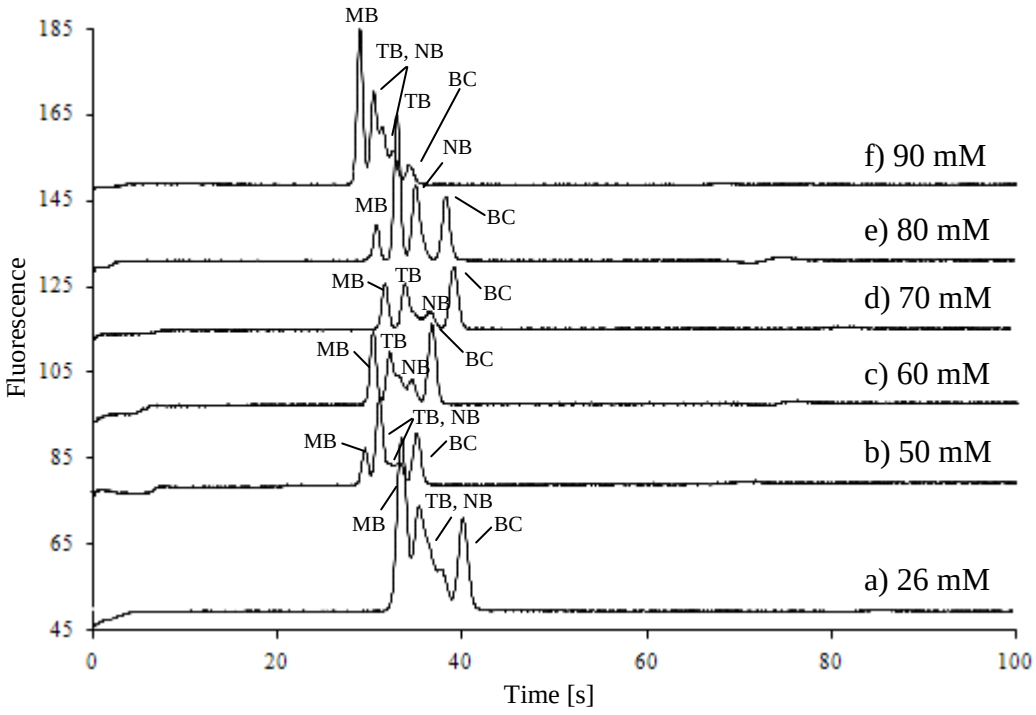

Figure 9.2 Effects of concentrations of NH_4OAc on the separation of the fluorescent dyes. Conditions: 870 mM acetic acid in DMSO containing NH_4OAc at the concentration of a) 26 mM, b) 50 mM, c) 60 mM, d) 70 mM, e) 80 mM and f) 90 mM; separation length 14 mm; injection/separation voltage 1,400/1,500 V; temperature 25°C and red LIF detection with λ_{ex} 634/38 nm and λ_{em} 685/22 nm. Peak identification: MB; methylene blue, TB; toluidine blue, NB; nile blue, BC; brilliant cresyl blue.

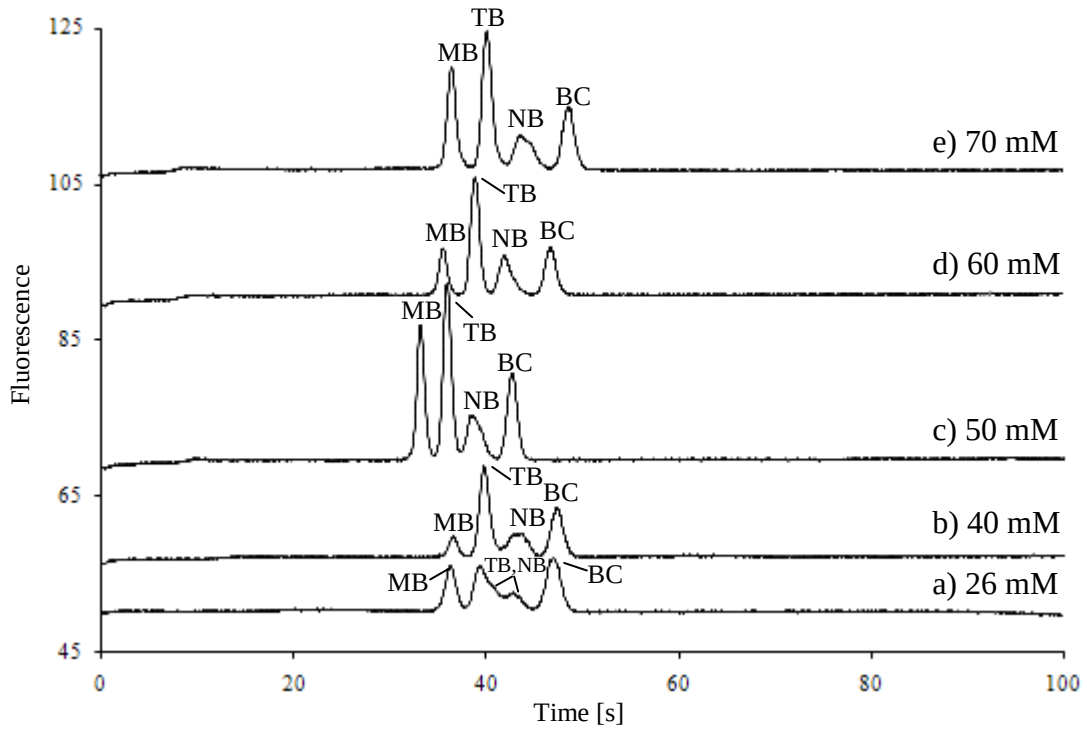

Figure 9.3 Effects of concentrations of NaOAc on the separation of the fluorescent dyes. Conditions: 870 mM acetic acid in DMSO containing NaOAc at the concentration of a) 26 mM, b) 40 mM, c) 50 mM, d) 60 mM and e) 70 mM,; separation length 14 mm; injection/separation voltage 1,400/1,500 V; temperature 25°C and red LIF detection with λ_{ex} 634/38 nm and λ_{em} 685/22 nm. Peak identification: MB; methylene blue, TB; toluidine blue, NB; nile blue, BC; brilliant cresyl blue.

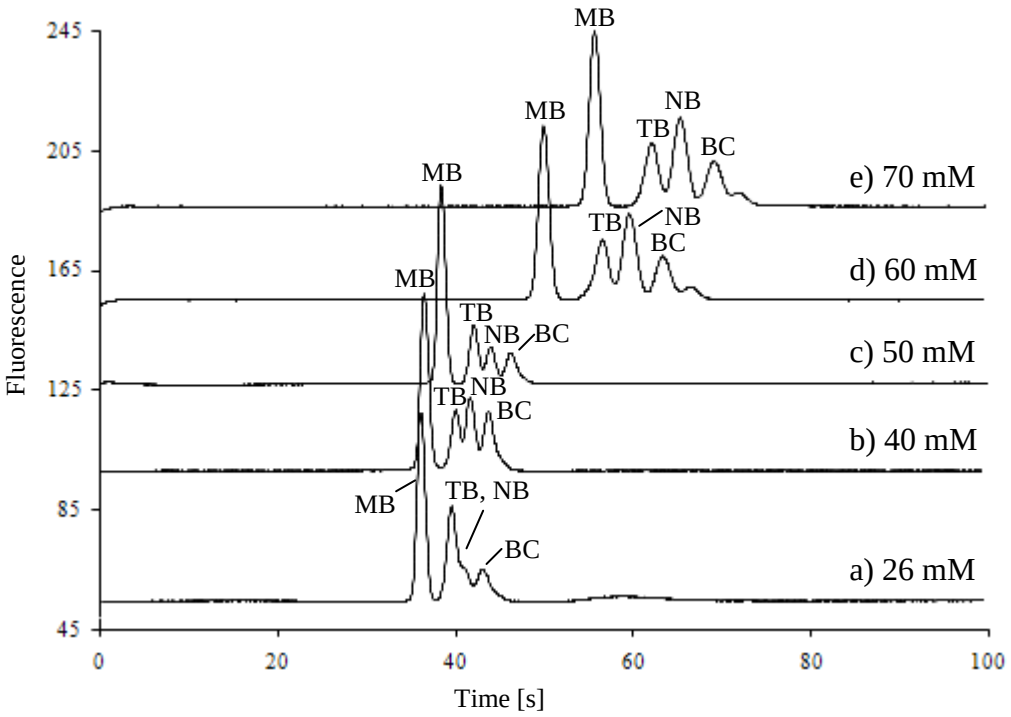

Figure 9.4 Effects of concentrations of LiCl on the separation of the fluorescent dyes. Conditions: 870 mM acetic acid in DMSO containing LiCl at the concentration of a) 26 mM, b) 40 mM, c) 50 mM, d) 60 mM and e) 70 mM,; separation length 14 mm; injection/separation voltage 1,400/1,500 V; temperature 25°C and red LIF detection with λ_{ex} 634/38 nm and λ_{em} 685/22 nm. Peak identification: MB; methylene blue, TB; toluidine blue, NB; nile blue, BC; brilliant cresyl blue.

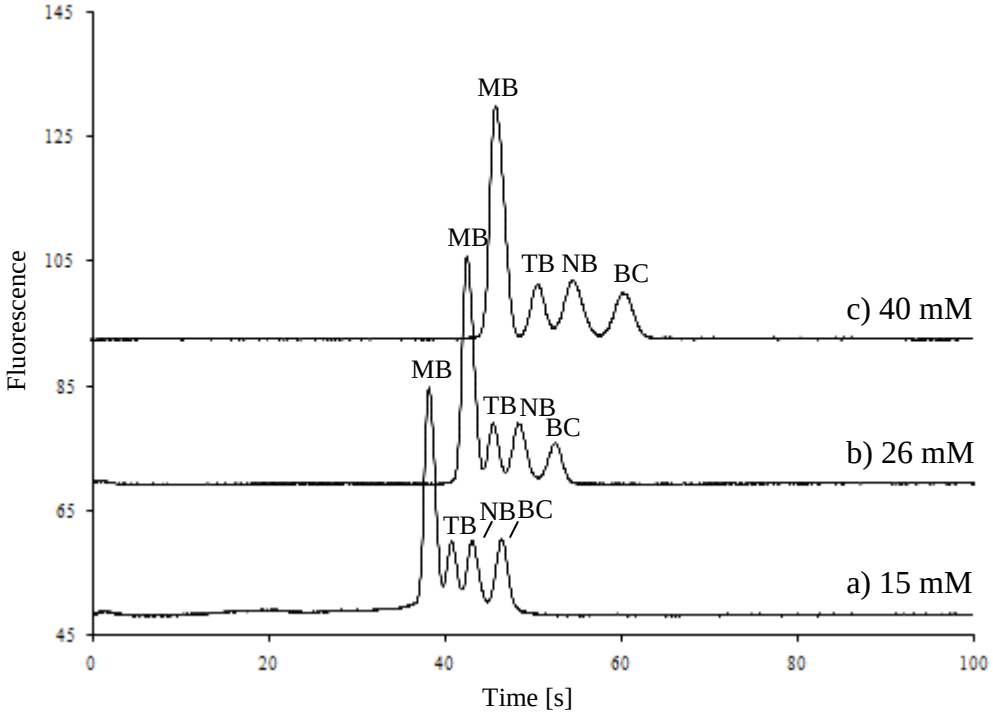

Figure 9.5 Effects of concentrations of $Ca(NO_3)_2$ on the separation of the fluorescent dyes. Conditions: 870 mM acetic acid in DMSO containing $Ca(NO_3)_2$ at the concentration of a) 15 mM, b) 26 mM and c) 40 mM; separation length 14 mm; injection/separation voltage 1,400/1,500 V; temperature 25°C and red LIF detection with λ_{ex} 634/38 nm and λ_{em} 685/22 nm. Peak identification: MB; methylene blue, TB; toluidine blue, NB; nile blue, BC; brilliant cresyl blue.

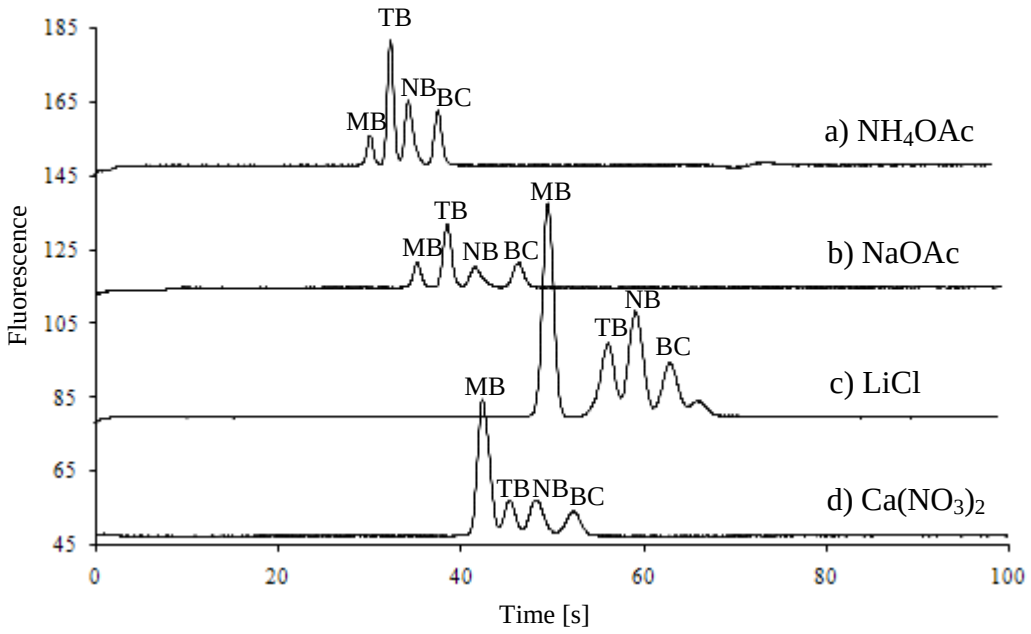

Figure 9.6 Effects of types of BGEs on the separation of the fluorescent dyes. Conditions: 870 mM acetic acid in DMSO containing a) 80 mM NH_4OAc, b) 60 mM NaOAc, c) 60 mM LiCl and d) 26 mM $Ca(NO_3)_2$; separation length 14 mm; injection/separation voltage 1,400/1,500 V; temperature 25°C and red LIF detection with λ_{ex} 634/38 nm and λ_{em} 685/22 nm. Peak identification: MB; methylene blue, TB; toluidine blue, NB; nile blue, BC; brilliant cresyl blue.

Table 9.2 Effects of types of BGEs on analytical parameters of the fluorescent dyes

Analyte / Parameter	MB	TB	NB	BC
%RSD of t_m				
NH_4OAc	2.39	1.95	1.93	1.93
NaOAc	1.59	1.41	1.45	1.80
LiCl	1.84	1.54	1.52	1.40
$Ca(NO_3)_2$	2.08	1.37	1.15	1.10
R_s		MB/TB	TB/NB	NB/BC
NH_4OAc		1.15	1.02	1.50
NaOAc		1.67	1.00	1.75
LiCl		1.78	0.00	1.27
$Ca(NO_3)_2$		0.00	0.00	1.79
TF				
NH_4OAc	0.93	1.05	1.26	0.73
NaOAc	0.91	1.02	1.28	0.74
LiCl	1.07	0.00	0.00	0.96
$Ca(NO_3)_2$	0.00	0.00	0.00	0.91
N				
NH_4OAc	6866.82	9803.33	6461.35	9388.46
NaOAc	5219.31	8339.77	4267.85	5670.21
LiCl	6707.66	0.00	0.00	5749.90
$Ca(NO_3)_2$	0.00	0.00	0.00	4523.44

*%RSD = percent relative standard deviation, t_m = migration time, R_s = resolution, TF = tailing factor, N = number of theoretical plates, MB = methylene blue, TB = toluidine blue, NB = nile blue and BC = brilliant cresyl blue

2.2 Effects of BGE solvent

Analyses of fluorescent dyes using 26 mM NH_4OAc in 870 mM acetic acid in various organic solvent (*i.e.* ACN, DMSO and MeOH,) were examined (1).

When MeOH and ACN were used as the solvents, no peaks were observed and no current was generated. However, in DMSO, excellent separation of the dyes were obtained. Four peaks could be achieved within 40 s with R_s= 1.05-1.50 (Figure 9.7a). Closer examination revealed that for MeOH and ACN, the wells became devoid of liquid after several minutes, which was attributed to the low volumes and high volatility of these solvents. This problem was not observed with DMSO because of its much lower volatility (Table 9.1). To circumvent this issue, 40% water was added to the BGE to decrease the volatility. Further experiments on the uses of MeOH and ACN as the solvent were performed in BGE containing 40% (v/v) water and 60% (v/v) solvent (Figure 9.7b and 9.7c). It can be seen that separations in aqueous ACN was the fastest (t_m < 30 s), while those in MeOH and DMSO required more time (t_m < 40 s). However, the separation in DMSO was superior, possibly due to differences in solvation and acidity/basicity, and prolong migration time (3-4). Sufficient resolution (R_s = 1.05-1.50) of the dyes could only be achieved using DMSO, whereas separations in MeOH and ACN gave co-migrating peaks.

2.3 Effects of water contents in BGE

Water might be present as water of hydration or as physically adsorbed water in organic solvents added BGE. Moreover, organic solvents might absorb water from the environment (3). Water content in the BGE influenced CE separation of the dyes. Results showed that addition of water (10-30%v/v) into 80 mM NH_4OAc and 870 mM acetic acid in DMSO decreased both the resolution and signal intensity of the dyes (Figure 9.8). Increasing amounts of water indicated that the dyes were not completely solubilized and their hydrophobicities caused the hydrophobic interaction with the chip surface. This leads to surface adsorption effects, which in turn contribute to significantly broad peaks and decreased reproducibility due to disruption of the electro-osmotic flow (EOF) (5).

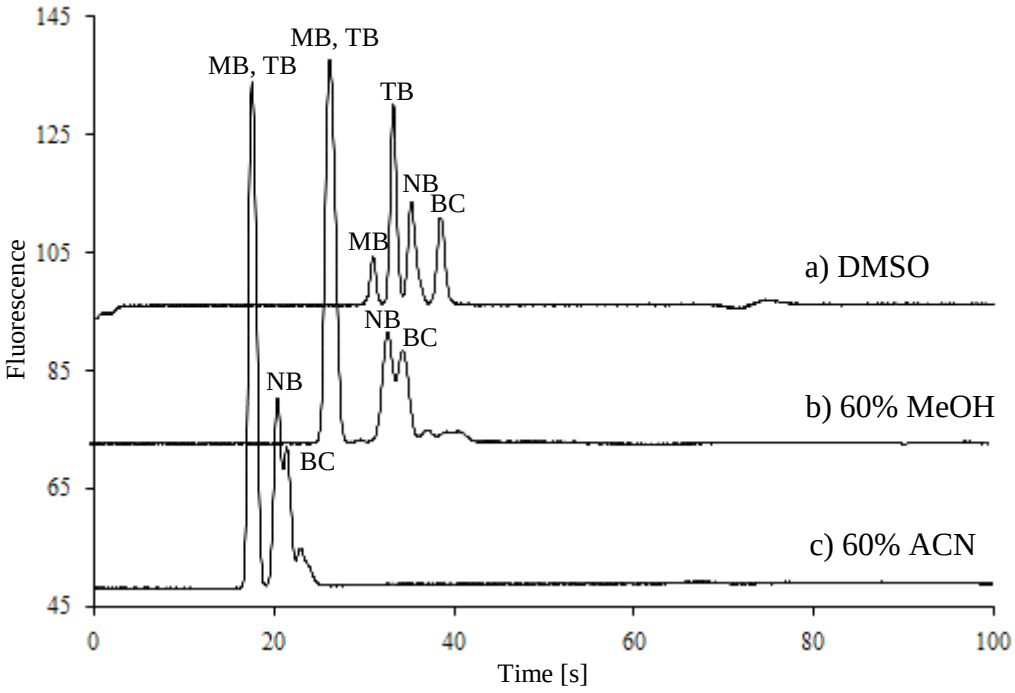

Figure 9.7 Effects of BGE solvent on the separation of the fluorescent dyes. Conditions: 80 mM NH_4OAc and 870 mM acetic acid in , b) 60% MeOH and c) 60% ACN; separation length 14 mm; injection/separation voltage 1,400/1,500 V; temperature 25°C and red LIF detection with λ_{ex} 634/38 nm and λ_{em} 685/22 nm. Peak identification: MB; methylene blue, TB; toluidine blue, NB; nile blue, BC; brilliant cresyl blue.

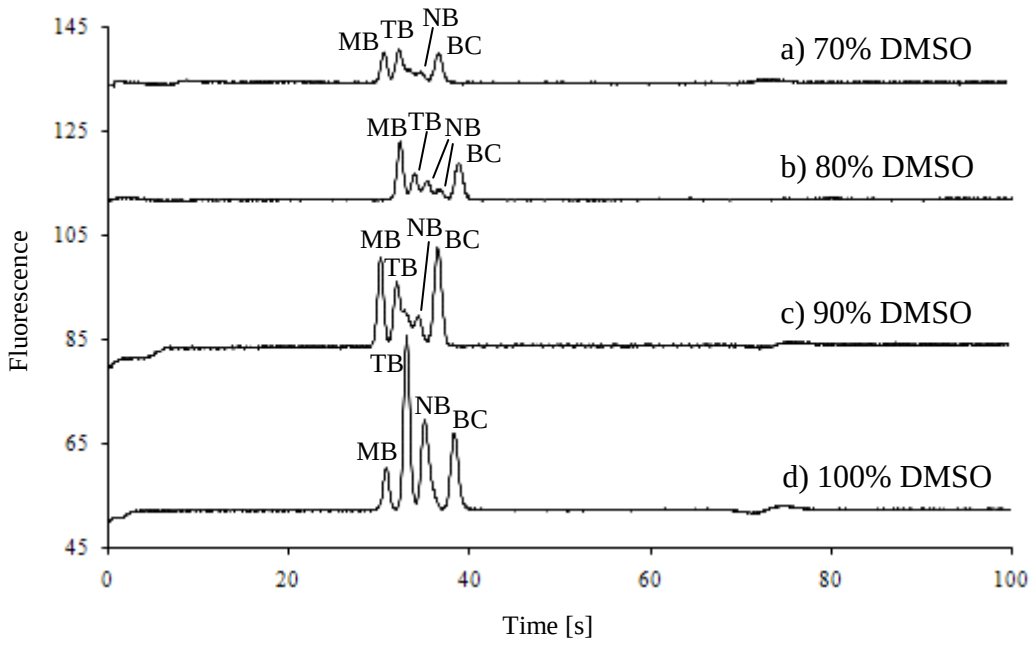

Figure 9.8 Effects of water contents in BGE on the separation of the fluorescent dyes. Conditions: 80 mM NH_4OAc and 870 mM acetic acid in a) 70% DMSO (30% H_2O), b) 80% DMSO (20% H_2O), c) 90% DMSO (10% H_2O) and 100% DMSO; separation length 14 mm; injection/separation voltage 1,400/1,500 V; temperature 25°C and red LIF detection with λ_{ex} 634/38 nm and λ_{em} 685/22 nm. Peak identification: MB; methylene blue, TB; toluidine blue, NB; nile blue, BC; brilliant cresyl blue.

3. Method validation of chip-based NACE for separation of fluorescent dyes

The optimized chip-based NACE condition for the separation of MB, TB, NB and BC was validated in terms of linearity, precision, recoveries, LOD and LOQ.

3.1 Linearity

Calibration curves of fluorescent dyes were established by triplicate injections of five different concentrations of the working standard solutions which were in ranges of 5-28 μM for MB, 10-100 μM for TB, 3.1-50 nM for NB and 5-75

nM for BC. Regression data calculated from peak area provided coefficient of determination (r^2) in ranges of 0.9744-0.9990 (Table 9.3).

3.2 Precision

Precision of the optimized NACE condition was evaluated from intra-day, inter-day and injection precision. Table 9.4 shows the precision of the method.

For intra-day precision, %RSDs of t_m and peak area were less than 2.08 and 2.26, respectively. For inter-day precision, the %RSD of t_m and peak area were less than 2.07 and 2.71, respectively. The %RSD of injection precision of t_m and peak area were less than 2.58 and 2.27, respectively.

3.3 Limit of detection (LOD) and limit of quantitation (LOQ)

LOD and LOQ of analytes were the concentration that can be determined with acceptable precision and recovery at the signal to noise ratio (S/N) of 3 and 10, respectively. Figures 9.9-9.12 and Table 9.5 show electropherograms at LODs and LOQs of MB, TB, NB and BC. The LOQs of the analytes were around three times greater than LODs. Table 9.5 summarized the LODs and LOQs of the dyes.

Table 9.3 Slope, y-intercept, standard error of slope and intercept and coefficient of determination of MB, TB, NB and BC

Analyte	Range	Slope	y-intercept	Standard error of mean		r^2
				slope	intercept	
MB	5-28 µM	141.7646	532.7822	0.3258	1.3121	0.9744
TB	10-100 µM	13.3635	-61.5780	0.0206	0.5690	0.9986
NB	3.1-50 nM	22.9908	43.7182	0.0167	0.5402	0.9990
BC	5-75 nM	1.4462	1.3050	0.0154	0.0149	0.9840

Table 9.4 Precision of MB, TB, NB and BC presented as %RSDs

Analyte	Concentration	Intra-day		Inter-day		Injection	
		t_m	area	t_m	area	t_m	area
MB	5	1.08	0.91	1.82	2.19	-	-
(µM)	15	1.41	1.07	1.53	1.57	2.45	1.32
	100	1.73	1.49	1.69	1.82	-	-
TB	10	1.90	2.23	1.12	1.90	-	-
(µM)	50	2.08	1.84	2.07	2.12	2.58	1.85
	100	1.73	1.10	1.82	1.90	-	-
NB	3.1	1.63	1.08	1.95	1.94	-	-
(nM)	10	1.35	1.61	1.33	1.83	2.36	1.62
	50	1.17	1.46	1.38	2.03	-	-
BC	5	1.46	2.26	1.65	2.71	-	-
(nM)	30	1.72	1.86	1.57	2.30	2.18	2.27
	75	1.70	2.22	1.12	2.31	-	-

*%RSD = percent relative standard deviation, t_m = migration time

Table 9.5 LODs and LOQs of MB, TB, NB and BC

Analyte	LOD (nM)	LOQ (nM) (n = 3)
MB	90	300 (1.76)
TB	1,000	3,200 (2.06)
NB	1.4	4.5 (1.98)
BC	2	6.2 (1.88)

*numbers in parentheses represent %RSDs (percent relative standard deviation), LOD = limit of detection, LOQ = limit of quantitation

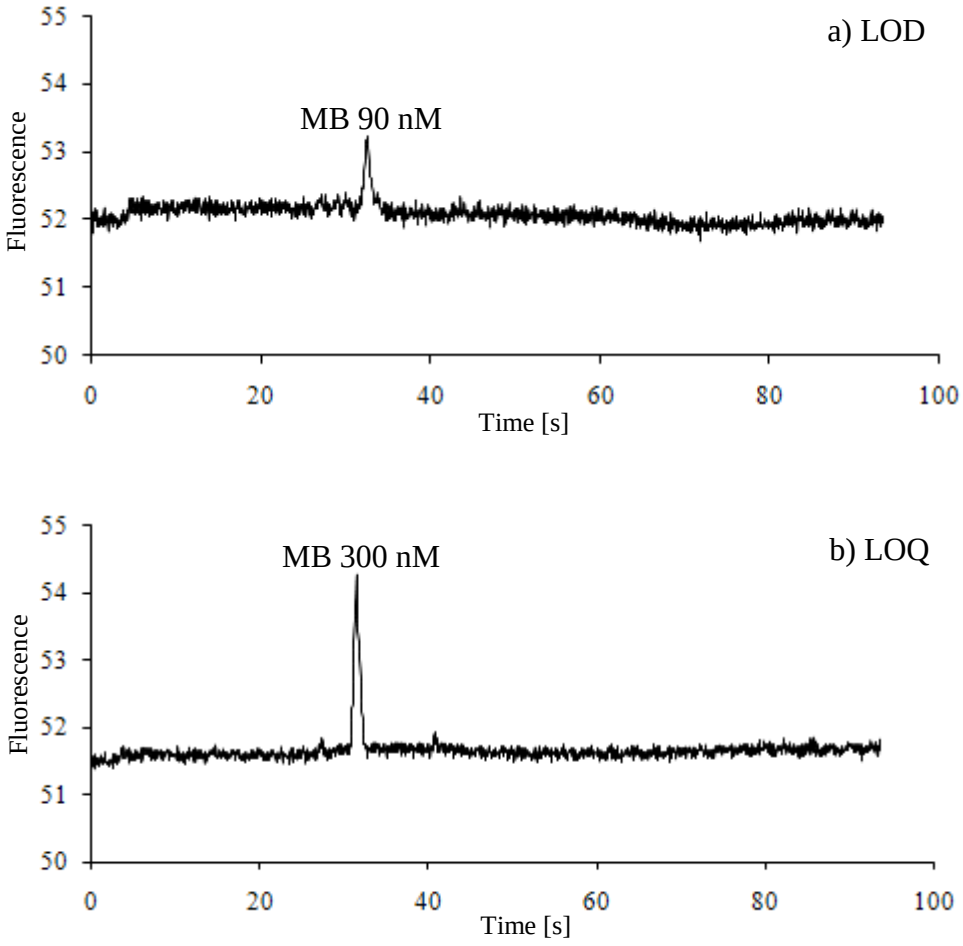

Figure 9.9 Electropherograms of methylene blue (MB) at limit of detection (LOD) and limit of quantitation (LOQ) levels. Microchip CE conditions see Figure 9.6a.

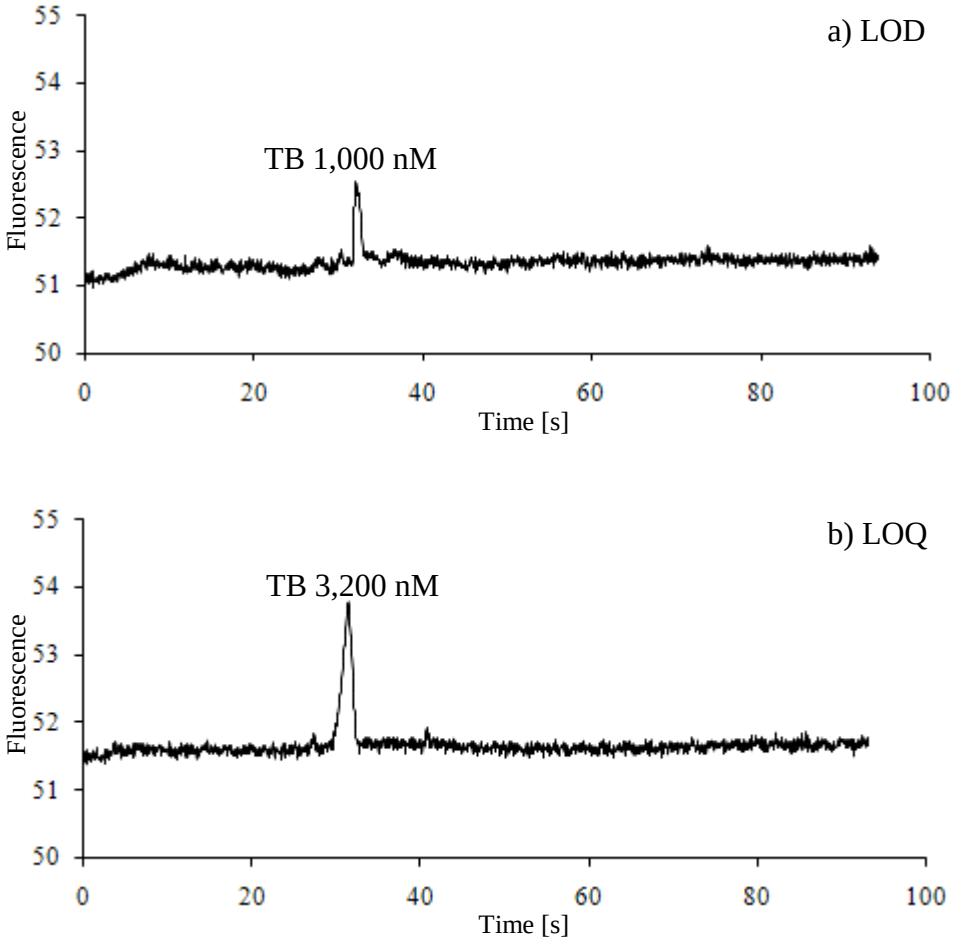

Figure 9.10 Electropherograms of toluidine blue (TB) at limit of detection (LOD) and limit of quantitation (LOQ) levels. Microchip CE conditions see Figure 9.6a.

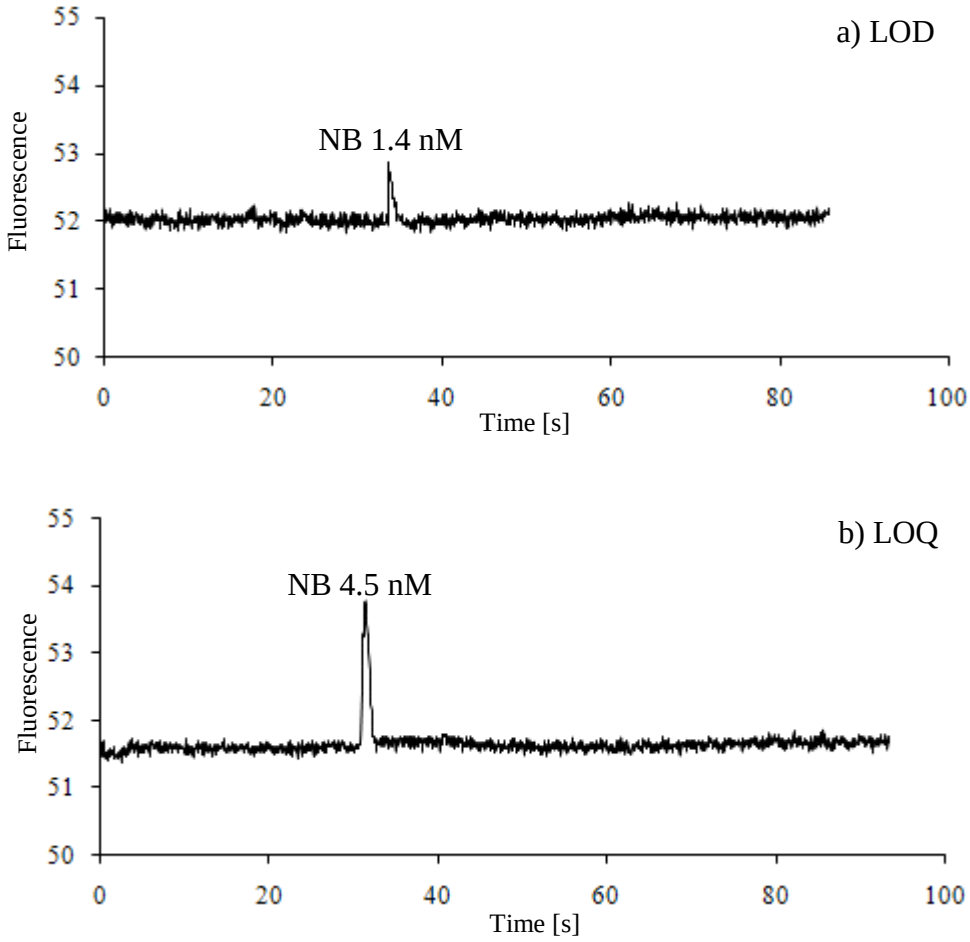

Figure 9.11 Electropherograms of nile blue (NB) at limit of detection (LOD) and limit of quantitation (LOQ) levels. Microchip CE conditions see Figure 9.6a.

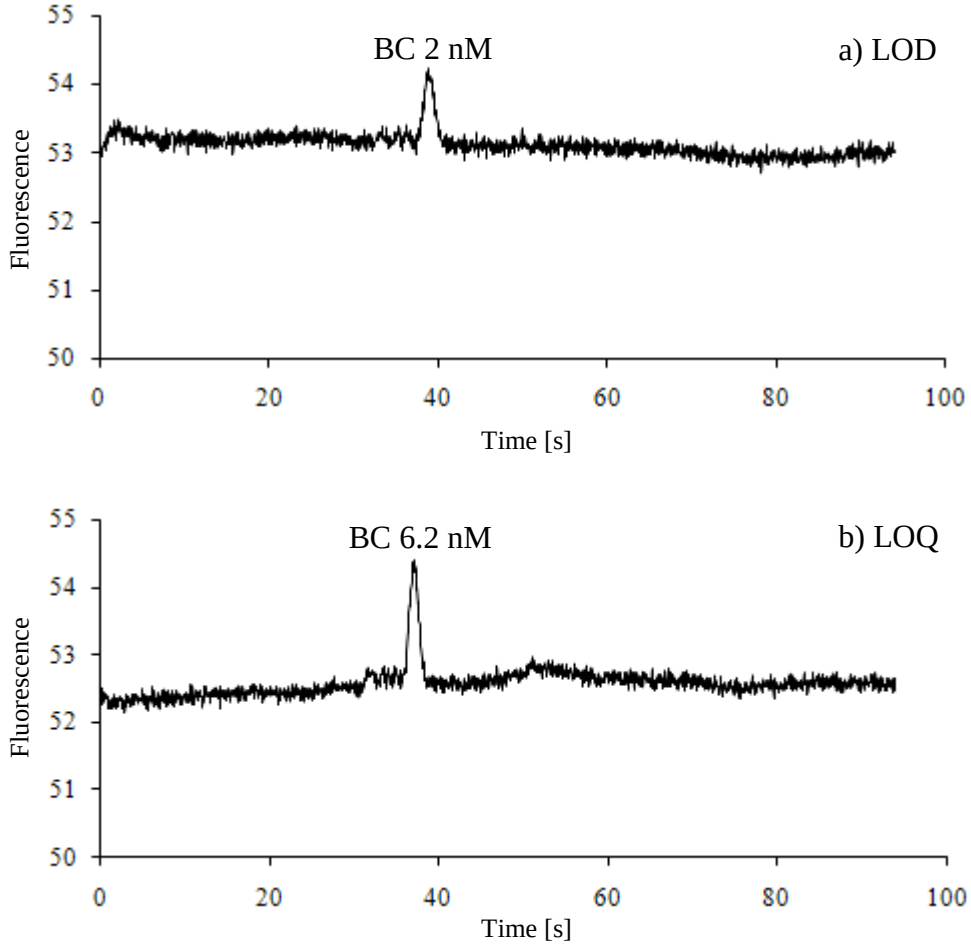

Figure 9.12 Electropherograms of brilliant cresyl blue (BC) at limit of detection (LOD) and limit of quantitation (LOQ) levels. Microchip CE conditions see Figure 9.6a.

4. Optimization of fluorescent staining of micoorganisms using on chip flow cytometry

NB is a hydrophobic basic fluorescent dye, which exhibits positive charge. The bacteria and fungi surface possess negative charges that could be attracted to nile blue. The optimization of NB concentration for bacteria and fungi staining was investigated in the range of 2.5-15 µM on the on-chip flow cytometry to ensure that the microorganisms were saturated with NB. The results showed that *E. coli, B. subtilis, M. luteus, S. aureus, C. albicans* and *L. fungicola* were saturated with NB at the concentration of 7.5, 7.5, 12.5, 12.5, 10 and 7.5 µM, respectively (Figure 9.13). However, 12.5 µM of NB was utilized for staining of all microorganisms to ensure complete cell staining and the excess NB was then removed in the washing step. The measured fluorescence values and cell number for the optimum stain of each microorganism are displayed as dot plots in Figure 9.14.

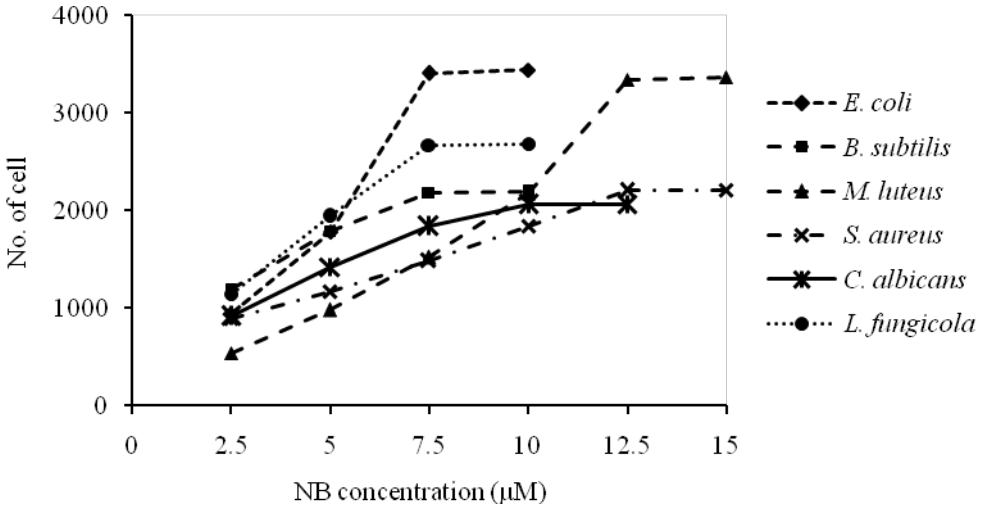

Figure 9.13 Optimization of NB concentrations for cell staining: *E. coli, B. subtilis, M. luteus, S. aureus, C. albicans* and *L. fungicola* stained with NB analyzed on the on-chip flow cytomety.

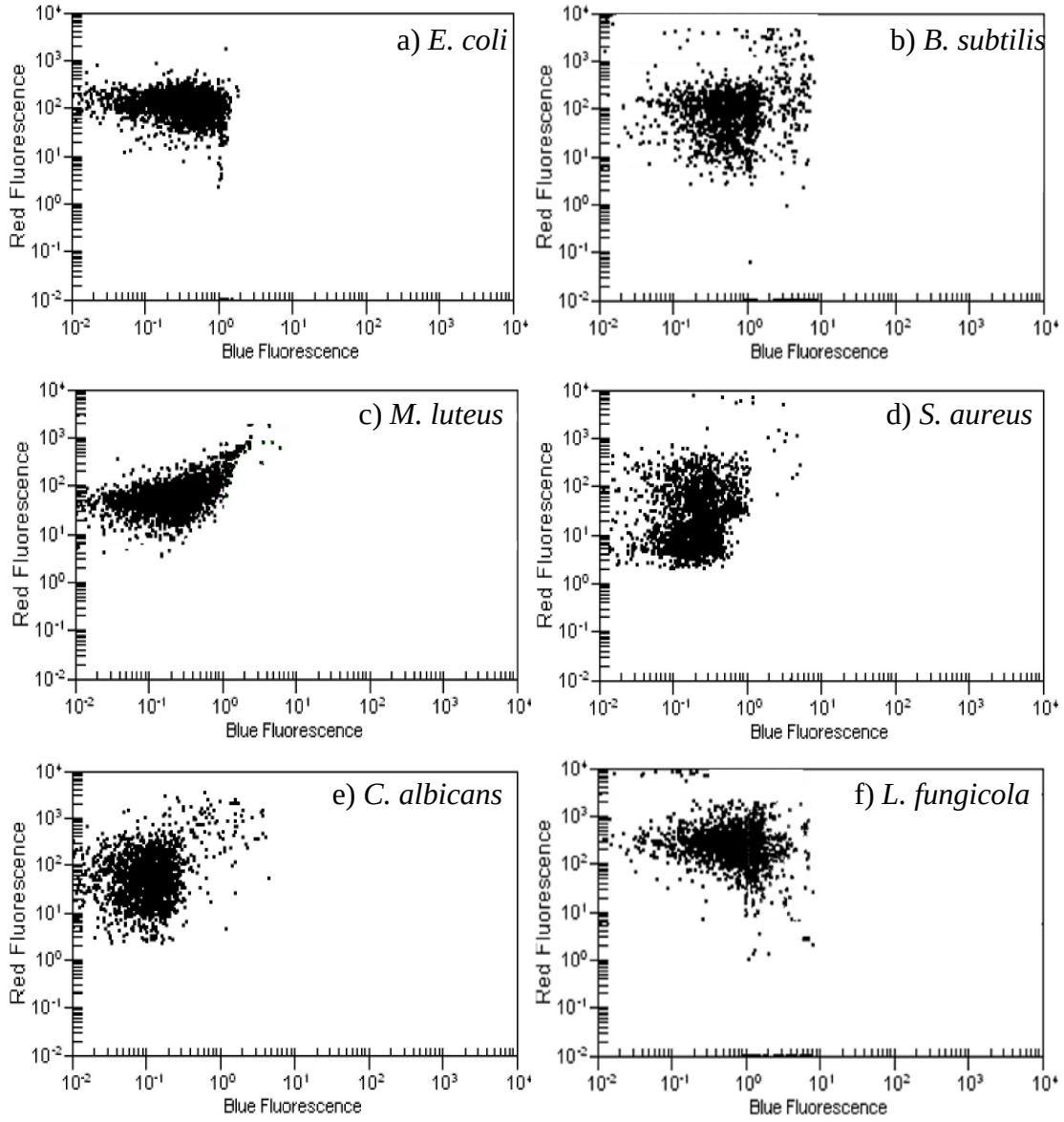

Figure 9.14 Dot plots of red fluorescence of a) *E. coli*, b) *B. subtilis*, c) *M. luteus*, d) *S. aureus*, e) *C. albicans* and f) *L. fungicola* stained with NB at the concentration of 7.5, 7.5, 12.5, 12.5, 10 and 7.5 µM, respectively and analyzed on the on-chip flow cytomety.

5. Analysis of single microorganism

Analyses of single microorganism (*i.e. E. coli, B. subtilis, M. luteus, S. aureus, C. albicans* and *L. fungicola*) on the microchip CE using spacer method (see section 3.5) were evaluated. The spacer method was previously applied for sample introduction in conventional CE (6-8) however, injection in microchip format differs from conventional CE in term of the microchip channel geometry, particularly at the intersection cross used for defining injection volume. Filling the injection intersection was achieved by application of different voltage to the sample waste and the sample reservoirs, and the small plug of sample was produced by application of different voltage to the buffer waste and the buffer reservoirs.

Presently, the microchip channels were filled with BGE containing CTAB before the injection of the cell suspensions in 1 mM Tris/0.33 mM citric acid buffer (pH 7.0) was made followed by a spacer of BGE containing CTAB and the blocking agents (nutrient broth or SB3-10). When the voltage was applied, the CTAB on the anodic side of the microbes migrated toward the cathode and coated the microbes as it moves through the sample zone. Positive charges on the microbes moved them toward the cathode until they met the blocking agent segment which was migrated with the EOF. Under these conditions, EOF was reversed and it flowed toward the anode. The combination of the anodic movement of the blocking agent segment and the cathodic movement of the microorganisms allowed the microorganism began to aggregate and eventually formed a large macroparticle. From this point on it became electrically neutral migrated in the anodic direction (towards the detector) while residing in the blocking agent (7). This allowed all of the aggregated microorganisms migrating together at the same velocity resulted in a narrow zone of sample and obtained a single and sharp peak.

Since the charges on microorganism surfaces caused electrophoretic heterogeneity. Uses of blocking agents which were the uncharged compounds, were purposed for elimination or minimization of the surface charges. Nutrient broth and the zwitterionic sulfobetaine surfactant, caprylyl sulfobetaine (SB3-10), were utilized for this approach (6). Figure 9.15-9.20 showed that SB3-10 demonstrated the superior effects on focusing the cells into a sharper peak (TF = 1.11-2.00) than nutrient broth

(TF = 0.82-4.22). Therefore, SB3-10 was chosen as an alternative blocking agent instead of the nutrient broth.

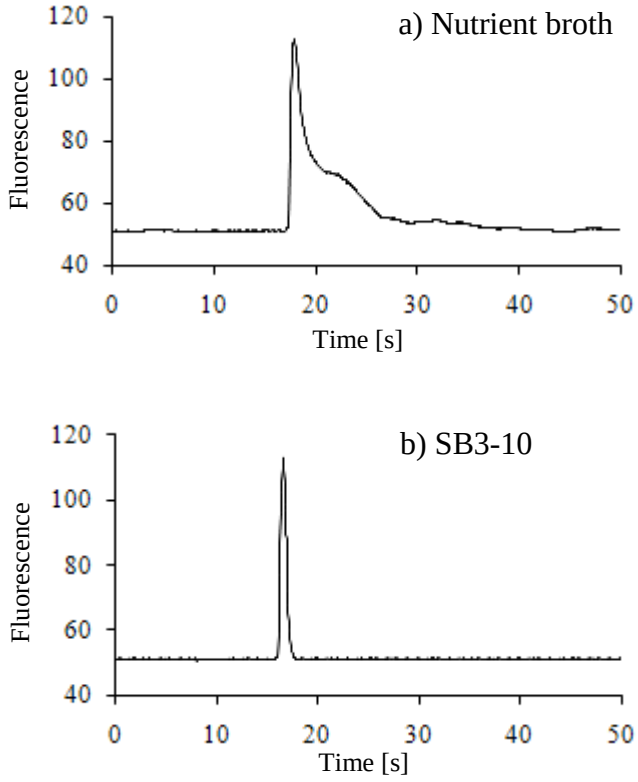

Figure 9.15 Analysis of *E. coli* using the spacer method. Conditions: 1 mg/mL CTAB in 1 mM Tris/0.33 mM citric acid, pH 7.0 using a) nutrient broth and b) 5 mg/mL SB3-10 as blocking agent; separation length 14 mm; injection/separation voltage -1,000/-1,000 V; temperature 25°C and red LIF detection with λ_{ex} 634/38 nm and λ_{em} 685/22 nm.

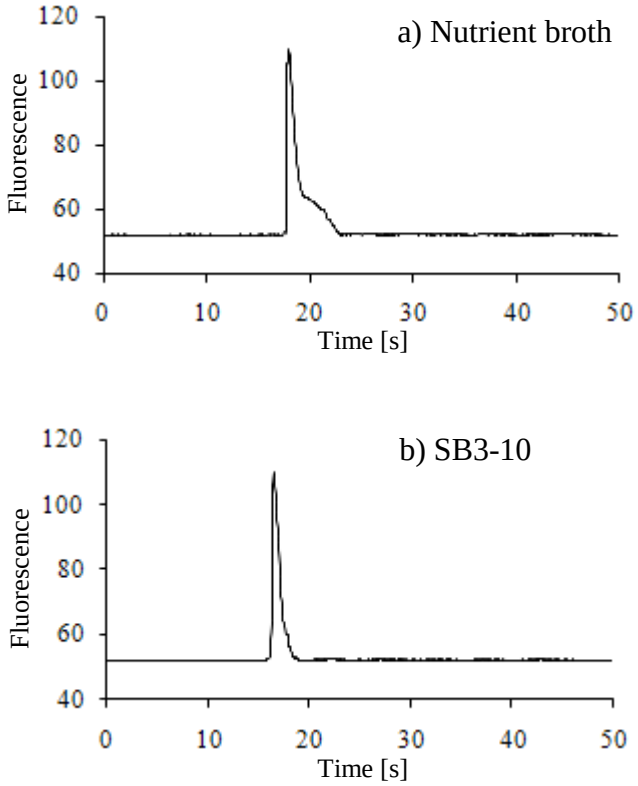

Figure 9.16 Analysis of *B. subtilis* using the spacer method. Conditions: 1 mg/mL CTAB in 1 mM Tris/0.33 mM citric acid, pH 7.0 using a) nutrient broth and b) 5 mg/mL SB3-10 as blocking agent; separation length 14 mm; injection/separation voltage -1,000/-1,000 V; temperature 25°C and red LIF detection with λ_{ex} 634/38 nm and λ_{em} 685/22 nm.

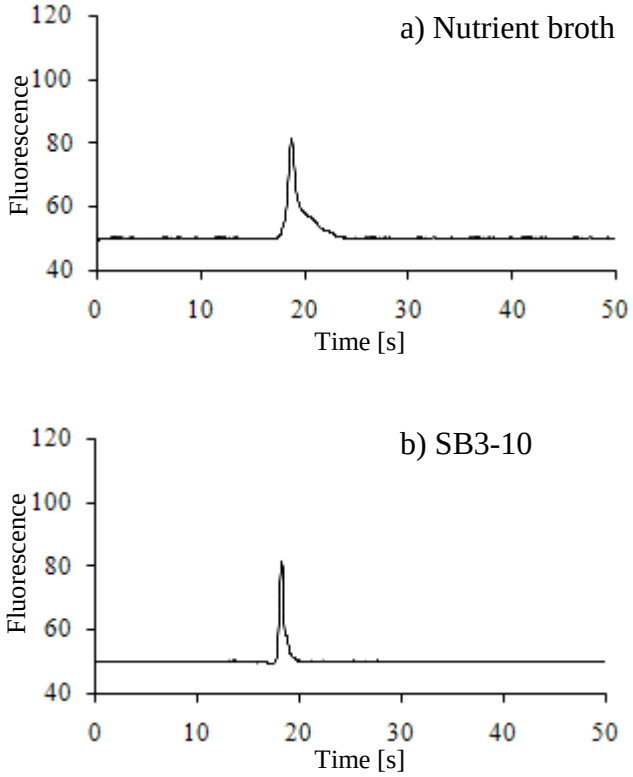

Figure 9.17 Analysis of *M. luteus* using the spacer method. Conditions: 1 mg/mL CTAB in 1 mM Tris/0.33 mM citric acid, pH 7.0 using a) nutrient broth and b) 5 mg/mL SB3-10 as blocking agent; separation length 14 mm; injection/separation voltage -1,000/-1,000 V; temperature 25°C and red LIF detection with λ_{ex} 634/38 nm and λ_{em} 685/22 nm.

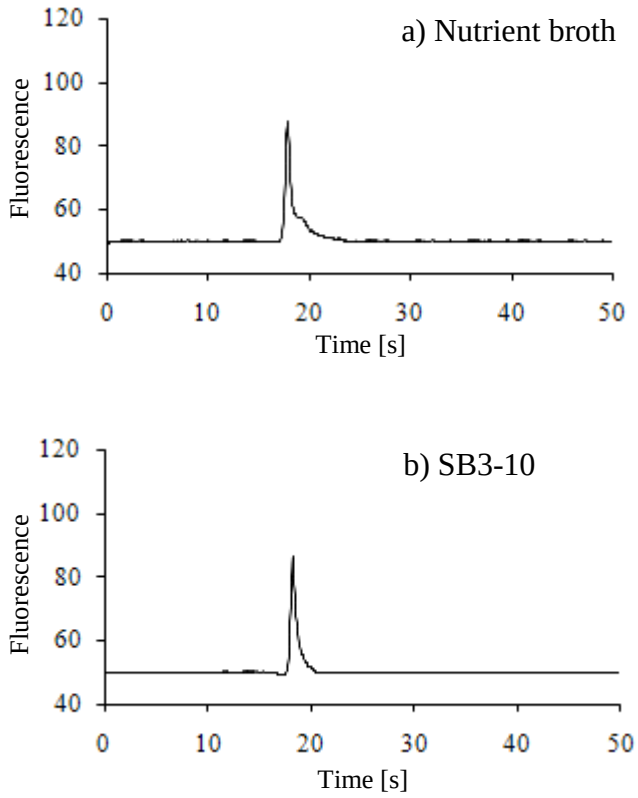

Figure 9.18 Analysis of *S. aureus* using the spacer method. Conditions: 1 mg/mL CTAB in 1 mM Tris/0.33 mM citric acid, pH 7.0 using a) nutrient broth and b) 5 mg/mL SB3-10 as blocking agent; separation length 14 mm; injection/separation voltage -1,000/-1,000 V; temperature 25°C and red LIF detection with λ_{ex} 634/38 nm and λ_{em} 685/22 nm.

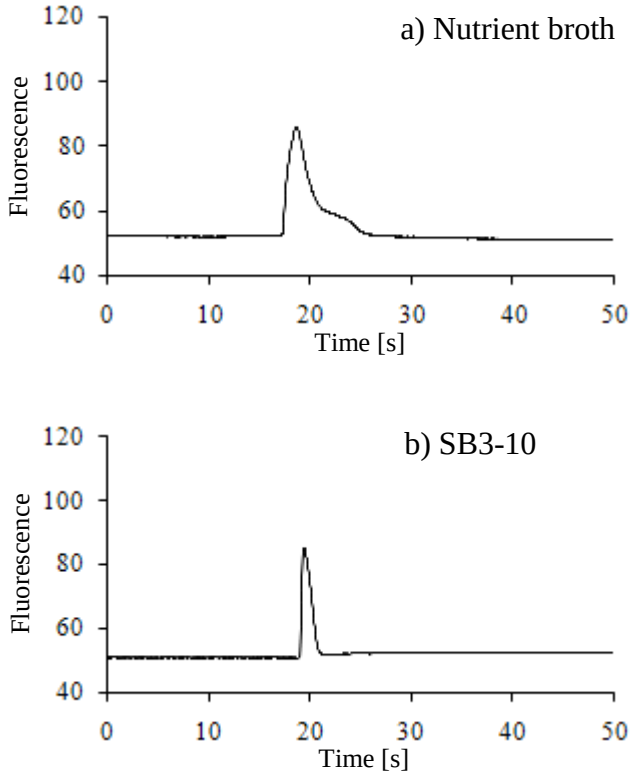

Figure 9.19 Analysis of *C. albicans* using the spacer method. Conditions: 1 mg/mL CTAB in 1 mM Tris/0.33 mM citric acid, pH 7.0 using a) nutrient broth and b) 5 mg/mL SB3-10 as blocking agent; separation length 14 mm; injection/separation voltage -1,000/-1,000 V; temperature 25°C and red LIF detection with λ_{ex} 634/38 nm and λ_{em} 685/22 nm.

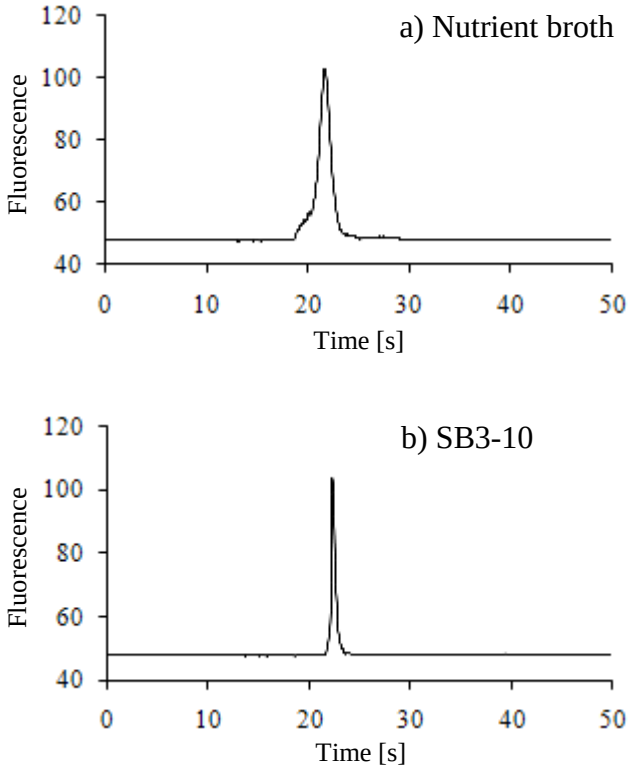

Figure 9.20 Analysis of *L. fungicola* using the spacer method. Conditions: 1 mg/mL CTAB in 1 mM Tris/0.33 mM citric acid, pH 7.0 using a) nutrient broth and b) 5 mg/mL SB3-10 as blocking agent; separation length 14 mm; injection/separation voltage -1,000/-1,000 V; temperature 25°C and red LIF detection with λ_{ex} 634/38 nm and λ_{em} 685/22 nm.

Fluorescence labeling is generally specific to the target analyte, thus interferences from sample matrices could be decreased resulting in low background noises. Additionally, SB3-10 greatly reduced the background fluorescence of the blocker plug. This background reduction allows a single cell to be detected, which is an essential for detecting of a microbial contamination or sterility test. In this work, injection volume was fixed at 24 pL based on chip dimension (40 x 40 x 15 μm). Thus, samples were prepared to finally obtain a single cell of bacteria or fungi while applying to the injection intersection and its signal to noise ratio was observed. Figure 9.21 shows electropherograms of single cell detection for both Gram negative and positive bacteria and fungi. The fluorescence intensity from the single cell analysis

displayed signal to noise ratios (S/N) of 25.6- 34.0 with %RSD of 1.91-2.45 (Figure 9.21).

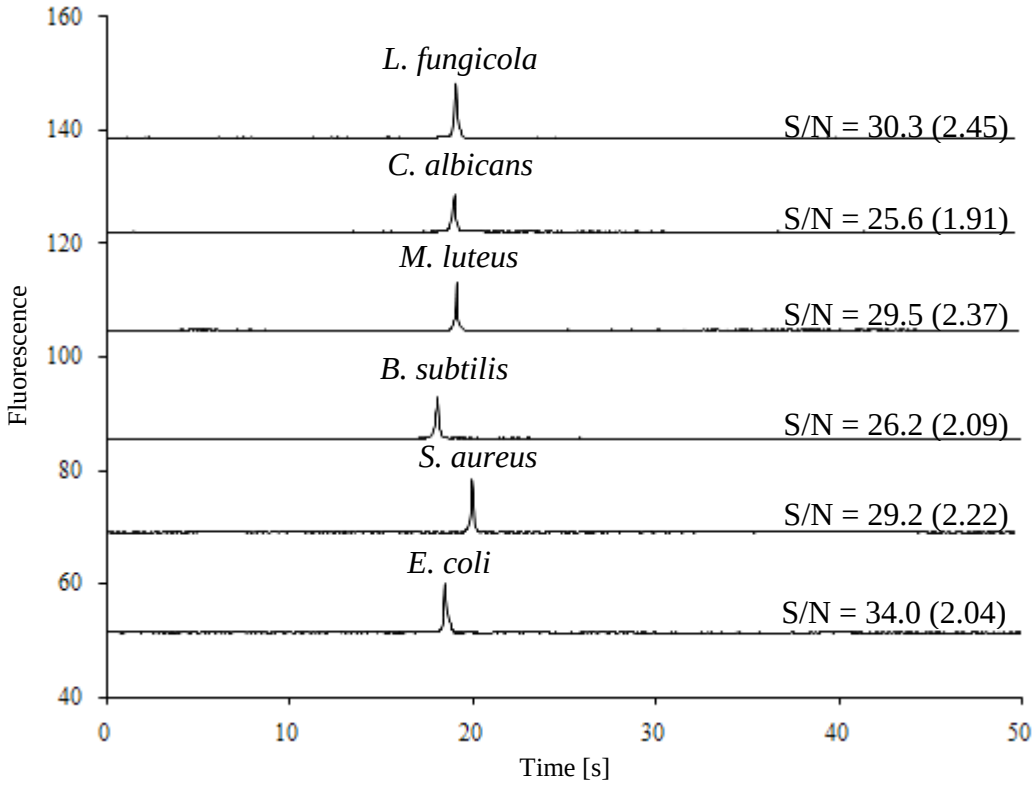

Figure 9.21 Electropherograms of single cells of bacteria and fungi. Conditions: 1 mg/mL CTAB in 1 mM Tris/0.33 mM citric acid, pH 7.0 using 5 mg/mL SB3-10 as blocking agent; separation length 14 mm; injection/separation voltage -1,000/-1,000 V; temperature 25°C and red LIF detection with λ_{ex} 634/38 nm and λ_{em} 685/22 nm.
S/N = signal-to-noise ratio and numbers in parentheses represent %RSDs (percent relative standard deviation).

6. Optimization of microorganism separation

From the analysis of single microorganism (previous section), each microbe showed a sharp peak in 1 mM Tris/0.33 mM citric acid buffer (pH 7.0) containing 1 mg/mL of CTAB. The microbe migrated with similar mobility resulting in the same migration time of about 20 s (Figure 9.21). Thus, this condition might not be suitable for separation of a microbe mixture. Addition of PEO into TBE buffer was considered to solve this problem. Utilization of dilute PEO as a non-bonded coating capillary was selected to prevent adsorption of cells to the capillary wall and to alter the EOF (9). The selected mixture containing *E. coli*, *S. aureus* and *C. albicans* was respresentatives of Gram negative bacteria, Gram positive bacteris and fungi, respectively.

At pH 8.5-9.5, baseline separation of the microbes could not be achieved (Figure 9.22). Increasing pH until pH 10.0-11.0, these microbes could be baseline separated with $R_s > 0.7$, however, at pH 11.0 their peak intensities decreased due to cell lyses. Figure 9.23 presents effects of pH on analytical parameters for the separation of the microbe mixture. The optimal pH was at 10.5, which provided %RSD of $t_m < 1.60$, $R_s > 1.3$, TF = 0.83 - 1.38 and N > 8,600. Furthermore, amounts of PEO in TBE buffer was optimized to improve the separation (Figure 9.24 and 9.25). Adding the PEO slowed the EOF resulting in well separated peaks of the microbes. TBE buffer (pH10.5) containing 0.0125 and 0.025% PEO provided better peak shapes of the microbes than the buffer with 0.05% PEO. Tailing peaks might occurs at high amount of PEO (0.05%) due to the weaker EOF, which was insufficient to focus samples into a narrow zone. The optimal PEO content in the buffer was 0.025% providing %RSD of $t_m < 1.80$, TF = 0.83 - 1.43, $R_s > 5.3$ and N > 20,000 (Figure 9.25). Finally, the optimal condition was applied for the separation of mixture of Gram positive bacteria (*i.e. B. subtilis*, *M. luteus* and *S. Aureus*) and the baseline separation was achieved (Figure 9.26).

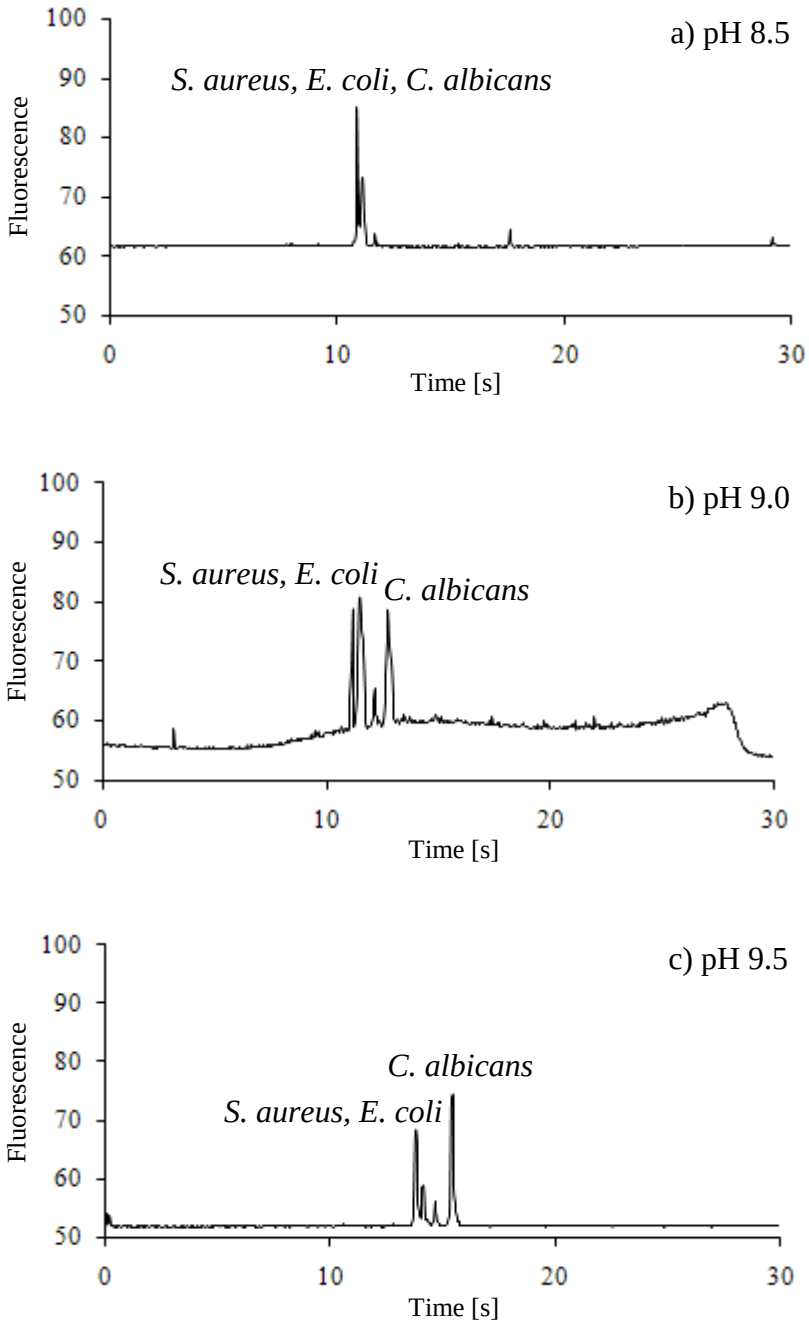

Figure 9.22 Effect of pHs of BGEs on the separation of *E. coli*, *S. aureus* and *C. albicans*. Conditions: 0.0125 % PEO in 3.94 mM Tris, 0.56 mM boric acid and 0.013 mM Na_2EDTA pH a) 8.5, b) 9.0, c) 9.5, d) 10.0, e) 10.5 and f) 11.0; separation length 14 mm; injection/separation voltage 1,000/1,000 V; temperature 25°C and red LIF detection with λ_{ex} 634/38 nm and λ_{em} 685/22 nm.

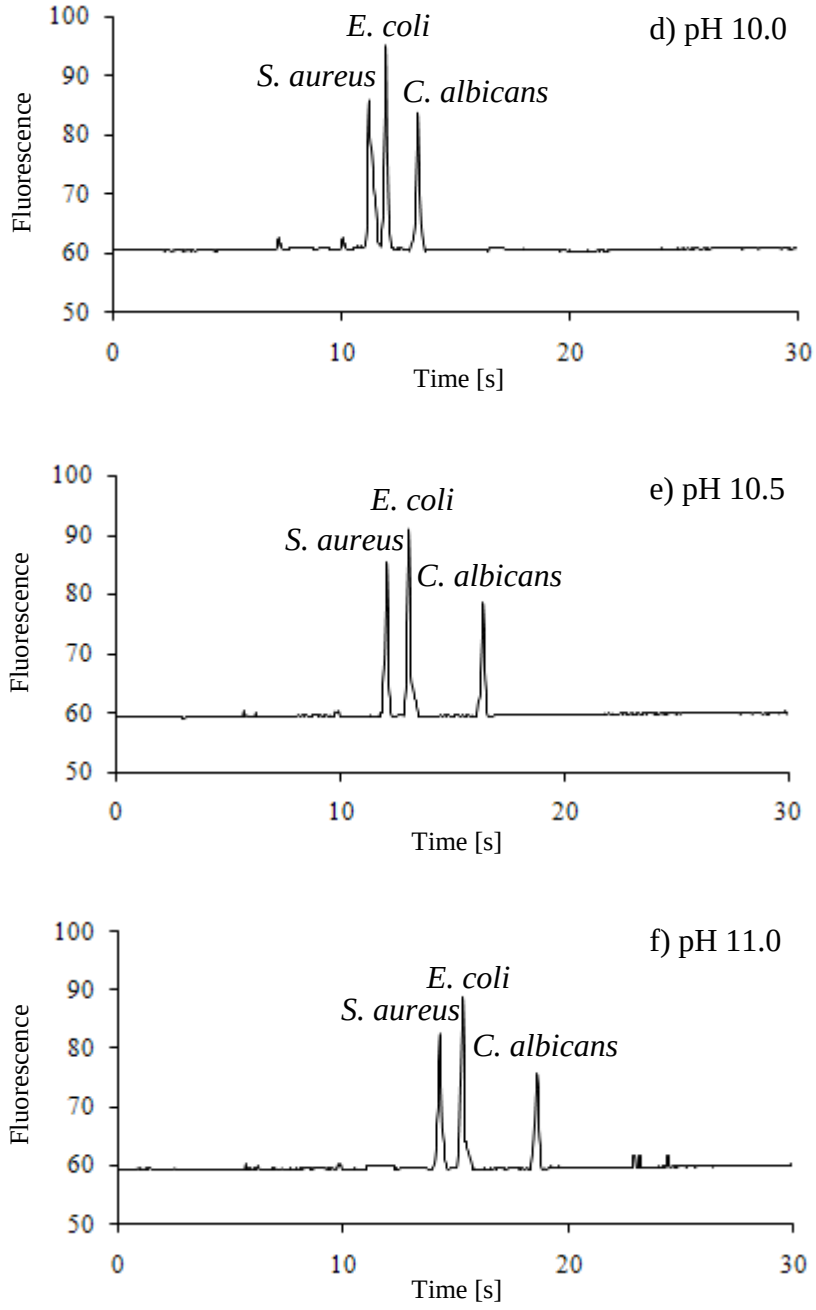

Figure 9.22 (continued) Effect of pHs of BGEs on the separation of *E. coli*, *S. aureus* and *C. albicans*. Conditions: 0.0125 % PEO in 3.94 mM Tris, 0.56 mM boric acid and 0.013 mM Na_2EDTA pH a) 8.5, b) 9.0, c) 9.5, d) 10.0, e) 10.5 and f) 11.0; separation length 14 mm; injection/separation voltage 1,000/1,000 V; temperature 25°C and red LIF detection with λ_{ex} 634/38 nm and λ_{em} 685/22 nm.

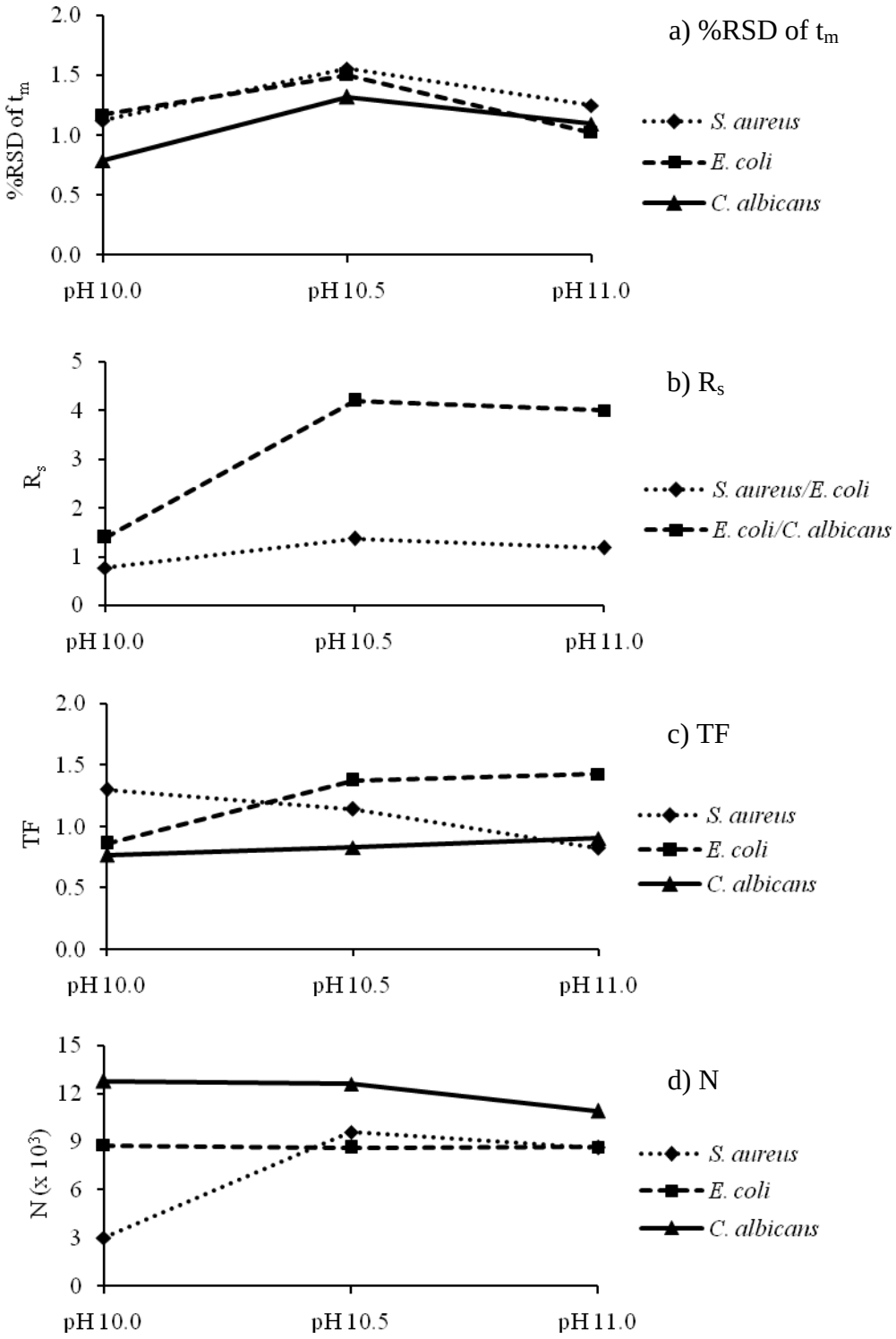

Figure 9.23 Effects of pHs of BGEs on analytical parameters of the investigated microorganisms, a) % relative standard deviation (%RSD) of migration time (t_m), b) resolution (R_s), c) tailing factor (TF) and d) number of theoretical plates (N).

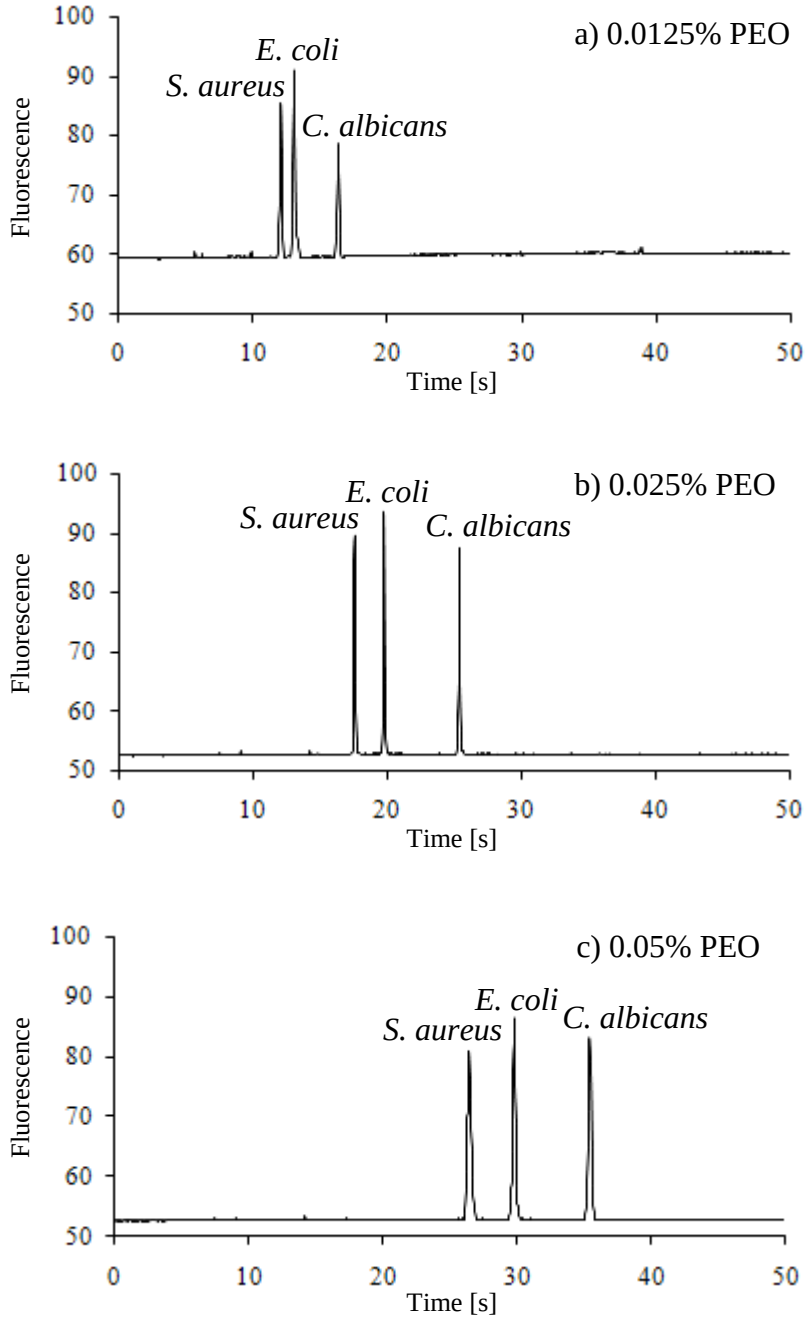

Figure 9.24 Effect of amount of PEO on the separation of *E. coli*, *S. aureus* and *C. albicans*. Conditions: 3.94 mM Tris, 0.56 mM boric acid and 0.013 mM Na_2EDTA pH 10.5 containing a) 0.0125%, b) 0.025% and c) 0.05% PEO; separation length 14 mm; injection/separation voltage 1,000/1,000 V; temperature 25°C and red LIF detection with λ_{ex} 634/38 nm and λ_{em} 685/22 nm.

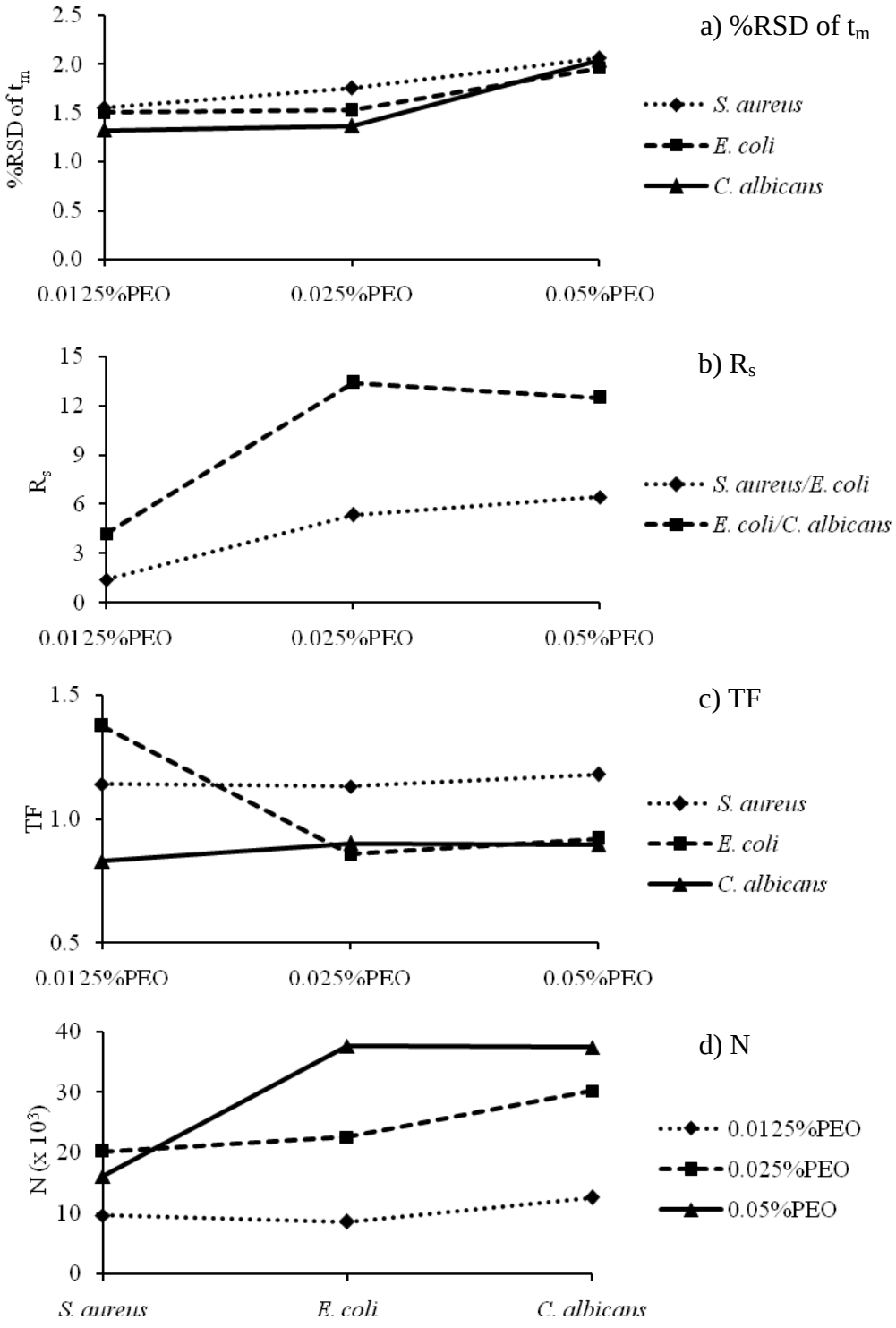

Figure 9.25 Effects of amount of PEO on analytical parameters of the investigated microorganisms, a) % relative standard deviation (%RSD) of migration time (t_m), b) resolution (R_s), c) tailing factor (TF) and d) number of theoretical plates (N).

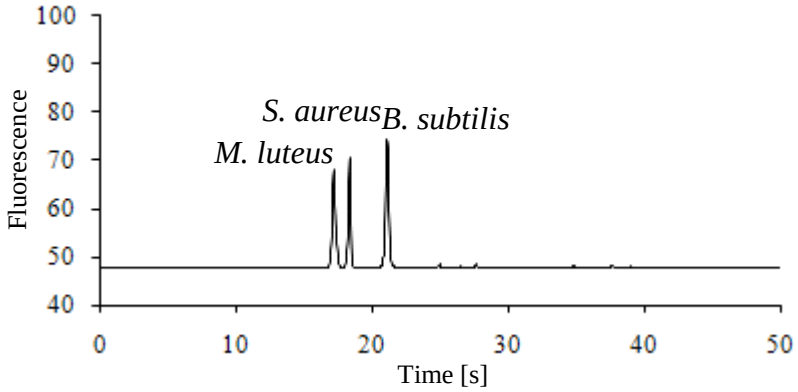

Figure 9.26 Electropherogram of the separation of *B. subtilis*, *M. luteus* and *S. aureus*. Conditions: 0.025% PEO in 3.94 mM Tris, 0.56 mM boric acid and 0.013 mM Na_2EDTA pH 10.5; separation length 14 mm; injection/separation voltage 1,000/1,000 V; temperature 25°C and red LIF detection with λ_{ex} 634/38 nm and λ_{em} 685/22 nm.

CHAPTER X
CONCLUSION

A simple and rapid chip-based non-aqueous CE separation of several structurally related basic dyes (*i.e.* MB, TB, NB and BC) was established using commercial chip-based CE instrument with a red LIF detection. Initially, the compatibility of the chips with organic solvent (*i.e.* ACN, DMF, DMSO and MeOH) was visually observed. DMSO, ACN and MeOH were compatible with the chips but ACN and MeOH were highly volatile. While the plastic covering chip was deformed in DMF. Presently, DMSO was selected as the solvent of choice. Optimization of the dye separation was performed by varying types and concentrations of BGE (*i.e.* 26-90 mM NH_4OAc, 26-70 mM NaOAc, 26-70 mM LiCl and 15-40 mM $Ca(NO_3)_2$ with 870 mM acetic acid in DMSO), BGE solvents (*i.e.* MeOH, ACN and DMSO), and water contents in BGE (10-30%). The NACE separation of fluorescent dyes was achieved in 80 mM NH_4OAc, 870 mM acetic acid in DMSO using DNA chip with separation length 14 mm, injection/separation voltage 1,400/1,500 V, temperature of 25°C and red LIF detection with λ_{ex} 634/38 nm and λ_{em} 685/22 nm. The optimum condition provided a baseline separation of all dyes in less than 40 s with the $R_s > 1.0$, $N > 6,400$, TF = 0.73-1.26 and %RSD of $t_m < 2.39$. The NACE condition was validated in term of linearity, precision, LOD and LOQ. Calibration curves were established over 5-28 μM, 10-100 μM, 3.1-50 nM and 5-75 nM for MB, TB, NB and BC, respectively. The good linearity (r^2 = 0.9744-0.9990) was obtained for all analytes. Method precision was performed by intra-, inter-day and injection precision. The %RSD of t_m and peak area were less than 2.58 and 2.71, respectively. The LODs were 90, 1,000, 1.4 and 2 nM and the LOQs were 300, 3,200, 4.5 and 6.2 nM (%RSD 1.76-2.06) for MB, TB, NB and BC, respectively. The results showed that red LIF facilitated sensitive detection of these dyes, especially NB, which was the most sensitive dye. Therefore, NB could be a potential fluorescent stain for microorganisms (*i.e. E. coli, B. subtilis, M. luteus, S. aureus, C. albicans* and *L. fungicola*).

The optimization of NB concentration for cell staining was investigated in the range of 2.5-15 μM on the on-chip flow cytometry to ensure fully stained. The results showed that *E. coli*, *B. subtilis*, *M. luteus*, *S. aureus*, *C. albicans* and *L. fungicola* were saturated with NB at the concentration of 7.5, 7.5, 12.5, 12.5, 10 and 7.5 μM, respectively. However, 12.5 μM of NB was utilized for staining of all microorganisms to facilitate complete cell staining. Then, analyses of the fluorescent stained cell were performed on the chip-based electrophoresis. The optimal condition for the analysis of single microorganism was carried out in 1 mg/mL CTAB in 1 mM Tris/0.33 mM citric acid, pH 7.0 using 5 mg/mL SB3-10 as blocking agent, separation length 14 mm, injection/separation voltage -1,000/-1,000 V, temperature of 25°C and red LIF detection. Single cell analysis of *E. coli*, *B. subtilis*, *M. luteus*, *S. aureus*, *C. albicans* and *L. fungicola* was achieved at ~20 s providing S/N of 34.0, 29.2, 26.2, 29.5, 25.6 and 30.3, respectively, with %RSD within 2.45%. However, separations of the mixture containing *E. coli*, *S. aureus* and *C. albicans*, respresentatives of Gram negative bacteria, Gram positive bacteris and fungi, respectively, could not be approached in this condition. Thus, the addition of PEO in TBE buffer was considered for the separation of microorganism mixture. Optimization was performed by varying pH of TBE buffer (pH 8.5-11.0) and amount of PEO (0.0125-0.05%). The optimized condition was achieved in 3.94 mM Tris, 0.56 mM boric acid and 0.013 mM Na_2EDTA pH 10.5 containing 0.025% PEO, separation length 14 mm, injection/separation voltage 1,000/1,000 V, temperature of 25°C and red LIF detection, providing %RSD of $t_m < 1.80$, TF = 0.83 - 1.43, $R_s > 5.3$ and $N > 20,000$. Addtionally, the optimal condition was successfully applied for the separation of Gram positive bacteria (*i.e. B. subtilis*, *M. luteus* and *S. aureus*).

Finally, the developed method on the commercially available microchip CE showed promising results, which enables the orientation of this instrument for the other applications using general CE method.

PART II: REFERENCES

1 Dittrich PS, Tachikawa K, Manz A. Micro total analysis systems. Latest advancements and trends. Anal Chem. 2006; 78(12): 3887-908.

2 Vilkner T, Janasek D, Manz A. Micro total analysis systems. Recent developments. Anal Chem. 2004; 76(12): 3373-86.

3 Reyes DR, Iossifidis D, Auroux P-A, Manz A. Micro total analysis systems. 1. introduction, theory, and technology. Anal Chem. 2002; 74(12): 2623-36.

4 Auroux P-A, Iossifidis D, Reyes DR, Manz A. Micro total analysis systems. 2. Analytical standard operations and applications. Anal Chem. 2002; 74(12): 2637-52.

5 Duffy DC, McDonald JC, Schueller OJA, Whitesides GM. Rapid prototyping of microfluidic systems in poly(dimethylsiloxane). Anal Chem. 1998; 70(23): 4974-84.

6 McDonald JC, Duffy DC, Anderson JR, Chiu DT, Wu H, Schueller OJA, et al. Fabrication of microfluidic systems in poly(dimethylsiloxane). Electrophoresis. 2000; 21(1): 27-40.

7 Seiler K, Harrison DJ, Manz A. Planar glass chips for capillary electrophoresis: repetitive sample injection, quantitation, and separation efficiency. Anal Chem. 1993; 65(10): 1481-8.

8 Harrison DJ, Fluri K, Seiler K, Fan Z, Effenhauser CS, Manz A. Micromachining a miniaturized capillary electrophoresis-based chemical analysis system on a chip. Science. 1993; 261(5123): 895-7.

9 Harrison DJ, Manz A, Fan Z, Luedi H, Widmer HM. Capillary electrophoresis and sample injection systems integrated on a planar glass chip. Anal Chem. 1992; 64(17): 1926-32.

10 Effenhauser CS, Manz A, Widmer HM. Glass chips for high-speed capillary electrophoresis separations with submicrometer plate heights. Anal Chem. 1993; 65(19): 2637-42.

11 Bousse L, Mouradian S, Minalla A, Yee H, Williams K, Dubrow R. Protein sizing on a microchip. Anal Chemistry. 2001; 73(6): 1207-12.

12 Mueller O, Hahnenberger K, Dittmann M, Yee H, Dubrow R, Nagle R, et al. A microfluidic system for high-speed reproducible DNA sizing and quantitation. Electrophoresis. 2000; 21(1): 128-34.

13 Fakhari AR, Breadmore MC, Macka M, Haddad PR. Non-aqueous capillary electrophoresis with red light emitting diode absorbance detection for the analysis of basic dyes. AnalChim Acta 2006; 580: 188–93.

14 Johns C, Macka M, Haddad PR. Design and performance of a light-emitting diode detector compatible with a commercial capillary electrophoresis instrument. Electrophoresis. 2004; 25(18-19): 3145-52.

15 Petr J, Jiang C, Sevcik J, Tesarova E, Armstrong DW. Sterility testing by CE: A comparison of online preconcentration approaches in capillaries with greater internal diameters. Electrophoresis. 2009; 30(22): 3870-6.

16 Ikeda M, Yamaguchi N, Nas M. Rapid on-chip flow cytometry detection of Listeria monocytogenes in milk. J Health Sci. 2009; 55(5): 851-6.

17 Herrera G, Martinez A, Blanco M, O'Connor J-E. Assessment of Escherichia coli B with enhanced permeability to fluorochromes for flow cytometric assays of bacterial cell function. Cytometry. 2002; 49(2): 62-9.

18 Lopez C, Pons MN, Morgenroth E. Evaluation of microscopic techniques (epifluorescence microscopy, CLSM, TPE-LSM) as a basis for the quantitative image analysis of activated sludge. Water Res. 2004; 39(2-3): 456-68.

19 Pascaud A, Amellal S, Soulas M-L, Soulas G. A fluorescence-based assay for measuring the viable cell concentration of mixed microbial communities in soil. J Microbiol Meth. 2009; 76(1): 81-7.

20 Khan MMT, Pyle BH, Camper AK. Specific and rapid enumeration of viable but nonculturable and viable-culturable Gram-negative bacteria by using flow cytometry. Appl Environ Microbiol. 2010; 76(15): 5088-96.

21 Portell X, Ginovart M, Carbo R, Gras A, Vives-Rego J. Population analysis of a commercial *Saccharomyces cerevisiae* wine yeast in a batch culture by electric particle analysis, light diffraction and flow cytometry. FEMS Yeast Res. 2011; 11(1): 18-28.

22 Sakamoto C, Yamaguchi N, Nasu M. Rapid and simple quantification of bacterial cells by using a microfluidic device. Appl Environ Microbiol, 2005; 71(2): 1117-21.

23 Palková Z, Váchová L, Valer M, Preckel T. Single-cell analysis of yeast, mammalian cells, and fungal spores with a microfluidic pressure-driven chip-based system. Cytometry Part A. 2004; 59A(2): 246-53.

24 Shadpour H, Musyimi H, Chen J, Soper SA. Physiochemical properties of various polymer substrates and their effects on microchip electrophoresis performance. J Chromatogr A. 2006; 1111(2): 238-51.

25 Landers JP, editor. Handbook of capillary and microchip electrophoresis and associated microtechniques. 3rd ed. New York: CRC Press; 2008.

26 Dolník V, Liu S, Jovanovich S. Capillary electrophoresis on microchip. Electrophoresis. 2000; 21(1): 41-54.

27 Becker H, Locascio LE. Polymer microfluidic devices. Talanta.. 2002; 56(2): 267-87.

28 Li PCH, editor. Microfluidic lab-on-a-chip for chemical and biological analysis and discovery. New York: CRC Press; 2005.

29 Tajalli H, Gilani AG, Zakerhamidi MS, Tajalli P. The photophysical properties of nile red and nile blue in ordered anisotropic media. Dyes Pigments. 2008; 78(1): 15-24.

30 Zheng H, Chen X-L, Zhu C-Q, Li D-H, Chen Q-Y, Xu J-G. Brilliant cresyl blue as a new red region fluorescent probe for determination of nucleic acids. Microchem J. 2000; 64(3): 263-9.

31 Breadmore MC, Henderson RD, Fakhari AR, Macka M, Haddad PR. Separation of nile blue-labelled fatty acids by CE with absorbance detection using a red light-emitting diode. Electrophoresis. 2007; 28(8): 1252-8.

32 Rahavendran SV, Karnes HT. Visible diode laser-induced fluorescence detection of phenylacetic acid in plasma derivatized with Nile blue and using precolumn phase transfer catalysis. Anal Chem. 1997; 69(15): 3022-7.

33 Law WS, Tay ETT, Feng H, Yu L, Zhao JH, Li SFY. Rapid identification of purified enteropathogenic Escherichia coli by microchip electrophoresis. J Sep Sci. 2007; 30: 1446 – 52.

34 Lim O, Suntornsuk W, Suntornsuk L. Capillary zone electrophoresis for enumeration of *Lactobacillus delbrueckii subsp. bulgaricus* and *Streptococcus thermophilus* in yogurt. J Chromatogr B. 2009; 877(8-9): 710-8.

35 Moon BG, Lee Y-I, Kang SH, Kim Y. Capillary electrophoresis of microbes. Bull Korean Chem Soc. 2003;24:81-5.

36 Gao P, Xu G, Shi X, Yuan K, Tian J. Rapid detection of *Staphylococcus aureus* by a combination of monoclonal antibody-coated latex and capillary electrophoresis. Electrophoresis. 2006; 27(9): 1784-9.

37 Jackowski M, Szeliga J, Kłodzińska E, Buszewski B. Application of capillary zone electrophoresis (CZE) to the determination of pathogenic bacteria for medical diagnosis. Anal Bioanal Chem. 2008; 391(6): 2153-60.

38 Bao Y, Lantz AW, Crank JA, Huang J, Armstrong DW. The use of cationic surfactants and ionic liquids in the detection of microbial contamination by capillary electrophoresis. Electrophoresis. 2008; 29(12): 2587-92.

39 Hoerr V, Stich A, Holzgrabe U. Critical aspects of analysis of *Micrococcus luteus, Neisseria cinerea*, and *Pseudomonas fluorescens* by means of capillary electrophoresis. Electrophoresis. 2004; 25(18-19): 3132-8.

40 Horká M, Růžička F, Holá V, Šlais K. Capillary isoelectric focusing of microorganisms in the pH range 2–5 in a dynamically modified FS capillary with UV detection. Anal Bioanall Chem. 2006; 385(5): 840-6.

41 Kłodzińska E, Dahm H, Różycki H, Szeliga J, Jackowski M, Buszewski B. Rapid identification of *Escherichia coli* and *Helicobacter pylori* in biological samples by capillary zone electrophoresis. J Sep Sci. 2006; 29(8): 1180-7.

42 Szumski M, Klodzinska E, Buszewski B. Separation of microorganisms using electromigration techniques. J Chromatogr A. 2005; 1084(1-2): 186-93.

43 Haugg M, Kaiser V, Schmidtkunz C, Welsch T. The effect of aggregation on the separation performance of bacteria in capillary electrophoresis. Electrophoresis. 2009; 30(2): 396-402.

44 Horká M, Růžička F, Kubesová A, Holá V, Slais K. Capillary electrophoresis of conidia from cultivated mMicroscopic filamentous fungi. Anal Chem. 2009; 81(10): 3997-4004.

45 Yu L, Yuan L, Feng H, Li SFY. Determination of the bacterial pathogen *Edwardsiella tarda* in fish species by capillary electrophoresis with blue light-emitting diode-induced fluorescence. Electrophoresis 2004; 25: 3139–44.

46 Armstrong DW, Schneiderheinze JM, Kullman JP, He L. Rapid CE microbial assays for consumer products that contain active bacteria. FEMS Microbiol Lett. 2001; 194(1): 33-7.

47 Kourkine IV, Ristic-Petrovic M, Davis E, Ruffolo CG, Kapsalis A, Barron AE. Detection of *Escherichia coli* O157:H7 bacteria by a combination of immunofluorescent staining and capillary electrophoresis. Electrophoresis. 2003; 24(4): 655-61.

48 Corneli S, Maragos CM. Capillary electrophoresis with laser-induced fluorescence: Method for the *Mycotoxin Ochratoxin A*. J Agri Food Chem. 1998; 46(8): 3162-5.

49 Lantz AW, Bao Y, Armstrong DW. Single-cell detection: Test of microbial contamination using capillary electrophoresis. Anal Chem 2007; 79: 1720-4.

50 Tong M-Y, Jiang C, Armstrong DW. Fast detection of *Candida albicans* and/or bacteria in blood plasma by "sample-self-focusing" using capillary electrophoresis-laser-induced fluorescence. J Pharm Biomed Anal. 2010; 53(1): 75-80.

51 Lantz AW, Bisha B, Tong M-Y, Nelson RE, Brehm-Stecher BF, Armstrong DW. Rapid identification of Candida albicans in blood by combined capillary electrophoresis and fluorescence in situ hybridization. Electrophoresis. 2010; 31(16): 2849-53.

52 He L, Jepsen RJ, Evans LE, Armstrong DW. Electrophoretic behavior and potency assessment of boar sperm using a capillary electrophoresis−laser induced fluorescence system. Anal Chem. 2003;75(4):825-34.

53 Alarcón B, García-Cañas V, Cifuentes A, González R, Aznar R. Simultaneous and sensitive detection of three foodborne pathogens by multiplex PCR, capillary gel electrophoresis, and laser-induced fluorescence. J Agri Food Chem. 2004; 52(23): 7180-6.

54 Preckel T, Luedke G, Chan SDH, Wang BN, Dubrow R, Buhlmann C. Detection of cellular parameters using a microfluidic chip-based system. JALA. 2002; 7(4): 85-9.

55 Rodriguez MA, Lantz AW, Armstrong DW. Capillary electrophoretic method for the detection of bacterial contamination. Anal Chem. 2006; 78(14): 4759-67.

56 Smallwood IM, editor. Handbook of organic solvent properties. London, Great Britain: Gray Publishing; 1996.

57 Tjørnelund J, Hansen S. The effect of water on separations in non-aqueous capillary electrophoresis systems. Chromatographia. 1997; 44(1): 5-9.

58 Geiser L, Veuthey J-L. Nonaqueous capillary electrophoresis in pharmaceutical analysis. Electrophoresis. 2007; 28(1-2): 45-57.

59 Vogt C, Vogt J, Becker A, Rohde E. Separation, comparison and identification of fountain pen inks by capillary electrophoresis with UV-visible and fluorescence detection and by proton-induced X-ray emission. J Chromatogr A. 1997; 781(1-2): 391-405.

APPENDICES

APPENDIX A

Table A.1 Analytical data from effects of types of BGEs (see Figure 4.2)

Parameter \ Analyte	NIC	TRI	NM	COT	NA
%RSD of t_m					
Citric acid	2.38	-	1.62	2.77	2.31
Phosphate	1.43	-	2.25	1.67	1.87
%RSD of t_r					
Citric acid	0.80	-	0.46	1.22	0.88
Phosphate	0.92	-	1.08	0.77	0.60
R_s		NIC/TRI	TRI/NM	NM/COT	COT/NA
Citric acid		20.30	4.48	8.74	35.29
Phosphate		29.55	5.87	12.20	47.68
TF					
Citric acid	1.50	1.70	1.72	1.58	1.94
Phosphate	1.35	1.63	1.52	1.79	0.79
N (x 10^3)					
Citric acid	116.08	58.77	47.86	73.90	39.77
Phosphate	264.93	152.88	133.67	89.51	69.21

Table A.2 Analytical data from effects of pHs of BGEs (see Figure 4.4)

Parameter \ Analyte	NIC	TRI	NM	COT	NA
%RSD of t_m					
pH 2.1	2.06	-	1.96	2.11	1.85
pH 2.5	1.43	-	2.25	1.67	1.87
pH 2.9	1.90	-	2.86	2.28	1.60
%RSD of t_r					
pH 2.1	0.37	-	0.12	0.28	0.23
pH 2.5	0.92	-	1.08	0.77	0.60
pH 2.9	0.62	-	1.32	0.74	0.76
R_s		NIC/TRI	TRI/NM	NM/COT	COT/NA
pH 2.1		21.32	3.38	9.84	19.19
pH 2.5		29.55	5.87	12.20	47.68
pH 2.9		13.29	9.11	1.63	42.69
TF					
pH 2.1	1.35	1.50	1.62	1.64	1.31
pH 2.5	1.33	1.56	1.47	1.58	1.94
pH 2.9	1.53	1.86	1.41	1.63	0.72
N (x 10^3)					
pH 2.1	104.566	73.526	48.515	42.118	100.278
pH 2.5	264.928	152.876	133.667	89.512	69.207
pH 2.9	75.428	41.403	38.274	24.811	20.848

Table A.3 Analytical data from effects of concentrations of BGEs (see Figure 4.6)

Parameter \ Analyte	NIC	TRI	NM	COT	NA
%RSD of t_m					
15 mM	1.83	-	2.27	2.32	1.94
20 mM	2.15	-	2.23	1.89	1.97
25 mM	2.06	-	1.96	2.11	1.85
30 mM	2.29	-	2.13	2.59	2.51
%RSD of t_r					
15 mM	0.33	-	0.76	1.72	0.55
20 mM	0.92	-	2.15	1.41	1.54
25 mM	0.37	-	0.12	0.28	0.23
30 mM	1.16	-	0.99	1.37	3.46
R_s		NIC/TRI	TRI/NM	NM/COT	COT/NA
15 mM		17.18	2.37	8.07	20.05
20 mM		20.13	3.35	8.99	18.99
25 mM		20.10	3.60	8.91	20.98
30 mM		23.10	3.38	11.54	27.92
TF					
15 mM	1.54	1.75	1.89	1.88	1.37
20 mM	1.50	1.72	1.88	1.88	1.32
25 mM	1.32	1.50	1.64	1.60	1.30
30 mM	1.32	1.70	1.73	1.72	1.32
N (x 10^3)					
15 mM	102.64	41.95	30.54	28.31	55.07
20 mM	104.57	55.08	38.74	36.51	65.99
25 mM	108.61	73.53	48.52	42.12	89.22
30 mM	110.61	67.38	54.13	34.62	47.28

Table A.4 Analytical data from effects of applied voltage (see Figure 4.8)

Analyte / Parameter	NIC	TRI	NM	COT	NA
%RSD of t_m					
20 kV	1.16	-	1.26	1.87	1.51
23 kV	1.09	-	2.26	2.98	2.77
25 kV	1.58	-	1.68	1.97	2.00
27 kV	2.35	-	2.23	2.12	2.51
30 kV	2.06	-	1.96	2.11	1.85
%RSD of t_r					
20 kV	0.58	-	0.11	1.12	1.50
23 kV	0.98	-	0.29	1.21	0.94
25 kV	1.30	-	0.68	1.17	1.29
27 kV	0.11	-	0.07	0.18	0.41
30 kV	0.37	-	0.12	0.28	0.23
R_s		NIC/TRI	TRI/NM	NM/COT	COT/NA
20 kV		24.13	2.99	11.80	20.30
23 kV		22.10	3.05	10.79	19.58
25 kV		20.92	3.54	8.72	20.41
27 kV		20.49	3.59	8.53	20.02
30 kV		20.11	3.60	8.92	21.03
TF					
20 kV	1.38	1.33	1.32	1.33	1.18
23 kV	1.36	1.54	1.50	1.54	1.28
25 kV	1.47	1.73	1.76	1.74	1.38
27 kV	1.52	1.72	1.71	1.70	1.48
30 kV	1.41	1.50	1.70	1.69	1.41
N (x 10^3)					
20 kV	92.21	53.06	41.48	32.58	32.16
23 kV	95.04	58.96	43.19	35.84	59.91
25 kV	96.23	59.36	45.07	38.51	66.28
27 kV	98.82	62.08	46.03	40.07	78.03
30 kV	108.61	67.38	48.52	42.12	89.22

Table A.5 Analytical data from effects of injection time (see Figure 4.10)

Analyte / Parameter	NIC	TRI	NM	COT	NA
%RSD of t_m					
5 s	1.76	-	0.93	1.17	2.29
10 s	2.06	-	1.96	2.11	1.85
15 s	1.15	-	1.69	0.93	2.45
20 s	0.36	-	1.40	0.84	1.81
%RSD of t_r					
5 s	1.45	-	0.48	0.74	1.76
10 s	0.37	-	0.12	0.28	0.23
15 s	0.94	-	1.37	0.44	1.96
20 s	0.20	-	0.84	0.30	1.49
R_s		NIC/TRI	TRI/NM	NM/COT	COT/NA
5 s		22.91	7.37	9.75	23.78
10 s		21.32	3.38	9.84	19.19
15 s		14.77	3.21	5.96	17.91
20 s		12.75	3.10	5.37	14.55
TF					
5 s	1.25	1.43	1.63	1.70	0.94
10 s	1.32	1.50	1.64	1.60	1.30
15 s	1.43	1.81	1.82	1.85	0.65
20 s	1.67	1.82	1.90	1.91	0.54
N (x 10^3)					
5 s	170.20	93.86	69.35	66.44	40.54
10 s	104.57	73.53	48.52	42.12	100.28
15 s	72.50	37.37	26.37	25.51	32.37
20 s	61.87	28.17	19.65	18.85	24.21

Day 1

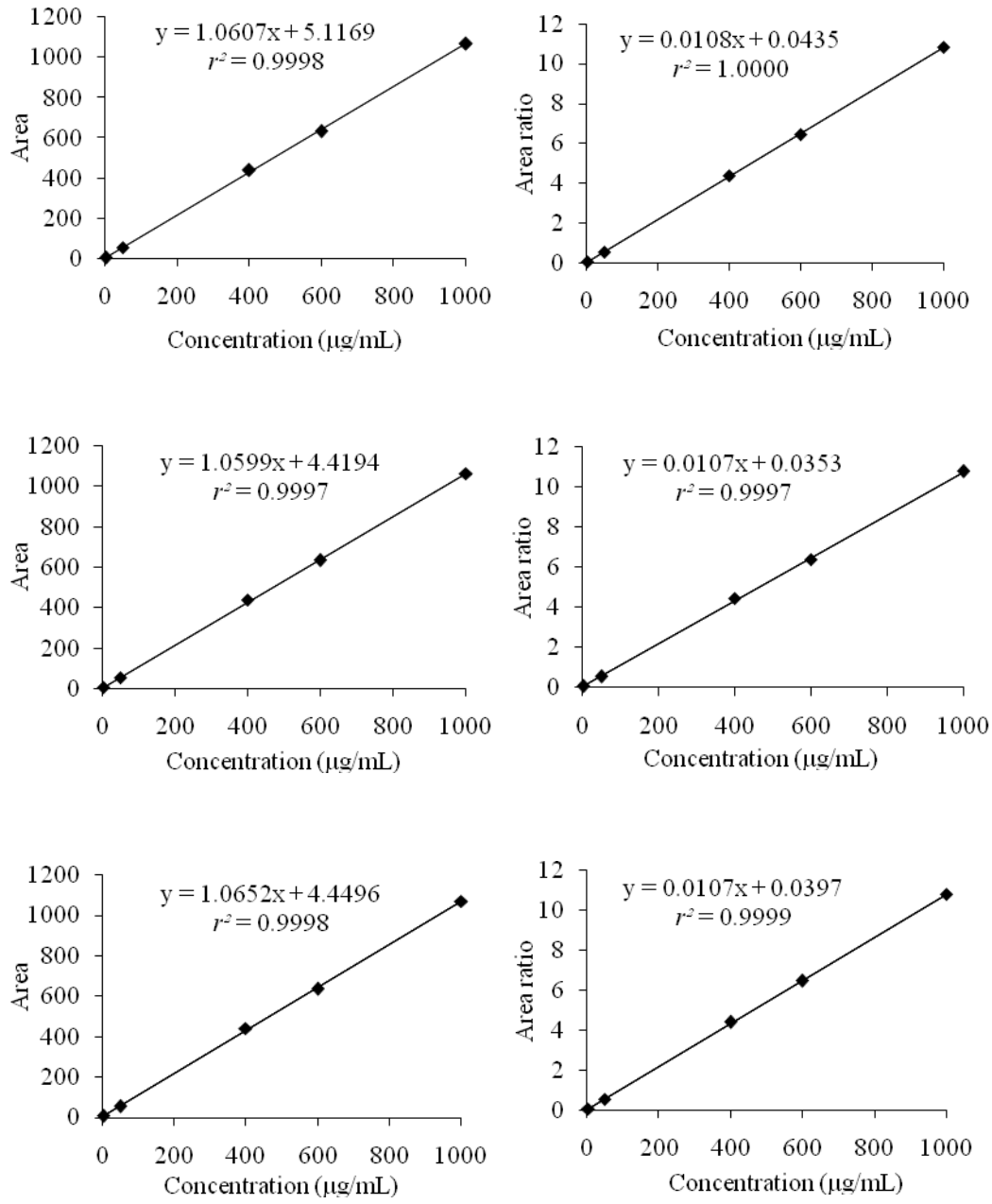

Figure A.1 Calibration curves of nicotine on three different days.

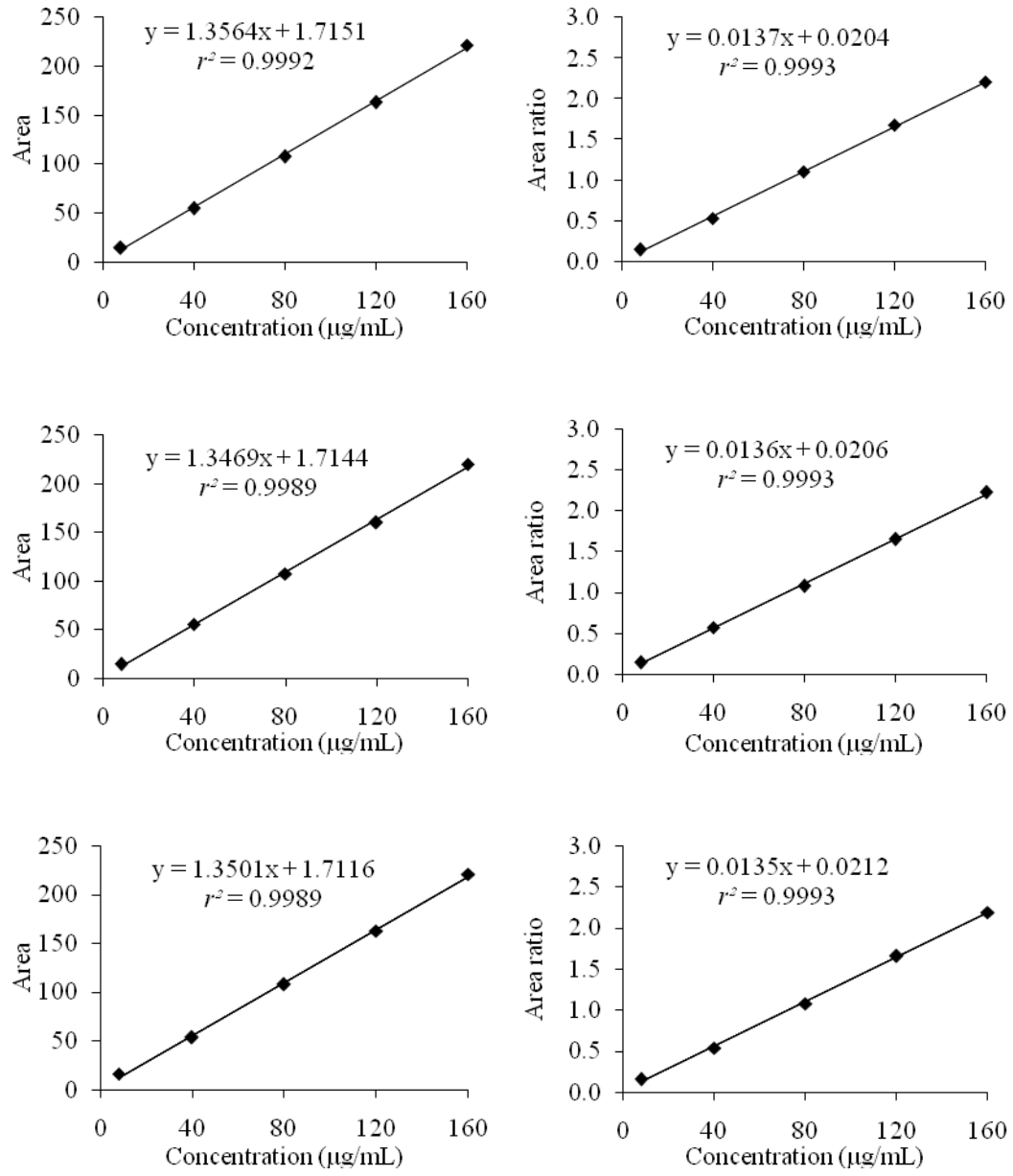

Figure A.2 Calibration curves of nicotinamide on three different days.

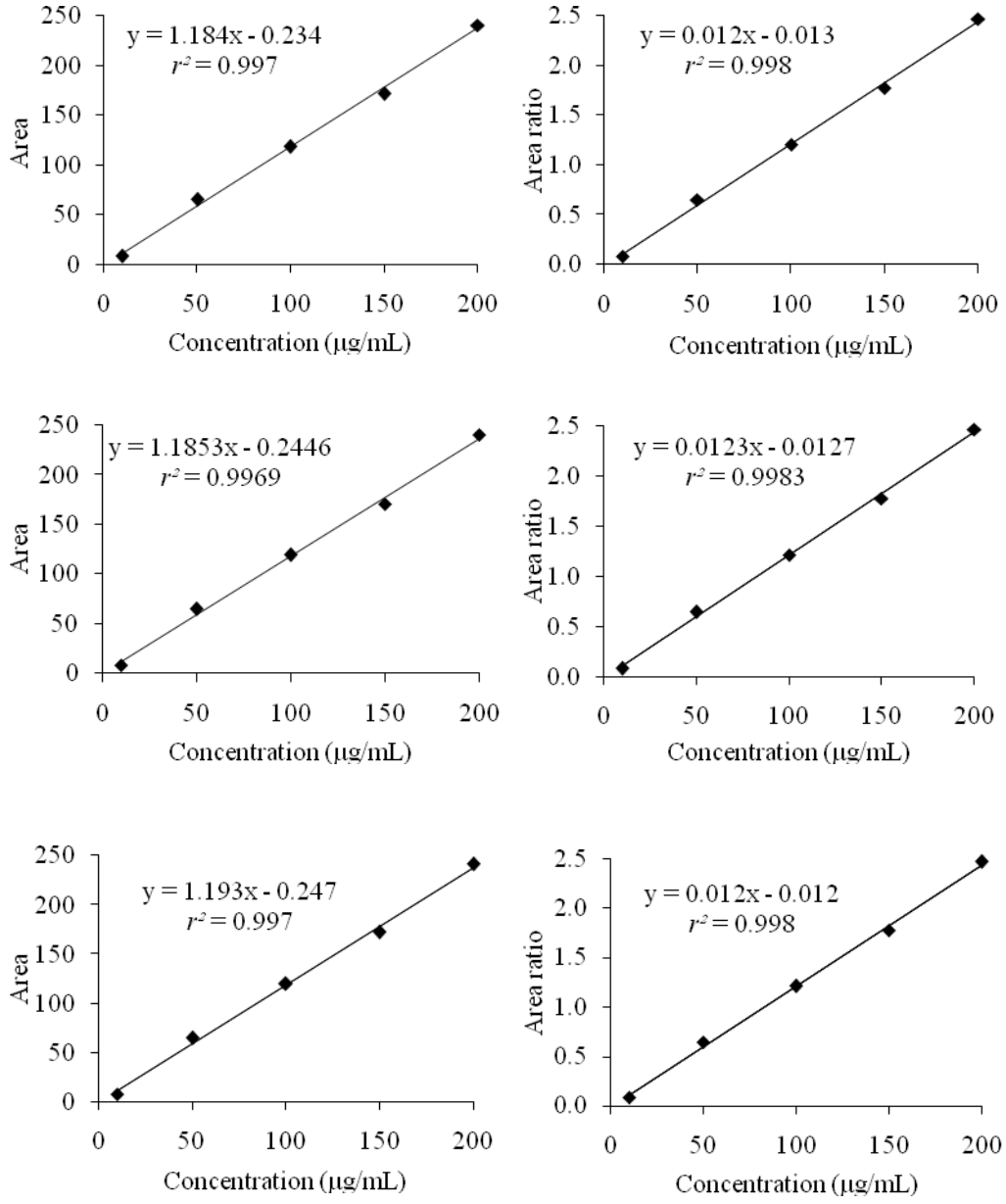

Figure A.3 Calibration curves of cotinine on three different days.

Day 1

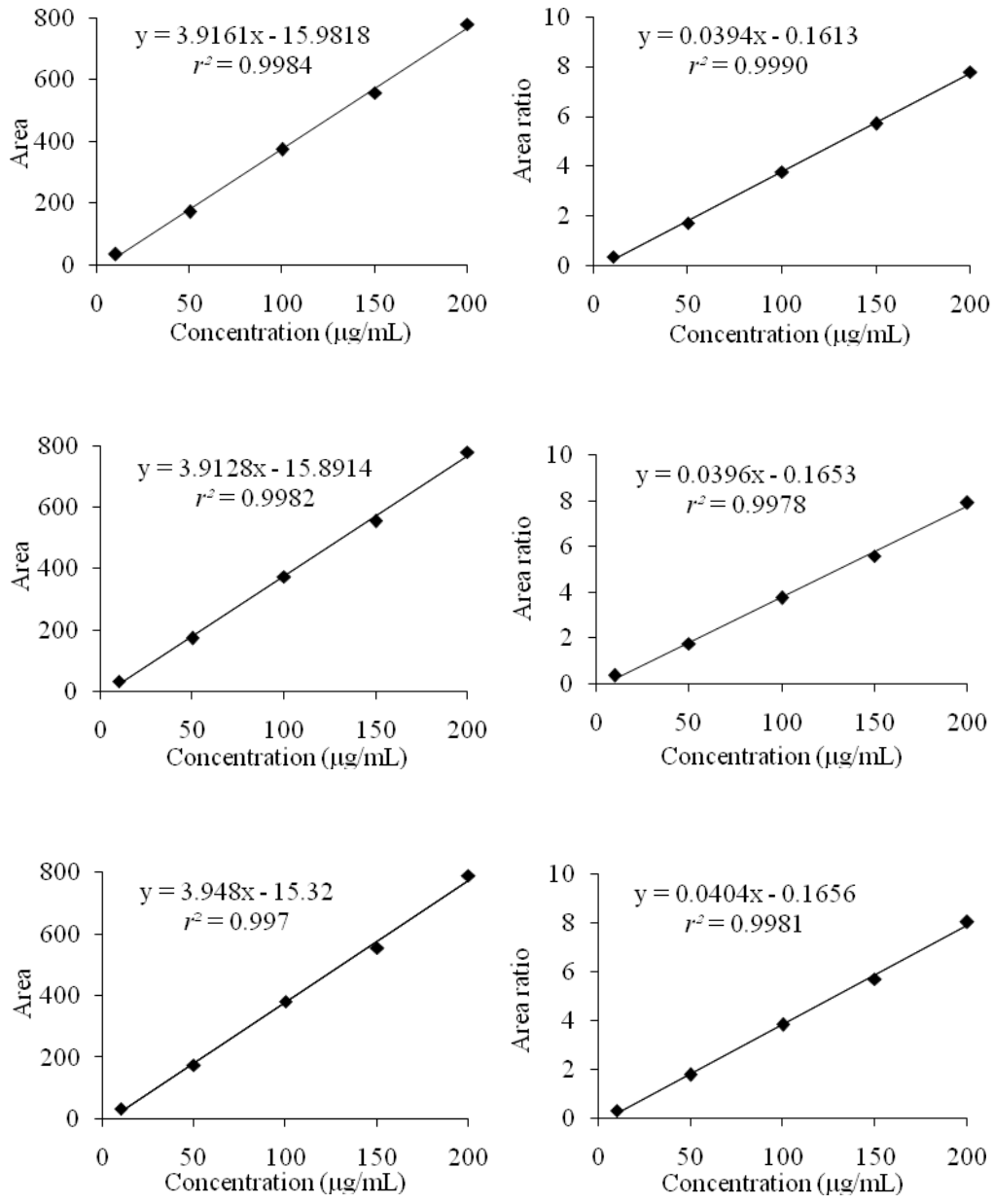

Figure A.4 Calibration curves of nicotinic acid on three different days.

APPENDIX B

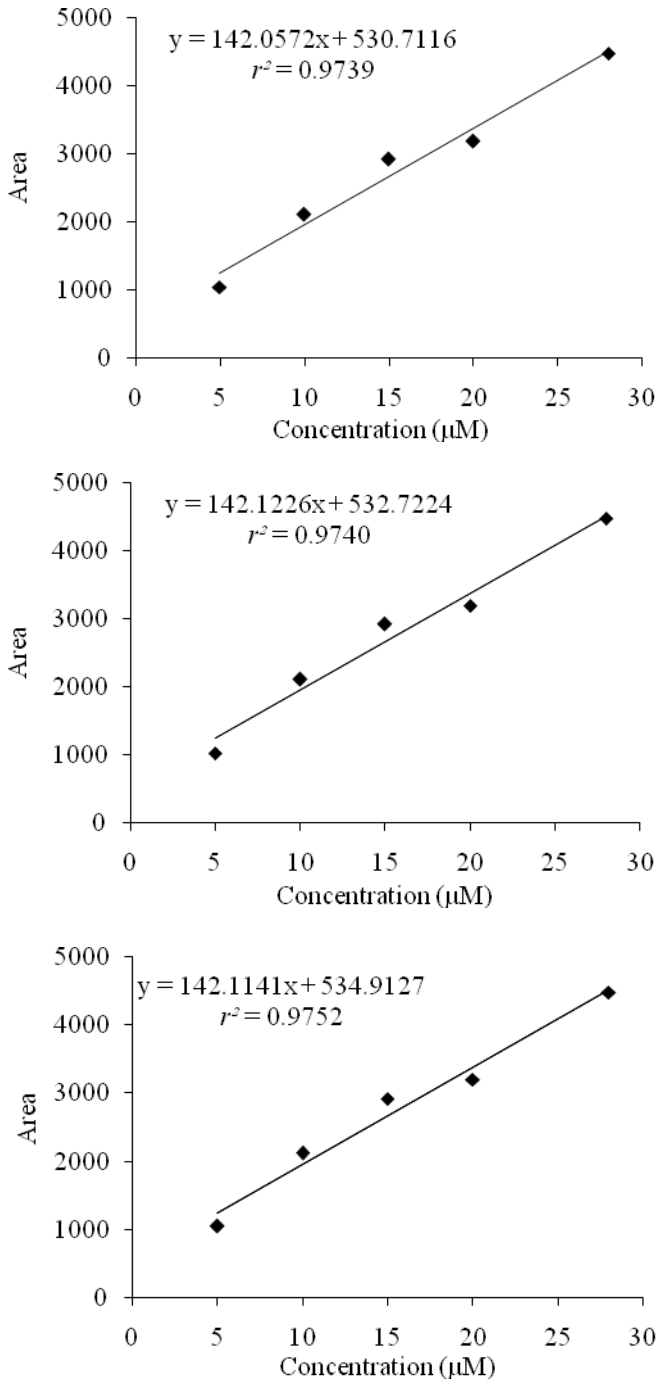

Figure B.1 Calibration curves of methylene blue on three different days.

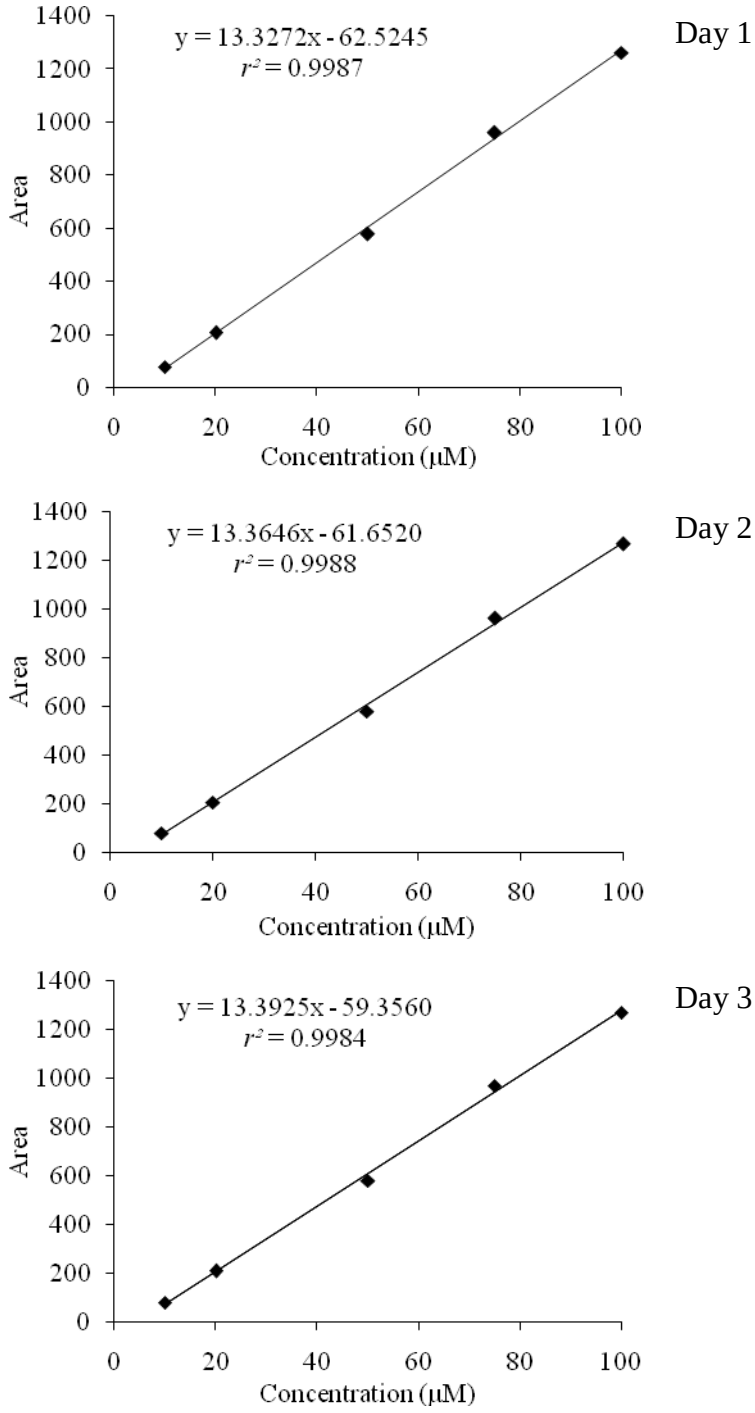

Figure B.2 Calibration curves of toluidine blue on three different days.

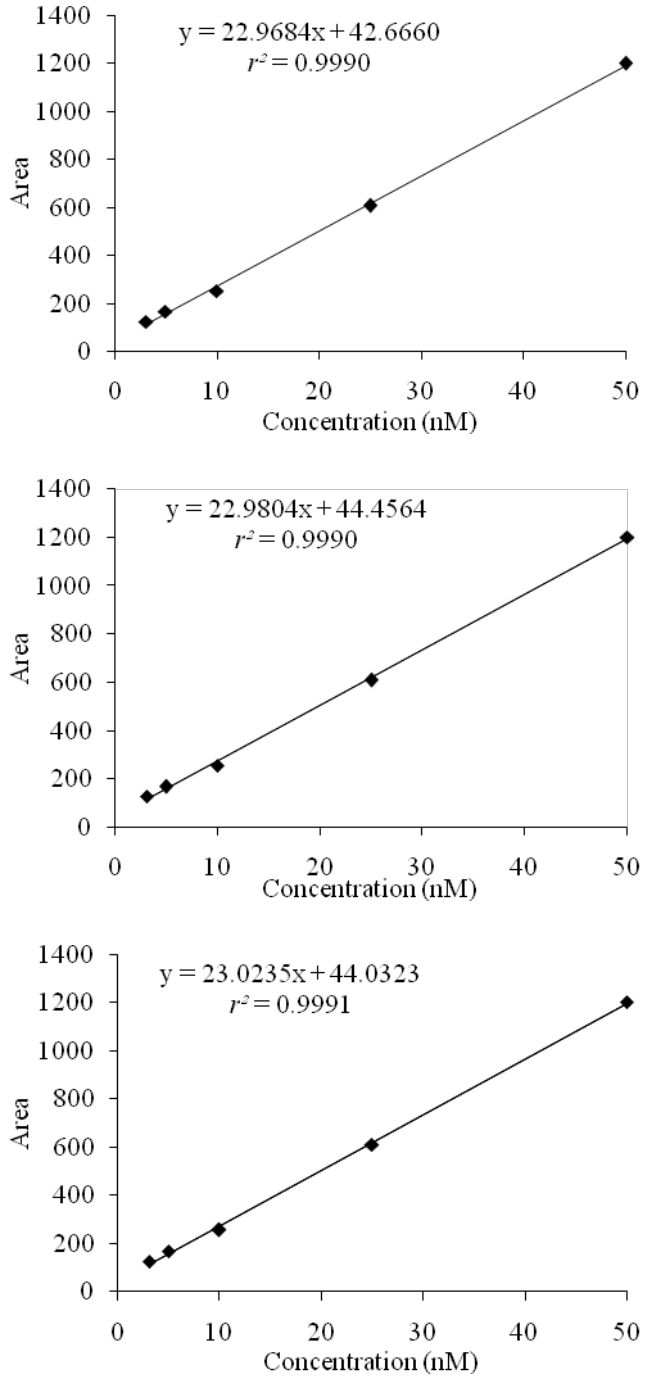

Figure B.3 Calibration curves of nile blue on three different days.

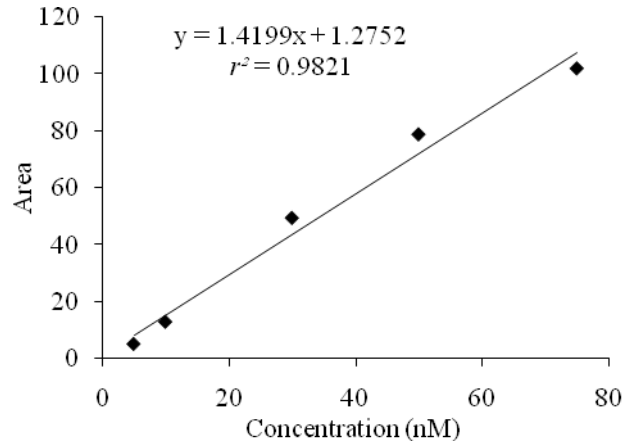

Day 1

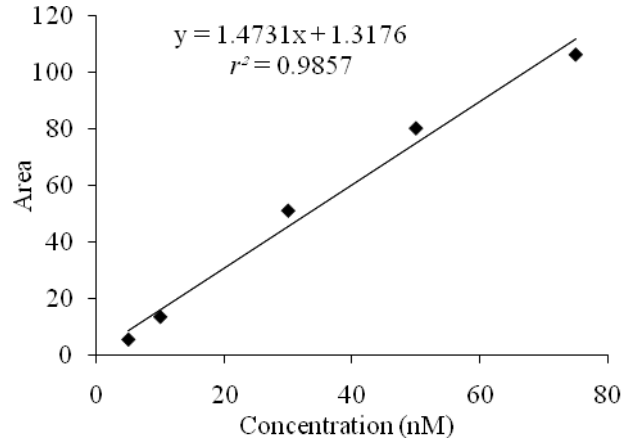

Day 2

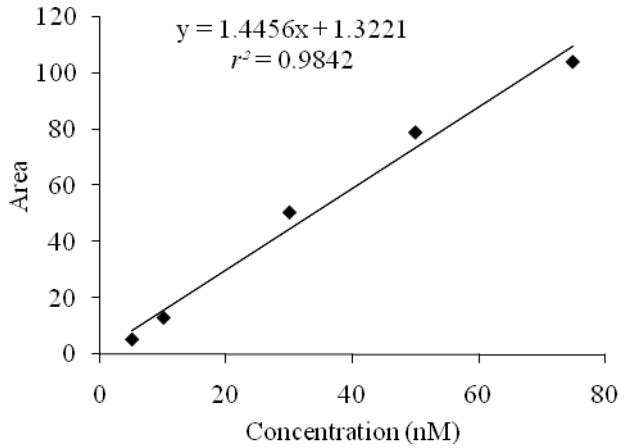

Day 3

Figure B.4 Calibration curves of brilliant cresyl blue on three different days.

BIOGRAPHY

NAME	Miss Nantana Nuchtavorn
DATE OF BIRTH	21 June 1983
PLACE OF BIRTH	Petchaburi, Thailand
INSTITUTIONS ATTENDED	Srinakharinwirot University, 2001-2006 Bachelor of Pharmacy Mahidol University, 2006-2011: Doctoral of Philosophy (Pharmaceutical chemistry and Phytochemistry)
RESEARCH GRANTS	Royal Golden Jubilee Ph.D. Program
HOME ADDRESS	284, Indramara 45, Sutthisarn road, Dindaeng, Bangkok 10400 E-mail: pang_nn@hotmail.com n.nuchtavorn@gmail.com
EMPLOYMENT ADDRESS	-
PUBLICATION/PRESENTATION	Publication: 1. Nuchtavorn N, Suntornsuk L, Simultaneous analysis of biological active pyridines in pharmaceutical formulations by capillary zone electrophoresis. J Chrom Sci. 2011. [accepted] 2. Nuchtavorn N, Clarke P, O'Connor B, Bek F, Macka M, Suntornsuk L, Rapid single cell detection of bacteria and fungi using microchip capillary electrophoresis with laser induced fluorescence, Proc. Pure and Applied

PUBLICATION/PRESENTATION

Chemistry International Conference (PACCON2011). [accepted]

3. Nuchtavorn N, Smejkal P, Breadmore MC, Doble P, Bek F, Guijt RM, Foret F, Suntornsuk L, Macka M, Exploring chip-CE-LIF platform flexibility: Separations of fluorescent dyes by chip-based non aqueous CE. J Chromatogr A. 2011. [In Review]

Presentation:

1. Nuchtavorn N, Suntornsuk L, Analysis of selected biologically active pyridines by capillary zone electrophoresis, Proc. 21st International Ion Chromatography Symposium (IICS 2009), Malahide, Co. Dublin, Ireland, 21-24 September 2009, poster presentation P504-T, p.142.

2. Nuchtavorn N, Suntornsuk L, Ryvolová M, Macka M, Separation of biologically active pyridines using capillary- and chip-based electrophoresis with various detection modes, Proc. 25th International Symposium on Microscale Bioseparations (MSB), Prague, Czech Republic, 21-25 March 2010, poster presentation P177, p.149.

3. Nuchtavorn N, Smejkal P, Breadmore MC, Ryvolová M, Bek F, Foret F, Guijt RM, Suntornsuk L, Macka M, A chip-based application oriented capillary electrophoresis

PUBLICATION/PRESENTATION

analyzer as a generic CE platform: Analysis of fluorescent dyes by NACE and the potential for derivatised bioanalytes with red LIF detection, Proc. 34th International Symposium on Capillary Chromatography (ISCC), Riva Del Garda, Italy, 1-4 June 2010, poster presentation R06, p.40.

4. Nuchtavorn N, Smejkal P, Breadmore MC, Ryvolová M, Guijt RM, Bek F, Foret F, Macka M, Suntornsuk L, Analysis of fluorescent dyes by non-aqueous CE on a chip and the potential for stained microorganisms with red LIF detection, Proc. 2nd REMSEA 2010: Regional Electrochemistry Meeting of South-East Asia on Applied Electrochemistry for Modern Life, Maha Chulalongkorn Building, Chulalongkorn University, Bangkok, Thailand, 16 – 19 November 2010, poster presentation PA28, p. 133.

5. Ryvolová M, Smejkal P, Nuchtavorn N, Piasecki T, Krčmová L, Akhter M, Foret F, Suntornsuk L, Maaskant P, Macka M, Solid-state light sources: an excellent match with the needs of portable and on-site analytical instrumentation, Proc. The 2010 International Chemical Congress of Pacific Basin Societies (Pacifichem), Honolulu, Hawaii, USA, 15-20 December 2010, oral presentation.

PUBLICATION/PRESENTATION

6. Smejkal P, Nuchtavorn N, Ryvolová M, Thompson R, Szekrényes A, Clarke P, Guijt RM, Breadmore MC, Foret F, Guttman A, O'Connor B, Bek F, Macka M, Chip based capillary electrophoresis analyzer: taking a commercial application-oriented instrumental platform back to research, Proc. 18th Annual RACI Environmental and Analytical Division R&D Topics Conference, University of Tasmania, Hobart, Tasmania, Australia, 5 – 8 December 2010, poster presentation. [Special Poster Prize for Poster with the Best Commercialisation Potential]

7. Nuchtavorn N, Clarke P, O'Connor B, Bek F, Macka M, Suntornsuk L, Rapid single cell detection of bacteria and fungi using microchip capillary electrophoresis with laser induced fluorescence, Proc. Pure and Applied Chemistry International Conference (PACCON2011), Miracle Grand Hotel, Bangkok, Thailand, 5-7 January 2011, poster presentation AC_A0008.

8. Nuchtavorn N, Clarke P, O'Connor B, Bek F, Macka M, Suntornsuk L, The potential of microchip capillary electrophoresis on microorganism detection, Proc. Pure and Applied Chemistry International Conference (PACCON2011), Miracle Grand Hotel, Bangkok, Thailand, 5-7 January 2011, oral presentation AC_A0009.

PUBLICATION/PRESENTATION

9. Nuchtavorn N, Smejkal P, Ryvolova M, Clarke P, Guijt RM, Bredmore MC, Foret F, O'Connor B, Bek F, Macka M, Suntornsuk L, A novel method for bioanalysis by on-chip capillary electrophoresis with fluorescence detection, Proc. RGJ-Ph.D. Congress XII, Jomtien Palm Beach Hotel & Resort, Pattaya, Chonburi, Thailand, 1 – 3 April 2011, oral presentation S5-O15.

10. Smejkal P, Nuchtavorn N, Breadmore MC, Foret F, Guijt RM, Bek F, Suntornsuk L, Macka M, Microfluidic chip-CE-LIF custom application oriented platform: Exploring the full potential as a generic rapid portable analyser, Proc. the 2nd Australian and New Zealand Micro and Nanofluidics Symposium, University of New South Wales, Sydney, Australia, 28-29 April 2011.

11. Smejkal P, Nuchtavorn N, Yi SG, Yi N, Breadmore MC, Foret F, Guijt RM, Suntornsuk L, Bek F, Macka M, Microfluidic electrophoresis with LIF and LED fluorescence detection for biomedical diagnostics and on-site analysis: How flexible can be a fixed-design chip-CE system?, Proc. 36th International Symposium on High-Performance Liquid Phase Separations and Related Techniques (HPLC 2011), Budapest, Hungary, 19-23 June 2011.

12. Ryvolová M, Krčmová L, Piasecki T, Smejkal P , Nuchtavorn N, Akhter M, Foret F, Suntornsuk L, Maaskant P, Breadmore MC , Macka M , Solid-State Light Sources: The 21st Century Light Sources for Miniaturised and Portable Analysis?, Proc. European Conference on Analytical Chemistry (Euroanalysis 2011), Congress Center SAVA, Belgrade, Serbia 11-15 September 2011.